

Aus dem Institut für Immunologie

Im Biomedizinischen Zentrum der Ludwig-Maximilians-Universität München

Vorstand: Prof. Dr. Thomas Brocker

**Impaired degradation of phagocytosed nuclear material  
contributes to inflammation in C1q-KO mice**

Dissertation

zum Erwerb des Doktorgrades der Naturwissenschaften  
an der Medizinischen Fakultät der  
Ludwig-Maximilians-Universität zu München

vorgelegt von

Ashretha Ashokkumar

aus

Krishnagiri/ Indien

Jahr

2019

Aus dem Institut für Immunologie

Im Biomedizinischen Zentrum der Ludwig-Maximilians-Universität München

Vorstand: Prof. Dr. Thomas Brocker

**Impaired degradation of phagocytosed nuclear material  
contributes to inflammation in C1q-KO mice**

Dissertation

zum Erwerb des Doktorgrades der Naturwissenschaften  
an der Medizinischen Fakultät der  
Ludwig-Maximilians-Universität zu München

vorgelegt von

Ashretha Ashokkumar

aus

Krishnagiri/ Indien

Jahr

2019

Mit Genehmigung der Medizinischen Fakultät  
der Universität München

**Betreuer:** Prof. Dr. Thomas Brocker

**Zweitgutachter:** Prof. Dr. Kirsten Lauber

**Dekan:** Prof. Dr. med. dent. Reinhard Hickel

**Tag der mündlichen Prüfung:** 14.01.2020

## Affidavit

I hereby declare, that the submitted thesis entitled **Impaired degradation of phagocytosed nuclear material contributes to inflammation in C1q-KO mice** is my own work. I have only used the sources indicated and have not made unauthorised use of services of a third party. Where the work of others has been quoted or reproduced, the source is always given.

I further declare that the submitted thesis or parts thereof have not been presented as part of an examination degree to any other university.

Munich, 31.01.2020

Ashokkumar, Ashretha

This work contains work presented in the following publications:

Ashokkumar, A., Kranich, J., Pacheco, N.F., Folytn-Kia, A., Dislich, B., Stefan F. Lichtenthaler., Schmidt, A., Imhof, A., Blume, J., Brocker, T. **“Impaired degradation of phagocytosed nuclear material contributes to inflammation in C1q-KO mice**, Manuscript in preparation

## ABBREVIATIONS

ANA	anti-nuclear antibody
APAF-1	Apoptotic protease activating factor 1
APC	antigen presenting cells
BAI1	brain specific angiogenesis inhibitor
BATF-3	basic leucin zipper transcription factor ATF-like 3
BCL-2	B-cell lymphoma
BSA	bovine serum albumin
CCL	chemokine (C-C motif) ligand
CD	cluster of differentiation
cDNA	complementary DNA
CSF	colony stimulating factor
CXCL	chemokine (C-X-C motif) ligand 1
DAMP	danger associated molecular pattern
DAPI	4',6-diamidino-2-phenylindole
DC	dendritic cells
DISC	death-inducing signaling complex
DMSO	dimethyl sulfoxide
DNGR-1	dendritic cell natural killer lectin group receptor-1
dNTP	deoxyribonucleotidtriphosphate
DOCK180	dedicator of cytokinesis 1
DTT	dithiothreitol
ECL	enhanced chemiluminescence
EDTA	ethylenediaminetetraacetic acid
ELMO1	engulfment and cell motility 1
ESAM	endothelial cell-selective adhesion molecule
FACS	fluorescence activated cell sorter

FcR	Fc Receptor
FCS	fetal calf serum
FDC	follicular dendritic cells
GC	germinal center
GPCR	G protein-coupled receptors
HMGB1	High mobility group protein B1
i.p.	intraperitoneal
IFNs	interferons
IL	interleukins
IRF	IFN regulatory factor
kDA	kilo Dalton
LAMP	lysosomal-associated membrane protein
MAC	membrane attack complex
MACS	magnetic cell sorting
MARCO	macrophage receptor with collagenous structure
MFGE8	Milk fat globule epidermal growth factor-factor 8
MFI	mean fluorescence intensity
MHC	major histocompatibility complex
MICL	myeloid inhibitory C-type lectin-like receptor
MLKL	mixed lineage kinase domain-like
mRNA	messenger RNA
MP	macrophage
MZ	marginal zone
NET	neutrophil extracellular traps
NF- KB	nuclear factor kappa B
NOD	nucleotide-binding oligomerization domain
PBS	phosphate buffer saline
pMP	peritoneal macrophage

qPCR	quantitative PCR
Rab	Ras-related protein
RIG-1	retinoic acid-inducible gene I
RIPK3	receptor-interacting serine/threonine-protein kinase
RT	reverse transcriptase
SD	standard deviation
SDS	sodium dodecyl sulfate
SLE	systemic lupus erythematosus
STING	Stimulator of Interferon Genes
TAM	tumour associated macrophages
TBK	tank binding kinases
TBM	tingible body macrophages
TBS	tris buffered saline
TEMED	tetramethylethylenediamin
TIM	T-cell immunoglobulin mucin
TLR	toll like receptor
TNF	tumor necrosis factor
TRAIL	TNF-related apoptosis-inducing ligand
VCAM	vascular cell adhesion molecule
WT	wild-type

# TABLE OF CONTENTS

<b>ABBREVIATIONS</b> .....	<b>iv</b>
<b>1 SUMMARY</b> .....	<b>1</b>
<b>2 ZUSAMMENFASSUNG</b> .....	<b>2</b>
<b>3 INTRODUCTION</b> .....	<b>3</b>
<b>3.1 The immune system</b> .....	<b>3</b>
<b>3.2 Mononuclear Phagocyte System</b> .....	<b>4</b>
3.2.1 MPs.....	4
<b>3.3 Cell death pathways</b> .....	<b>9</b>
3.3.1 Apoptosis .....	9
3.3.2 Necrosis .....	11
3.3.3 NETosis .....	11
<b>3.4 Phagocytosis</b> .....	<b>12</b>
3.4.1 Communication between phagocytes and apoptotic cells.....	13
3.4.2 Scavenging receptors .....	15
3.4.3 Apoptotic cargo processing .....	17
3.4.4 Implications of impaired phagocytosis .....	18
<b>3.5 SLE - an autoimmune disorder</b> .....	<b>18</b>
3.5.1 Epidemiology .....	19
3.5.2 Etiological factors for SLE.....	19
3.5.3 Pathogenesis of SLE .....	20
3.5.4 Complement deficiencies and SLE .....	21
3.5.5 Current therapeutic strategies .....	24
<b>3.6 Study motivation</b> .....	<b>26</b>
<b>4 MATERIALS AND METHODS</b> .....	<b>27</b>
<b>4.1 Materials</b> .....	<b>27</b>
4.1.1 Devices .....	27
4.1.2 Consumables .....	28
4.1.3 Chemicals and buffers .....	28
4.1.4 FACS antibodies .....	31
4.1.5 Western blot antibodies .....	32
4.1.6 Immunohistochemistry antibodies .....	32
4.1.7 Mouse strains.....	33
<b>4.2 Methods</b> .....	<b>33</b>
4.2.1 Immunological and cell biology methods.....	33
4.2.2 Molecular Biology.....	36
<b>5 RESULTS</b> .....	<b>43</b>
<b>5.1 Does C1q deficiency affect phagocytosis pathways?</b> .....	<b>43</b>
5.1.1 <i>in vivo</i> tracking of apoptotic cells .....	43
5.1.2 An unbiased proteomics screen .....	45
5.1.3 Confirmation of the proteomics screen.....	49
5.1.4 Does C1q-KO pMPs exhibit an acidification defect? .....	53
5.1.4 Why is the phagocytic machinery disturbed in C1q-KO mice?.....	55
<b>5.2 Do phagocytosis defects trigger inflammatory pathways in C1q-KO mice?</b> .....	<b>57</b>
<b>5.3 Can MFGE8-DNASE2A restore the DNA degradation?</b> .....	<b>60</b>
5.3.1 Generation of MFGE8-DNASE2A fusion protein.....	60
5.3.2 Enzymatic activity of MFGE8-DNASE2A fusion protein .....	60
5.3.3 Functional activity of MFGE8-DNASE2A fusion protein .....	61
5.3.4 Efficacy of MFGE8-DNASE2A to recover phagocytosis defect.....	62
5.3.5 Efficacy of MFGE8-DNASE2A to reduce inflammation in C1q-KO mice.....	64

<b>6 DISCUSSION .....</b>	<b>67</b>
6.1 C1q-KO mice exhibit a phagocytosis defect.....	67
6.2 Inflammation is a consequence of phagocytosis defect in C1q-KO mice .....	68
6.3 C1q-KO mice exhibit a dysfunctional phagocytic machinery.....	71
6.4 Diminished TFEB expression in C1q-KO MPs.....	72
6.5 MFGE8-DNASE2A administration does have a therapeutic potential.....	73
<b>7 GRAPHICAL ABSTRACT.....</b>	<b>75</b>
<b>8 OUTLOOK.....</b>	<b>76</b>
<b>9 APPENDIX .....</b>	<b>77</b>
9.1 Spleen enriched MPs proteomics.....	77
9.2 pMPs proteomics.....	78
9.3 Primer sequences.....	80
<b>10 REFERENCES .....</b>	<b>81</b>
<b>11 ACKNOWLEDGEMENT.....</b>	<b>102</b>
<b>12 PRESENTATIONS .....</b>	<b>103</b>

# 1 SUMMARY

C1q-deficiency is strongly associated with the development of systemic lupus erythematosus (SLE) in humans and lupus-like autoimmunity in mice. Often, macrophages (MPs) show a reduced ability to engulf apoptotic cells in SLE patients. In agreement with this, it has been shown that C1q-KO mice show impaired engulfment of dead cells. However, the precise mechanisms how this leads to the development of SLE is unclear. Using apoptotic cells with fluorescently-labeled H2B histones, we could show that C1q-KO peritoneal macrophages (pMPs) exhibit a delayed degradation of nuclear material derived from phagocytosed apoptotic cells. We found a significant reduction of lysosomal DNASE2A in C1q-KO splenic enriched MPs and pMPs which is necessary for digesting the engulfed apoptotic nuclear material. As a consequence, C1q-KO MPs show elevated levels of factors involved in the STING-pathway, which is activated by recognition of cytosolic DNA. We also found significant reduction of RAB5 in C1q-KO MPs which is necessary for maintaining the endo-lysosomal system. In addition, enlarged lysosomal compartments were seen in C1q-KO MPs which is an indication of dysfunctional lysosomes. In order to restore the degradation of phagocytosed nuclear material, we coated apoptotic cells with a DNASE2A fused to the apoptotic-cell binding protein MFGE8, to deliver DNASE2A directly to the lysosomes containing DNA of phagocytosed apoptotic cells. This not only restored DNA-degradation in C1q-KO MPs, but also lead to reduced production of inflammatory cytokines upon phagocytosis. Hence, we postulate that C1q-deficiency leads to accumulation of non-degraded DNA in phagocytic cells triggering production of pro-inflammatory cytokines via the STING pathway. In addition, reduced DNASE2A expression could be a consequence of the disrupted endo-lysosomal system seen in C1q-KO MPs.

## 2 ZUSAMMENFASSUNG

Der C1q-Mangel ist stark mit der Entwicklung des systemischen Lupus erythematoses (SLE) beim Menschen und der lupusartigen Autoimmunität bei Mäusen verbunden. Häufig zeigen Makrophagen eine verminderte Fähigkeit, apoptotische Zellen bei SLE-Patienten zu aktivieren. In Übereinstimmung damit wurde gezeigt, dass C1q-defiziente Mäuse eine beeinträchtigte Phagozytose toter Zellen aufweisen. Die genauen Mechanismen, wie dies zur Entwicklung von SLE führt, sind jedoch unklar. Wir fanden eine signifikante Reduktion von lysosomaler DNase2a bei C1q-defizienten Milz- und Peritonealmakrophagen, die für den Abbau des phagozytierten apoptotischen Kernmaterials notwendig ist. Unter Verwendung von apoptotischen Zellen mit fluoreszenzmarkierten H2B-Histonen konnten wir zeigen, dass C1q-defiziente peritoneale Makrophagen einen verzögerten Abbau von Kernmaterial aus phagozytierten apoptotischen Zellen aufweisen. Infolgedessen zeigen C1q-defiziente Makrophagen erhöhte Werte von Faktoren, die am STING-Signalleitungsweg beteiligt sind, der durch die Erkennung zytosolischer DNA aktiviert wird. Wir fanden auch eine signifikante Reduktion von RAB5 in C1q-defizienten Makrophagen, die für die Aufrechterhaltung des endo-lysosomalen Systems notwendig ist. Darüber hinaus wurden vergrößerte lysosomale Kompartimente in C1q-KO-Makrophagen beobachtet, was ein Hinweis auf dysfunktionale Lysosomen ist. Um den Abbau von phagozytiertem Kernmaterial wiederherzustellen, haben wir apoptotische Zellen mit DNASE2A beschichtet, die mit dem apoptotischen Zellbindungsprotein MFGE8 fusioniert ist, um DNASE2A direkt an die Lysosomen zu liefern, die DNA von phagozytierten apoptotischen Zellen enthalten. Dadurch wurde nicht nur der DNA-Abbau in C1q-defizienten Makrophagen wiederhergestellt, sondern auch die Produktion von inflammatorischen Zytokinen bei Phagozytose reduziert. Daher postulieren wir, dass C1q-Mangel zu einer Anhäufung von nicht abgebauter DNA in phagozytischen Zellen führt, die die Produktion von proinflammatorischen Zytokinen über den STING-Weg auslöst. Darüber hinaus könnte eine reduzierte DNASE2A-Expression eine Folge des gestörten endo-lysosomalen Systems sein, das in C1q-defizienten Makrophagen beobachtet wird.

## 3 INTRODUCTION

### 3.1 The immune system

Multicellular organisms have evolved their own defense strategies to fight off pathogens. The body is protected from various infectious and harmful agents by a variety of effector cells and molecules that together make up the immune system. The collective and coordinated signals from the immune system to pathogens (eg., protozoans, virus and bacteria) are termed immune response. The immune system is broadly classified as innate and adaptive immunity. Innate immunity comprises physical barriers (skin and mucosal), chemical barriers (anti-microbial peptides), blood proteins (complement) and cellular components (macrophages (MPs), neutrophils and NK cells). Innate immunity serves as the first line of defense and relies on a limited number of receptors and secreted proteins that recognize a wide variety of pathogens. Early responses to pathogens are mediated by innate immunity followed by a very specific immune responses termed adaptive immunity.

When an infection overwhelms innate immune defense mechanisms, an adaptive immune response is initiated. Nevertheless, the adaptive immune system with its large range of repertoire of antigen-specific receptors produced by somatic recombination is able to recognize virtually any microbial and non-microbial antigen. The high affinity receptors of B cells and T cells are accomplished through a process called V(D)J-recombination which allows the generation of a very large number of different specificities from a limited number of genetic segments. B cells and T cells with high affinity receptors are the cellular components that exert their immune responses towards pathogens. Some specialized antigen presenting cells (APCs) act as a bridge between innate and adaptive immune system in order to activate T and B cells thereby initiating the adaptive immune responses. Adaptive immunity is further subdivided into humoral immunity and cell-mediated immunity. Humoral immunity is mediated by antibodies produced by B cells. Successful elimination of extracellular microbes and toxins is facilitated by binding of secreted antibodies to the pathogen surface. On the other hand, cell-mediated immunity is effective against intracellular pathogens proliferating inside the MPs or other host cells.

The failure or breakdown of mechanisms maintaining self-tolerance in B and T cell results in autoimmunity. Loss of self-tolerance results in abnormal selection of self-reactive lymphocytes thereby presenting self-antigens to the immune system [1]. MPs contribute to autoimmunity and inflammation through their ability to present autoantigens and through its potent effector mechanisms during innate and adaptive immunity.

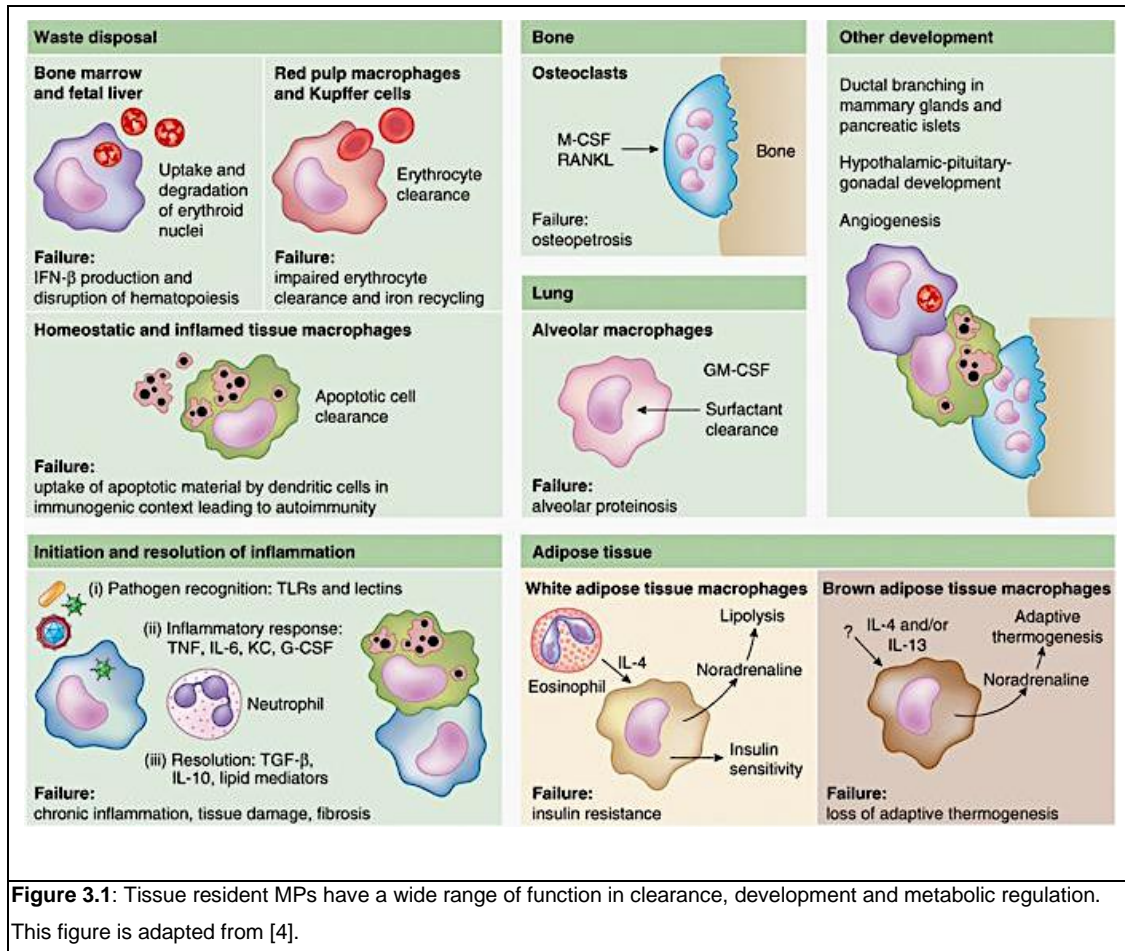
## **3.2 Mononuclear Phagocyte System**

The mononuclear phagocyte system (MPS) was established by van Furth [2] that consists of myeloid immune cells such as monocytes, MPs but not granulocytes though dendritic cells were included following their discovery. The homeostasis of tissue resident MPs relies on the constant recruitment of blood monocytes developed from committed bone marrow precursors [3]. Tissue resident MPs are heterogeneous immune cells which fulfill tissue-specific and niche-specific functions. Tissue resident MPs have dedicated homeostatic functions such as apoptotic cell clearance, response to infection and the resolution of inflammation [4]. In the beginning, it was considered that both monocytes and MPs are related cell types arising from a continuous differentiation. Nevertheless, these initial concepts were later challenged with fate mapping studies to identify their respective origin. At present it is established that classical MPs and DCs reside in tissues whereas monocytes reach the inflammation site from blood circulation only on demand. The origin and characteristics of each cell types are discussed further in detail.

### **3.2.1 MPs**

MPs are specialized immune cells of innate immune system involved in the phagocytosis and neutralization of potential pathogens. The MP functions are mainly restricted to their immediate surroundings in which they differ from mobile DCs specialized in triggering remote T cell responses upon their translocation to tissue-draining lymph nodes [5]. MPs are functionally grouped into two classes, known as “M1-M2” paradigm [6]. M1 MPs are classically activated MPs associated with inflammatory responses while the tissue resident MPs are

categorized as “M2-like” with their functions contributing towards the maintenance of tissue homeostasis and resolution of inflammation [4], [6].



Tissue MPs play an important role in immunosurveillance in their close surroundings. This patrolling function of MPs is achieved with the help of wide array of danger sensing molecules like scavenging receptors, pattern recognition receptors (TLRs, C-type lectins receptors, RIG-1 and NOD), cytokine receptors and adhesion molecules. Once pathogens are sensed by MPs they eliminate them with the help of a highly developed lysosomal compartment abundant in critical protease and bactericidal activity [7]. However, the wide array of receptor and effector functions of MPs are dependent on their local adaptation to different tissues [8]. The wide range of tissue resident MPs and their functions are shown in Figure 3.1

### 3.2.1.1 Development and heterogeneity of tissue MPs *in vivo*

The majority of adult tissue MPs is seeded prenatally from embryonic progenitors and can maintain themselves by self-renewal. Primitive MPs appear at first within the yolk sac blood

islands. These MPs follow a 'fast-track' differentiation pathway without a monocytic intermediate to become mature fetal tissue MPs completely dependent on transcription factor PU.1 [9], [10]. Once the circulatory system is fully established, yolk-sac derived MPs migrate into the embryonic tissues via circulation and develop into a fetal MP population [11]. However, it is unclear if yolk-sac derived MPs persist into adulthood and if they act as a sole source of adult tissue specific MPs. Following the appearance of yolk-sac derived MPs, monocytes differentiate in the fetal liver from pro-monocytic intermediates and resemble adult monocytes as they express CD11b, F4/80, Ly6C and CSF1R [12], [13]. CD11b mediates inflammation, chemotaxis, phagocytosis and is also involved in the complement system by binding iC3b. F4/80 is a member of adhesion G-protein coupled receptor (GPCR) family widely expressed in mouse MPs and some circulating monocytes. Ly6C is expressed on MP and DC-precursors, granulocytes and wide range of endothelial cells, B and T cell subpopulations. These monocytes are released into circulation and later recruited to fetal tissues. Once they reach embryonic fetal tissues, these monocytes proliferate and differentiate locally into MPs thus superseding the existing yolk-sac derived MPs as seen in alveolar MPs from lungs and heart MPs [14], [15]. Thus, tissue resident MPs derived either from embryonic or adult monocytic origin are exposed to many tissue-specific factors which influences their further development, function, and polarization. The specific functions and phenotype of splenic MPs and pMPs are discussed further in detail as they are extensively used in this current study.

### **3.2.1.2 pMPs**

pMPs are one of the best characterized MP population and contributed much to our understanding of MP biology. These MPs are easily accessible and were used to study phagocytosis and signaling cascades [16], [17]. However, the specific functions and ontogeny of pMPs are still largely unknown. There are two different pMPs subsets which differ in phenotype and function. One minor subset represents F4/80<sup>int</sup>CD11b<sup>int</sup> pMPs which act as an on-demand precursor for F4/80<sup>hi</sup>CD11b<sup>hi</sup> pMP population. The F4/80<sup>hi</sup>CD11b<sup>hi</sup> pMP population dominates under steady-state conditions and is long-lived with limited self-renewal potential [18]. During inflammatory conditions, Ly6C<sup>hi</sup> monocytes infiltrate the peritoneum and

differentiate into a F4/80<sup>int</sup>CD11b<sup>int</sup> and subsequently into a F4/80<sup>hi</sup>CD11b<sup>hi</sup> population thereby integrating into the pMP network [19].

### 3.2.1.3 Splenic MPs

Spleen is the largest lymphoid organ and a major site for initiation of T and B cell responses against blood-borne antigens. The various MP sub-populations are compartmentalized into specific splenic zones and perform their respective roles to maintain homeostasis [20]. The splenic microarchitecture consists of the white and red pulp separated by an interface termed marginal zone (MZ). The red pulp is involved in erythrophagocytosis as it is well equipped with a unique and efficient venous system [21]. The marginal zone is a region rich in B cells and several types of MPs. This zone contains two different MP sub-populations defined as marginal zone macrophages (MZMs) and marginal metallophilic macrophages (MMMs). MZMs are localized in the outer layer of marginal zone and express CD204, MARCO and SIGN-R1 as pattern recognition receptors. These cells play a major role in the capture of blood borne antigens [22]–[24]. MZMs also interact with MZ B cells which play an important role in attracting and retaining MZMs by chemokine secretion (CCL19 and CCL2) [25]. MMMs or MZMs located in the inner layer of marginal zone are identified by CD169 expression which mediates the uptake of sialic acid expressing bacteria [26]. On the other hand, CD169<sup>+</sup> MPs also trap viruses and immune complex and present them in an intact form to follicular B cells and induce GC B cell responses [27]. In addition, CD169<sup>+</sup> MPs are important to initiate T cell responses [28]. When antigens are specifically targeted to CD169<sup>+</sup> MPs, BATF-3 dependent cross-presentation to CD8<sup>+</sup> DCs is required for cross-priming of CD8<sup>+</sup> T cells [29].

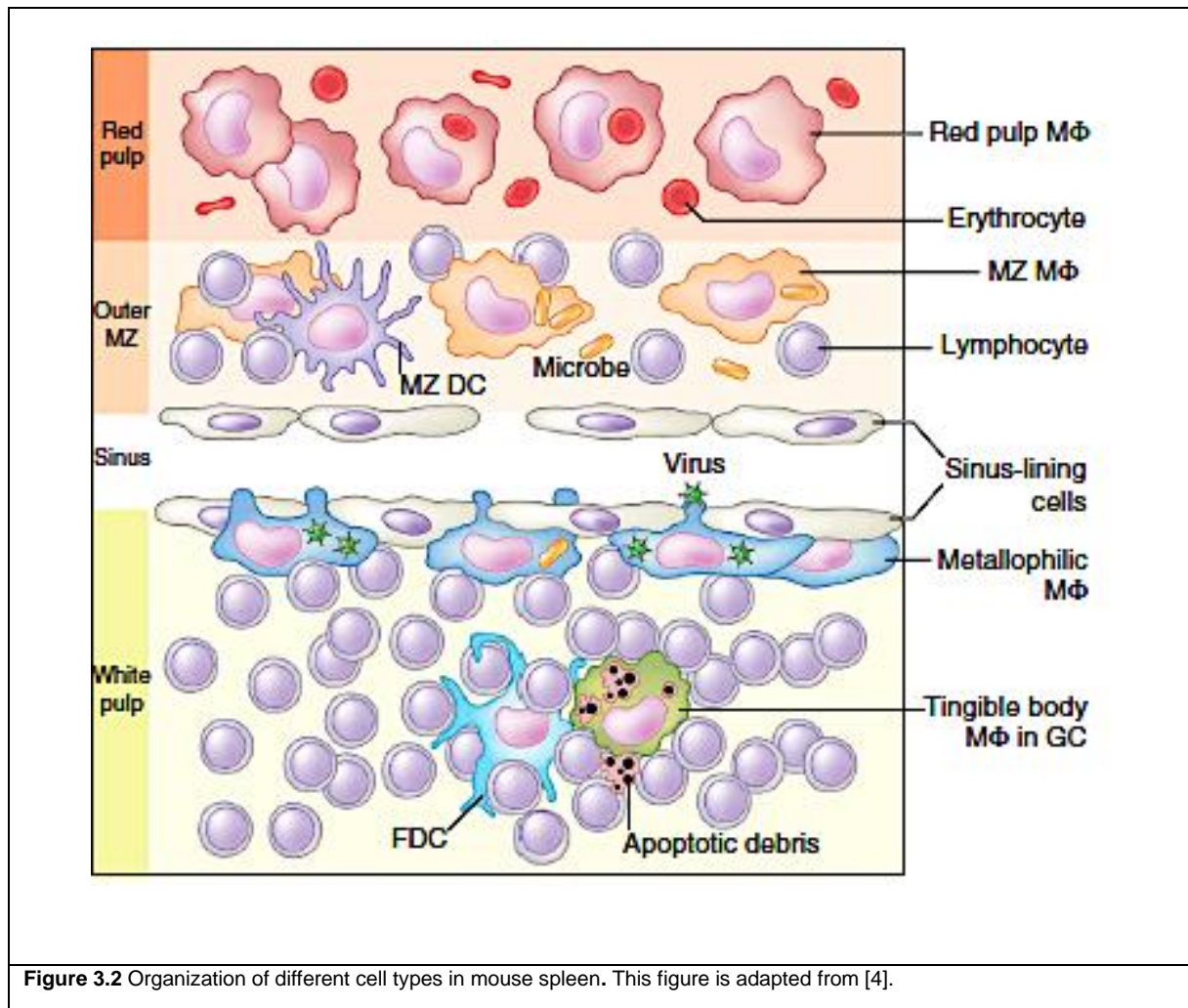


**Figure 3.2** Organization of different cell types in mouse spleen. This figure is adapted from [4].

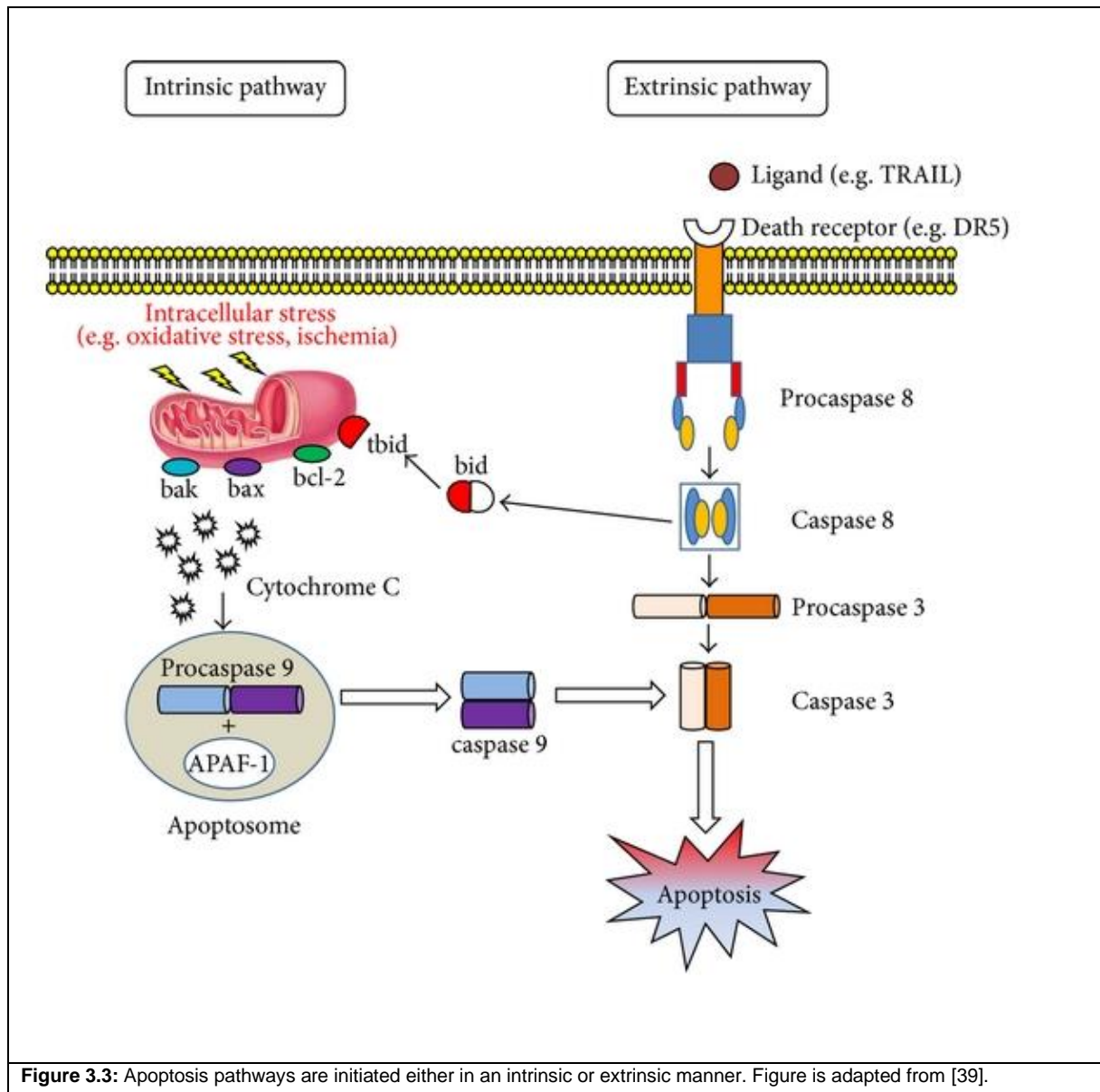
Follicular dendritic cells (FDCs) are located in the primary B cell follicles and germinal centers (GCs) of spleen. FDCs retain immune complexed antigen in B cell follicles to facilitate the GC-reaction [30]. The white pulp MPs are identified by CD68 and include tingible body macrophages (TBMs). These TBMs are located in germinal centers and play crucial role in phagocytosis of apoptotic GC B cells during a germinal center reaction. Milk-Fat Globule Epidermal growth factor 8 (MFGE8) and receptor tyrosine kinase MerTK play important roles in clearance of apoptotic cells by TBMs. FDCs provide TBMs with MFGE8 thereby favoring the disposal of apoptotic B cells [31], [32]. The major cell components in splenic microarchitecture is depicted in Figure 3.2. The functions of MFGE8 are discussed more in detail under section 3.4.2.1.

### **3.3 Cell death pathways**

During the developmental or inflammatory processes and from mechanical stress billions of cells die as an everyday routine in a programmed fashion and is hence termed programmed cell death [33]. Based on the biochemical and morphological characteristics, cell-death processes are classified into three major categories as follows: Apoptosis, necrosis and NETosis [34]. Some of the other forms of programmed cell death identified are ferroptosis, necroptosis and pyroptosis. Any one of the above process could cause the modification of self-antigens coupled with its inefficient clearance, acting as a driving force for tolerance break, further augmented by generation of an inflammatory milieu [35].

#### **3.3.1 Apoptosis**

Apoptosis is considered to be immunologically silent. It is required to maintain homeostasis by efficient replacement of many dying cells with healthy cells which occur during development, aging and immune responses for example. This mode of cell death is accompanied by a change in morphological features such as cell shrinkage, chromatin condensation, cytoskeletal remodeling, nuclear fragmentation and plasma membrane blebbing [36]. During apoptosis, the membrane integrity is maintained avoiding leakage of intracellular auto-antigens and hence triggering of immune responses by such antigens is prevented [37]. Effector caspases are proteolytically activated from apoptosis which could be initiated either extrinsically (death-receptor mediated) by caspase-8 or intrinsically (mitochondrial) by caspase-9 [38]. The high amount of protein cleavage during apoptosis is probably responsible for morphological and biochemical changes which lead to subsequent killing of cells.



Intrinsic pathways are activated by intrinsic lethal signals such as DNA damage, hypoxia and metabolic stress. These signals further activate BCL-2 family members (BH<sub>3</sub> - members) which are transcriptionally up-regulated and further stimulate the release of cytochrome C from mitochondria whereas anti-apoptotic members inhibit the release of cytochrome C. The released cytochrome C functions together with APAF-1 and activated caspase 9 which leads to the activation of downstream caspases (caspase 3 and caspase 7). The extrinsic death pathway is activated by Fas ligand (FasL), Tumor necrosis factor (TNF) and TNF-related apoptosis-inducing ligand (TRAIL). The binding of FasL to its Fas receptor leads to the formation of death inducing signal complex (DISC). The major components of DISC are Fas, adaptor proteins and procaspase-8. The activation pathways downstream of

caspase 8 is different in each cell type. Caspase 8 directly activates caspase 3 to kill dying thymocytes. On the other hand, caspase 8 cleaves Bid and then cleaved Bid (tBid) stimulates cytochrome C release and further leads to activation of caspase 9 - caspase 3 pathway in hepatocytes [40]–[42]. The sequential steps for intrinsic and extrinsic cell death pathways are shown in Figure 3.3.

### **3.3.2 Necrosis**

Necrosis was once considered to be an uncontrolled mode of cell death that happens due to severe membrane damage. This results in a rapid redistribution of cellular constituents followed by massive cell swelling and cell rupture liberating intracellular danger signals called danger associated molecular pattern (DAMPs). DAMPs act as endogenous danger signals to promote inflammation. Some of the most common DAMPs are high mobility group box-1 (HMGB1), calgranulin A, calgranulin B and serum amyloid A (SAA). However, from recent studies it is evident that necrosis is also a process that occurs in a tightly regulated manner completely unrelated to cell injury [43], [44]. This programmed form of necrosis is known necroptosis or inflammatory cell death. Necroptosis represents an alternative cell death mode that is a consequence of RIPK3 activation due to the presence of TNF, Fas, TRAIL, TLR stimulation and some caspase inhibitors [45]–[50]. Necroptosis seems to be highly dependent on RIPK3 and MLKL, however not all cell tissues express RIPK3. As a consequence, not all cells are able to follow a necrotic cell death pathway [49], [51].

### **3.3.3 NETosis**

Neutrophils are one of the major cellular components of first line defense mechanism against invading pathogens. These cells migrate to the site of inflammation, and their defense mechanisms include phagocytosis of pathogens, degranulation, cytokine production and neutrophil extracellular trap (NET) formation [52], [53]. NETs are made up of fibrous network assembly from nuclear and granular components which protrudes from activated neutrophils [54]. The special structure of NETs helps to trap the pathogens followed by killing with respiratory bursts followed by cell death [55]. NETosis is a process of active NET formation

and subsequent release of NETs. The release of mitochondrial ROS mediated by NADPH oxidase activation is an important requirement for an effective NETosis. Inflammasomes are activated by NETs and favor subsequent synthesis of IL-1 $\beta$  and IL-18 which in turn further induces NET formation [56]. IL-8 is known to adhere locally to activated endothelial cells and generates NETs positive for Proteinase-3 and Myeloperoxidase [57], [58]. NETs are a potent source of autoantigens and their impaired clearance has been reported in many cases of SLE [59].

### 3.4 Phagocytosis

Cell death pathways release many particles which are efficiently taken up by phagocytes to maintain homeostasis. The cellular uptake of particles (<0.5  $\mu\text{m}$ ) within a plasma membrane envelope is termed phagocytosis. The maintenance of homeostasis by the removal of dead cells depends much on the presence and nature of phagocytes [60]. The uptake mechanisms differ depending on the particle size and receptor-ligand interactions. Following the engulfment, early phagosome vacuoles fuse with primary lysosomes or with products from the endoplasmic reticulum (ER) and Golgi complex which results in formation of a secondary phagolysosome. The entire process is highly dynamic and tightly regulated which involves fusion and fission events with endocytic and secretory vesicles resulting in acidification. This aids in cargo digestion and is accompanied by membrane recycling [61]. The phagocytic particles can be generated from apoptosis, necrosis or microbial infection. It is a specific task for the phagocytes to distinguish between live or senescent cells, pathogens from commensals and infected from uninfected cells [62].

The phagocytes which take up apoptotic cells are classified as “professional”, “non-professional” and “specialized” phagocytes. Apoptotic cells generated *in vivo* are recognized by professional phagocytes and subsequently engulfed to prevent the release of intracellular material which could be immunogenic at some point. MPs and immature DCs are categorized as professional phagocytes which show higher capabilities with respect to apoptotic cell engulfment both *in vitro* and *in vivo* [63]. Tissue resident MPs such as pMPs, Kupffer cells in

the liver, microglia in the brain and alveolar MPs in the lungs are also classified as professional phagocytes [3]. Apart from this, circulating monocytes are recruited at the time of inflammation and tissue injury. These recruited phagocytes may either compete or co-operate with tissue resident MPs in taking up dead cells [64]. Epithelial cells and fibroblasts are categorized as “non-professional” phagocytes as they engulf dead cells with lower efficiencies during a MP deficient situation as in PU.1 deficient mouse embryos [65]. Specialized phagocytes are multi-functional phagocytes such as Sertoli cells in testes and retinal pigment epithelial cells (RPE) which exert their function only in specific tissue-contexts [66], [67].

### **3.4.1 Communication between phagocytes and apoptotic cells**

The major source of particles for phagocytosis can be either apoptotic and necrotic cells or microbial material [62]. The engulfment of apoptotic material by phagocytes depends on a number of early steps. For an effective dead cell clearance, positioning of professional phagocytes close to apoptotic cells is important. This is achieved by maintaining phagocyte migration and apoptotic cell motility [68]. Phagocytes face the challenge to find dying cells among healthy cells. This is facilitated with the release of certain molecules from dying cells termed “*find me signals*” which recruit or activate phagocytes. The attracted phagocytes through their engulfment receptors sense “*eat me signals*” produced by dying cells [69].

Such “*find me signals*” are Sphingosine-1-Phosphate (S1P) and CX<sub>3</sub>CL<sub>1</sub>/fractalkine. SIP binds to its SIP-1R receptor on MPs and promotes chemotaxis of MPs. SIP1 is generated by Sphingosine kinase and secreted by apoptotic cells in a caspase dependent manner. CX<sub>3</sub>CR<sub>1</sub> released from apoptotic cells activates MPs by its subsequent binding to its receptor CX<sub>3</sub>CR [70], [71]. The role of ATP and UTP produced by apoptotic cells to serve as “*find me signals*” is yet to be clearly established [72].

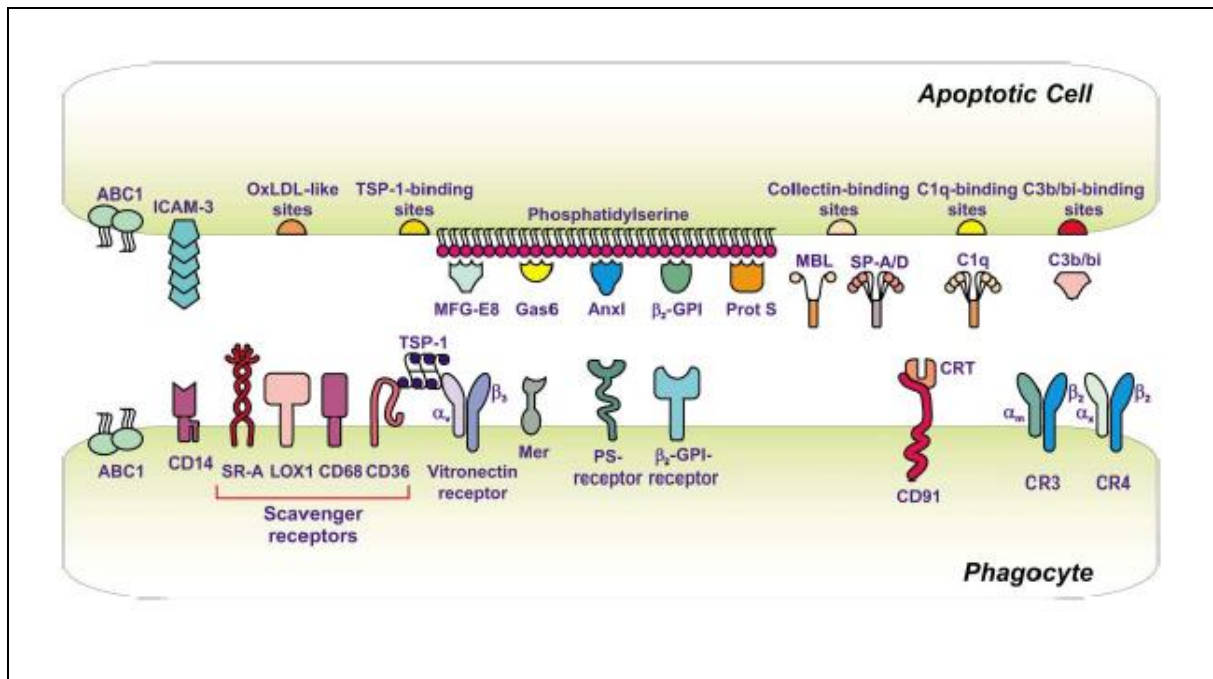


**Figure 3.4:** Apoptotic cell recognition by phagocytes. A number of membrane receptors on the phagocytes are involved in sensing the molecules produced by apoptotic cells. Figure is adapted from [73].

Phosphatidylserine (PS) is a plasma membrane component which remains exclusively on the inner side of the lipid bilayer in healthy cells [74]. PS is exposed on the outer side of the lipid bilayer when a cell undergoes apoptosis [75]. PS is mostly externalized in a caspase 3-mediated cleavage of scramblase Xkr8 [76]. The inhibition of apoptotic cell engulfment has been observed when PS is masked in both *in vitro* and *in vivo* studies [77], [78]. Thus, PS is one of the best described “*eat me signal*”. In addition to PS some of the moieties expressed on apoptotic cells include calreticulin, complement C1q, annexin I and a modified form of intracellular adhesion molecule-3 (ICAM-3) [73]. On the other hand, CD47 has been proposed as “*don’t eat me signal*” following the observation that CD47<sup>-</sup> red blood cells are cleared more rapidly by splenic MPs compared to CD47<sup>+</sup> apoptotic cells [79]. The wide range of membrane receptors involved in sensing apoptotic cells are shown in Figure 3.4. Following the successful recognition of an apoptotic cell by phagocytes, an extensive cytoskeletal rearrangement occurs to internalize corpses thereby processing the ingested cargo. The uptake of apoptotic cells is followed by secretion of “*tolerate me signal*” such as Transforming Growth Factor  $\beta$  (TGF- $\beta$ ) and Interleukin-10 (IL-10) which further inhibits the recruitment of other MPs to the site of ongoing cell death and stops the secretion of pro-inflammatory cytokines such as TNF- $\alpha$ , IL-1

and IL-12 [80]. This elicits anti-inflammatory responses which dampen the local immune responses at the sites where apoptotic cell death occurs [63].

### **3.4.2 Scavenging receptors**

Phagocytosis can occur either via opsonic or non-opsonic dependent mechanisms. Opsonic dependent phagocytosis is dependent on the molecules called opsonin that bind to the cell surface thereby enhancing phagocytosis by other phagocytes. Opsonic phagocytosis is dependent either on the binding of IgG antibodies or complement proteins to be taken up either via Fc or complement receptors respectively. Some of the notable opsonic receptors are FcR (activating or inhibitory) and complement receptor CR3. Fc receptors (FcR) bind conserved domains of IgG antibodies. CR3 is responsible for recognizing iC3b deposited by classical IgM or IgG or alternate lectin pathways of complement activation [81]. Other cell derived opsonin includes fibronectin, mannose-binding lectin, MFGE8 and other phagocyte receptor ligands [82]. Non-opsonic phagocytosis is dependent mostly on pattern recognition receptors (PRRs). Non-opsonic receptors include CD169 and CD33 recognizing sialylated residues [83]. Dectin-1 recognizes fungal beta-glucan [60], [84] and other related C-type lectins such as Dectin-2, Mincle, Mincle and DNGR-1 recognizes many fungal related structures [85], [86]. Though TLRs are considered as good sensors, they always function together with other non-opsonic receptors to aid efficient uptake and signaling [62].

#### **3.4.2.1 Milk-fat globule epidermal growth factor 8 (MFGE8)**

MFGE8, also known as lactadherin, has been found associated with milk fat globules in mammary glands which is a secreted protein present on many phagocytes involved in apoptotic cell engulfment [87]. MFGE8 is predominantly expressed mostly by MPs, immature DCs, mammary epithelial and retinal pigment epithelial cells [31], [88], [89]. MFGE8 acts as a link between MPs and their target apoptotic cells thereby establishing its role as opsonin [82].

Murine MFGE8 comprises two repetitive mouse epidermal growth factor (EGF) domains on the N-terminus carrying a highly conservative RGD (Arg, Gly, Asp) motif in the B-loop of EGF domain. It carries two factors-VII-homologous domains (C1 and C2) in its

C-terminal region together with Proline-Threonine (PT)-rich domain. MFGE8 is bound by  $\alpha_v\beta_3$  or  $\alpha_v\beta_5$  integrins on phagocytes through its RGD motif [90]. It binds tightly to PS through its C2 domain thereby further promotes the apoptotic cell engulfment [91].

MFGE8<sup>-/-</sup> mice develop an age-dependent SLE type of autoimmune diseases. This is also characterized with increased levels of anti-double stranded DNA (dsDNA), anti-nuclear antibodies (ANA), immune complex deposits in glomeruli of kidneys and proteinuria. Tingible body macrophages (TBMs) from MFGE8<sup>-/-</sup> mice show an impaired removal of apoptotic cells from germinal centers. Without MFGE8, many apoptotic cells are left unengulfed by TBMs in the germinal center. These unengulfed cells undergo secondary necrosis and release cellular components thereby providing a trigger to activate immune system resulting in the generation of autoantibodies. The onset of disease in MFGE8<sup>-/-</sup> mice aggravate upon immunization as this induces germinal centers and thereby increases the load of apoptotic cells [88], [92].

#### **3.4.2.2 Additional PS receptors**

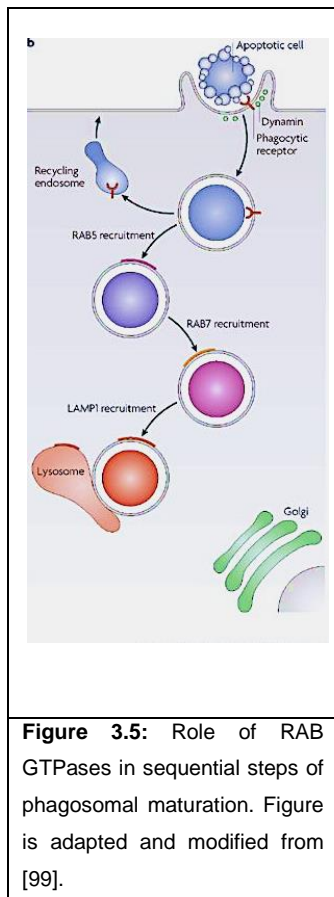
Furthermore, there are other receptors such as TIM-1, TIM-4, BAI1 and MerTK which also have the ability to recognize PS on apoptotic cells. These receptors play their role in the absence of MFGE8 in cells such as pMPs [93]–[95]. First, TIM-1 and TIM-4 are composed of an immunoglobulin V (IgV) domain, a mucin-like domain, a transmembrane domain, a cytoplasmic region and a signal sequence. The bridging between TIM-1/TIM-4 and PS occurs via their respective IgV domain [93]. TIM-4 acts only as a tethering receptor but does not activate the downstream signaling pathways [96]. TIM-4 is highly expressed on tissue resident MPs, dendritic cells and pMPs [97]. TIM-3 has also been shown to bind PS and facilitate apoptotic cell engulfment however, less efficiently compared to TIM-1/TIM-4 [98]. Secondly, brain specific angiogenesis inhibitor (BAI1), is capable for PS engagement and initiates intracellular signaling to mediate apoptotic cell engulfment. Once BAI1 recognizes PS, BAI1 interacts with a cytoplasmic module consisting of ELMO1 and DOCK180 which further induces actin cytoskeletal rearrangements facilitating the apoptotic cell uptake [94]. Lastly, Mer tyrosine kinase (MerTK) belongs to Tumor associated macrophages (TAM) receptor family. TAM receptors engage PS on apoptotic cells indirectly via other soluble bridging molecules such as

Protein-S and GAS-6 [95].

### **3.4.3 Apoptotic cargo processing**

Phagocytes recognize apoptotic material via appropriate cell-surface receptors followed by engulfment, by surrounding the dying cells with pseudopod-like structures. These pseudopods then fuse leading to the formation of an apoptotic cell containing membrane vacuole termed phagosome [99]. The nature of phagosomes is similar to an extracellular environment which has no degradation capacity. This nascent phagosome further undergoes phagosomal maturation leading to degradation of the ingested phagosomal contents. Phagosomal maturation involves a sequential fusion with early endosomes, late endosomes and eventually lysosomes [100]. During this process, nascent phagosomes acquire the properties from donor organelles such as specific markers as well as gradual acidification of phagosomal lumen [99]. Following this fusion, an intracellular hybrid compartment called phagolysosomes is formed which contains various digestive enzymes such as hydrolases, proteases, lipases, and glycosides. These digestive enzymes exhibit their optimal activities in an acidic environment of  $\text{pH} \leq 5.0$  to effectively degrade the luminal contents [101].

A continuous alteration of phagosome-associated molecules is required for the interaction with distinct endocytic organelles and thus leads to a successful phagosomal maturation [102]. The small Rab GTPases and lipid second messenger phosphatidylinositol 3-phosphate are known for their critical role in phagosomal maturation. Rab GTPases regulate the membrane trafficking events by delivering apoptotic cargo to the appropriate subcellular destination [103]. Rab proteins associate themselves with the phagosome at different maturation states and facilitate the docking and fusion of intracellular organelles to phagosomes (Figure 3.5). Among the identified Rab GTPases; RAB-5, RAB-2, RAB-14 and RAB-7 are recruited sequentially to phagosomes undergoing the maturation process in



*C. elegans* [104]–[107].

RAB-5 through its conserved tethering activity, aids the anchoring of early endosomes to phagosomes containing apoptotic cells irrespective of phagocytic cargo identity [108]. RAB-2 and RAB-7 play an important role in the recruitment and fusion of lysosomes to phagosomes. In addition, RAB-2 also plays an important role in the acidification of phagosomal lumen [104], [107]. The acidification of lysosomes is also aided by the activity of vacuolar type proton transporting ATPase (V-ATPase) which gains energy from ATP hydrolysis to pump protons from the cytosolic space to the phagosomal lumen [109]. Thus, an acidic environment acts as a favorable condition for an effective degradation of phagocytic content.

### 3.4.4 Implications of impaired phagocytosis

Professional and non-professional phagocytes engulf apoptotic cells in an immunologically silent manner. This is essential in a number of physiological processes such as development and normal tissue homeostasis and in the resolution of inflammation [110]. When clearance of apoptotic cells is impaired, release of autoantigens such as double-stranded DNA (dsDNA) and the Sm antigens of the U1 small nuclear ribonucleoprotein complex can be the consequence. This can then result in the development of autoantibodies and autoimmunity [80], [111]. The inefficient clearance of apoptotic remnants could be an intrinsic defect and responsible for initiation of systemic autoimmunity in diseases such as Systemic Lupus Erythematosus (SLE) which is discussed in detail below.

## 3.5 SLE - an autoimmune disorder

SLE is a multi-system autoimmune disorder with defective clearance of apoptotic cells

and which is assumed to be involved in the development of autoimmunity. SLE is characterized by impaired immune tolerance resulting in production of pathogenic auto-antibodies and immune complexes [112], [113]. These immune complexes are deposited in various organs which in turn cause inflammation and tissue damage. The most common disease manifestations include fever, facial rashes (“butterfly pattern”), arthritis, serositis, glomerulonephritis, thrombocytopenia, proteinuria, photosensitivity and, psychosis [114].

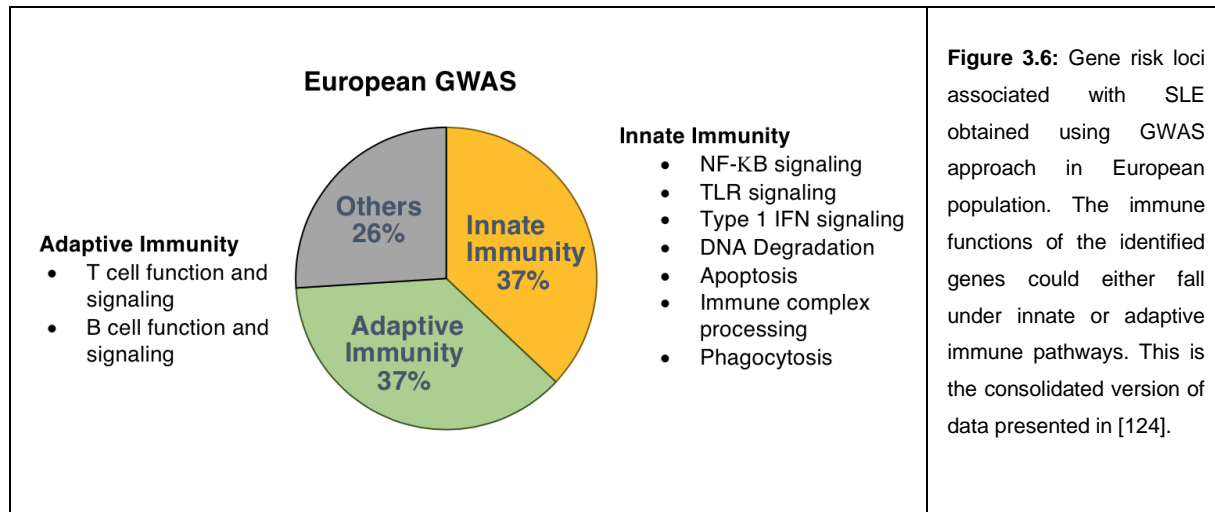
### **3.5.1 Epidemiology**

There is great variation in the extent of SLE pathogenesis across countries and different ethnic groups. Early disease phases may differ across ethnic groups which depends on their genetic makeup whereas at later stages it depends on their socio-economic status and access to medical treatment [115]. Populations of non-European ancestry are more affected as Europeans. Asian Americans, African Americans and Hispanic Americans are more susceptible and exhibit more complex manifestations than Caucasians [116]–[118]. Aboriginal Australians are more susceptible than non-Aboriginal Australians [119], [120]. About 65% of patients are in the age group of 16-55 years and 20% are diagnosed before the age of 16. The onset of Juvenile Systemic Lupus Erythematosus (JSLE) is mostly in the range of 14-20 years rarely before the age of 5 years [121], [122]. SLE is more prevalent in women compared to men which is attributed to immune-activating effects of estrogen via signaling by estrogen receptor  $\alpha$ . However, a clear correlation between female hormone concentrations and disease activity has not been established in human patients due to the complexity of other contributing genetic and environmental factors [123].

### **3.5.2 Etiological factors for SLE**

SLE is a very complex disease and it is impossible to narrow it down to a single factor responsible for triggering the disease. Genome-wide association studies (GWAS) are based on screening millions of genetic variants distributed throughout the whole-genome with respect

to a phenotype. There are about 60 risk loci identified from various GWAS studies many of which are associated with important signaling pathways (Fig. 3.6).



Epigenetic modifications such as reduced DNA methylation, histone hypoacetylation and overexpression of certain miRNAs act as major contributors for SLE susceptibility. These epigenetic modifications could either be due to environmental triggers or genetic inheritance [125], [126]. Smoking has been shown to have a considerable effect on the disease especially on causing active SLE rashes and photosensitivity [127]. Epidemiological data have suggested a relationship between EBV infection and SLE incidence as various SLE susceptibility genes play important roles in EBV replication and immune evasion [128], [129].

### 3.5.3 Pathogenesis of SLE

The efficient removal of dead cells is a very important process to prevent the accumulation of cellular debris which might act as a potential source of auto-antigens. The accumulation of cellular debris triggers inflammation followed by leakage of cytoplasmic and nuclear auto-antigens such as ribonucleoproteins, DNA, or histones. Phagocytic activity of TBMs from SLE patients show a reduced ability to engulf apoptotic material compared to healthy donors [130]. The inadequate removal of cellular debris by TBMs in the germinal centers (GCs) of secondary lymphoid organs results in release of modified auto-antigens. FDCs may present these modified auto-antigens to auto-reactive B cells which results in loss

of self-tolerance and auto-antibody production. When autoantibodies are bound to uncleared cellular debris in tissues or blood it results in immune complex formation. These immune complexes deposit in different tissues such as kidneys, skin, or joints which further leads to irreversible organ damage [80], [131]. In addition, studies show that *in vitro* differentiated MPs from SLE patients had reduced and delayed engulfment capacity for autologous apoptotic material [132]. Indeed, MPs differentiated from CD34<sup>+</sup> HSC and monocytes show reduced differentiation and adhesion compared with those derived from healthy individuals [133], [134]. Also, peripheral lymphocytes from SLE patients show an increased rate of apoptosis [135]. These findings also support the notion that impaired phagocyte function is a primary defect in some SLE patients. In addition, anti-ribonucleoprotein autoantibodies detectable in sera of SLE patients switch neutrophil death from apoptosis to NETosis [136]. NETosis releases harmful intracellular components such as heat shock proteins, HMGB1 or modified histones thereby resulting in DC activation [137]. The prevalence of increase in antibodies against NET proteins such as defensins or HMGB1 has been previously reported in blood samples from lupus patients [138], [139]. These autoantibodies also recognize some components of NETs (Neutrophil elastase, Myeloperoxidase, LL-37). The activation of pDCs by these immune complexes further result in elevated expression of IFN- $\alpha$  regulated genes [140]. This results in upregulation of CD80 and CD86 which serves as signal for survival and expansion of autoreactive CD4<sup>+</sup> autoreactive T cells. Elevated levels of IFN- $\alpha$  also lead to upregulation of TLR7 which mounts its enhanced response against immune complexes fueling an inflammatory loop [141]. During disease progression, tightly regulated apoptosis and necrosis turns into a potential source of autoantigens and immunostimulatory signals which is favorable to maintain a sustained chronic autoimmune response [142].

### **3.5.4 Complement deficiencies and SLE**

The importance of complement pathways in the immunopathogenesis of lupus and other autoimmune disorders was shown many years ago [143], [144]. The complement system consists of proteins which can be activated either directly by pathogens or by pathogen bound antibodies. The complement proteins of each pathway interact with each other and results in

complement activation. As a consequence, pathogens are killed either directly or by facilitating phagocytosis and inflammatory responses. There are three pathways of complement activation as follows: classical, lectin and alternative cascades which serve to clear pathogens. The classical pathway is activated when the C1q complex (C1q, C1r, C1s) interacts with immune complexes or when C1q binds to the pathogen surface. The lectin pathway is initiated when mannose binding ligand (MBL) or ficolins bind to carbohydrate moieties on pathogen surfaces [145], [146]. The alternative pathway is activated during spontaneous hydrolysis of C3 or via properdin [147]. Complement proteins exert their effects against infection by either promoting phagocytosis of complement coated particles or by promoting inflammation through complement factor cleavage products. They also exert their effect directly on pathogens causing lysis by forming the membrane attack complex [148], [149].

C1q is a soluble macromolecule which has six subunits with each subunit composed of three unique polypeptide chains (A, B, C). Members of the classical and lectin complement pathway (C1q, adiponectin, MBL, ficolins) share similar structural features such as: a carboxyl globular head region, and an extended N-terminal collagen like sequence [150]. The globular C1q head binds directly to PS-exposed on apoptotic cells and promotes phagocytosis [151], [152]. In addition, C1q also binds to immune complexes, bacteria, virus, DNA, myelin and  $\beta$ -amyloid [145], [153], [154]. C1q is expressed by cells that are derived from monocyte/MP lineage, microglia and DCs [155], [156]. It has also been shown that C1q binds many immune cells such as B cells, monocytes, MPs, DCs, neutrophils [157]–[161]. cC1qR, LRP-1/CD91, CR1/CD35,  $\alpha$ 2 $\beta$ 1, CD93/C1qRp and gC1qR are the identified C1q receptors to date [161]–[166] (Fig. 3.7). The various C1q dependent apoptotic cells engulfment pathways are shown in Figure 3.7.

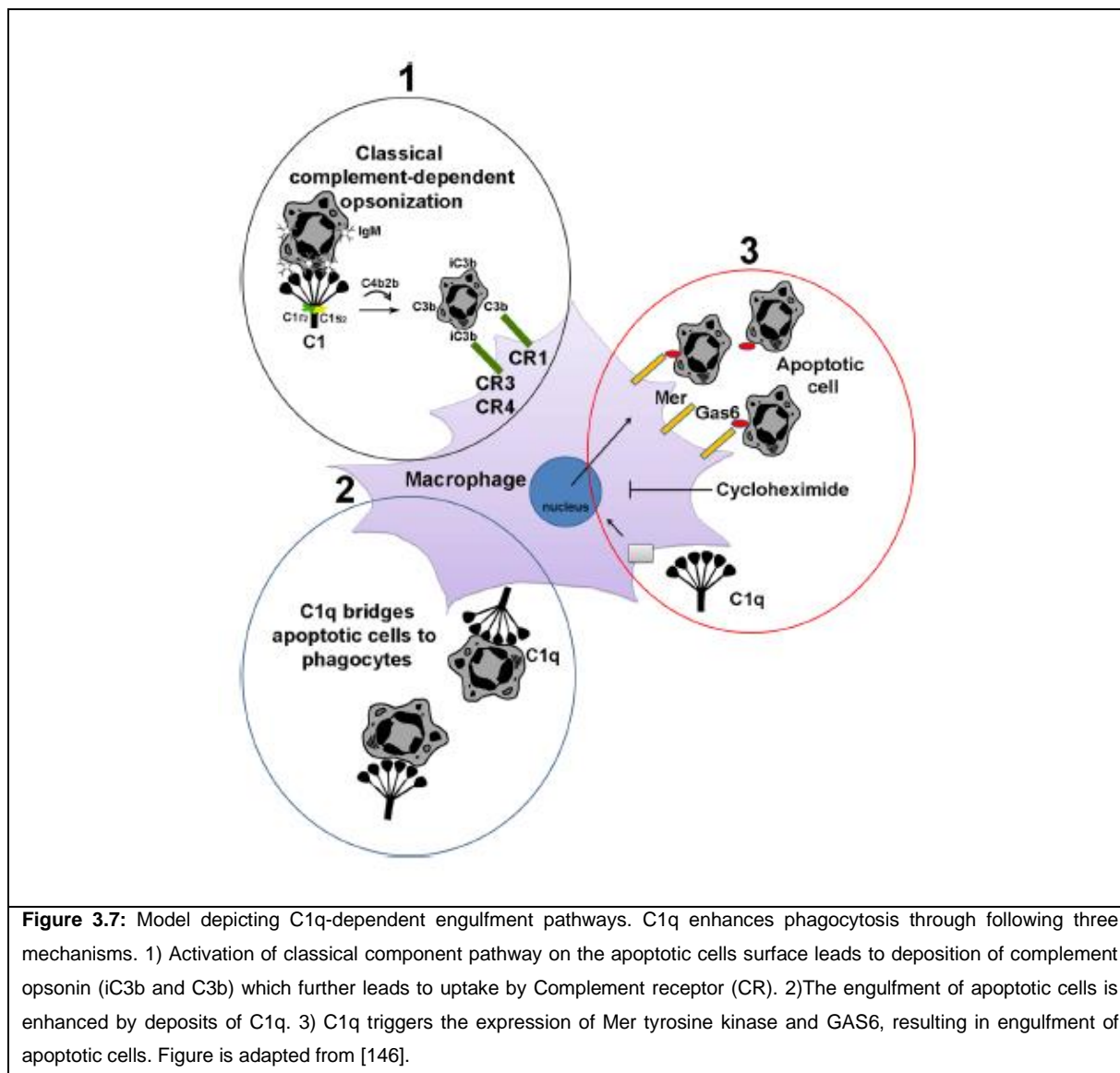


**Figure 3.7:** Model depicting C1q-dependent engulfment pathways. C1q enhances phagocytosis through following three mechanisms. 1) Activation of classical component pathway on the apoptotic cells surface leads to deposition of complement opsonin (iC3b and C3b) which further leads to uptake by Complement receptor (CR). 2)The engulfment of apoptotic cells is enhanced by deposits of C1q. 3) C1q triggers the expression of Mer tyrosine kinase and GAS6, resulting in engulfment of apoptotic cells. Figure is adapted from [146].

The disease incidence varies between classical complement deficiencies. The homozygous C1q deficiency is the highest single gene risk factor known, with more than 90% of the affected individuals developing SLE. C1q is considered as a strong opsonin for phagocytosis of apoptotic cells and late necrotic cells. The importance of C1q in effective uptake of degraded chromatin by monocyte-derived phagocytes was also shown [167]. Although homozygous C1q deficiencies are rare, many SLE patients without C1q gene mutation also have been reported to have reduced serum C1q activity due to increased consumption, reduced production or neutralization by anti-C1q autoantibodies. About 53-92% of SLE patients are reported to have low C1q levels in the serum [168]. It has been also shown that C1qa<sup>-/-</sup> mice exhibit increased levels of antinuclear antibodies, develop glomerulonephritis

and accumulate apoptotic bodies in the kidneys. However, the genetic background of the mice plays an important role in SLE susceptibility [169], [170]. C4 and C2 deficiencies show a lower disease incidence [171]. Though the incidence of C4 and C2 is low, it is unclear why their deficiency results in a SLE phenotype such as glomerulonephritis and recurrent bacterial infection [172], [173]. Only a very few cases of SLE patients were reported to have a C3 deficiency. In line with this no disease manifestations are seen in C3 deficient mice on a mixed 129xC57BL/6 background. This further shows that C3 is not critical for SLE development [174]. Deficiency of the late complement components C4-C9 is only rarely associated with SLE cases but these patients are more prone to develop recurrent bacterial infections [175].

There are number of murine models used to study the cellular and genetic requirements for SLE induction. The spontaneous lupus models include the F1 hybrid (NZB/WF1) generated between the New Zealand Black (NZB) and New Zealand White (NZW) strains. Other spontaneous lupus model is MRL/lpr developed from several inbred strains. From initial MRL sub-strain characterization, MRL/lpr mice displayed a high mortality rate and unlike the NZB/WF1 mice both males and females are affected. The induced lupus models include pristane-induced model and chronic graft-versus-host-disease models [176]. These murine models also exhibit autoimmune phenotype whereby free nucleosomes including DNA and histones were detected similar to active SLE patients [177], [178]. As discussed earlier, NETs are a rich source of DNA and are more prone to DNASE1 degradation. Some SLE patients show reduced DNASE1 function due to the presence of anti-DNASE1 antibodies or genetic variations. A proper co-operation between DNASE1 and C1q is necessary for effective removal of necrosis derived remnants [171], [179]. So, deficiency of C1q might prevent the access of DNASE1 to NETs resulting in uncleared apoptotic remnants which increases the exposure of modified autoantigens to the immune system [180]. pDCs are also stimulated by NET-derived immune complexes to release IFN- $\alpha$  in a Fc $\gamma$ RII and TLR-9 dependent pathway [140].

### **3.5.5 Current therapeutic strategies**

SLE is considered as a heterogenous group of diseases in which environmental exposures or genetic deficiencies act as a trigger to activate both innate and adaptive immune

responses which results in loss of tolerance to self-antigens. There is a long pre-clinical phase characterized by accumulation of auto-antibody specificities, followed by inflammation and tissue injury. This is followed by onset of clinical symptoms, persistent immune amplification and finally irreversible tissue damage. New therapies for SLE are aimed at any of the following pathways: Innate immunity, T cells, B cells or tissue injury and inflammation. Many animal studies provide valuable information into the therapeutic potential of many experimental drugs for SLE. Nevertheless, additional considerations are required when predicting the possible outcomes of treatment in SLE patients. There is a huge difficulty in predicting the outcomes due to the complex pathogenesis, heterogeneous clinical manifestation of SLE and inadequacy in clinical trial design [123]. Patients with refractory SLE are treated with a B cell depleting chimeric anti-CD20 antibody which temporarily depletes B cells as well as short lived plasma cells [181]. Belimumab is a monoclonal antibody which specifically targets the B cell stimulator protein (BLys) thereby preventing the binding of BLys to receptors on B lymphocytes which is important for its survival and has been currently approved for SLE treatment [182]. Another approach uses Tocilizumab, a monoclonal antibody which targets IL-6 receptor and effectively blocks IL-6 signaling which is important in maturation of B cells into plasma cells [183].

### 3.6 Study motivation

Despite substantial evidence supporting the crucial role of C1q in apoptotic cell clearance the exact mechanism by which C1q-deficiency causes lupus remains to be explored. It is known that C1q deficiency results in SLE as described earlier, however, the mechanisms in SLE development are still ambiguous. This ambiguity in establishing a relationship between C1q deficiency and lupus development is addressed by two hypotheses. According to waste disposal hypothesis, C1q plays an important role in the prevention of autoimmunity by disposal of dying cells and failure of this mechanism would lead to autoantigen driven autoimmunity [148], [149]. On the other hand, C1q has been shown to play a role in the induction of tolerance to autoantigens [184]. So, during a C1q-deficiency the normal tolerance mechanism is disturbed thereby favoring SLE induction.

The main aim of the project was to identify the mechanisms how C1q deficiency contributes to lupus. Therefore, C1q<sup>-/-</sup> mice were used as a model to study the disease mechanisms and to identify susceptibility factors for SLE development. To this end an unbiased proteomic screen was performed to identify proteins that were important to disease pathogenesis in C1q-KO mouse model. As a result, the identified proteins which might contribute towards disease development were investigated further.

## 4 MATERIALS AND METHODS

### 4.1 Materials

#### 4.1.1 Devices

Devices	Company
Analytic scale	Adventurer, Ohaus Corp., Pine Brooks, NJ, USA
Chemical scale	Kern, Albstadt, Germany
Automatic pipettors	Integra Biosciences, Baar, Switzerland
Pipettes	Gilson, Middleton, WI, USA
Power supply	Amersham Pharmacia, Piscataway, NJ, USA
Water bath	Grant Instruments Ltd., Barrington Cambridge, UK
Vacuum pump	KNF Neuberger, Munzingen, Germany
Vortex-Genie2	Scientific Industries, Bohemia, NY, USA
Magnetic stirrer	Ika Labortechnik, Staufen, Germany
Tissue homogenizer	FastPrep-24, MP Biomedicals, Santa Ana, CA, USA
Centrifuge	Rotixa RP, Hettich, Tuttlingen, Germany
Bench centrifuge	Centrifuge 5415 D, Eppendorf, Germany
pH-meter	Inolab, Weilheim, Germany
Incubator	Hera cell, Heraeus Kendro Laboratory Products, Hanau, Germany
Laminar airflow cabinet	Heraeus, Hanau, Germany
PCR-machine	Biometra, Goettingen, Germany
Real-time PCR machines	CFX96 Real Time System, BIO-RAD, Hercules, CA, USA
ELISA-reader	µmax kinetic microplate reader, Molecular Devices, Biberach, Germany
Cell counter	CASY cell counter and analyzer, OMNI life science, Bremen, Germany
Flow cytometer	FACSCalibur, FACSCantoll, FACSAria Fusion, AMNIS ImageStream BD, Heidelberg, Germany
Gel Electrophoresis	BIO-RAD, Hercules, CA, USA
Western blot developer	Optimax

#### 4.1.2 Consumables

Items	Supplier
BD Microtainer	BD, Franklin Lakes, NJ, USA
Disposable cell strainer (100 $\mu$ m nylon)	Falcon a Corning Brand, One Riverfront Plaza, Corning, USA
Disposable injection needle (26 G x 1/2"), (23 G X 1/2"), (21 G x 1/2")	Terumo Medical Corporation, Tokyo, Japan
Disposable syringe (1+5+20 ml) Reaction	Braun, Melsungen, Germany
Disposable MACS filters	Milltenyi Biotech
Disposable MACS columns	Milltenyi Biotech
Disposable glass Pasteur pipettes	VWR International bvba, Leuven, Belgium
Serological pipette, sterile (10 ml)	Greiner, Frickenhausen, Deutschland
TipOne filter tips (10 $\mu$ l, 200 $\mu$ l, 1000 $\mu$ l)	STARLAB GmbH, Hamburg, Germany
Laboratory gloves Latex Gentle Skin Grip	Meditrade GmbH, Kiefersfelden, Germany
PCR strips tubes (0.2 mL)	VWR International, West, Belgium
qPCR strips tubes (0.2 mL)	BIO-RAD
Reaction container 1.5 ml, 2 ml, 5 ml	Eppendorf, Hamburg, Germany
Reaction container 5 ml (FACS)	BD, Franklin Lakes, NJ, USA
Petri dish	Greiner Bio-One GmbH, Germany
Tissue culture plates (96 wells-U, 6 and 12 well sterile)	VWR International bvba, Leuven, Belgium
Tissue culture flasks (T25, T75 and T175)	Nunc
8-well chamber glass slides	Nunc, Lab-Tek
Lysing matrix tubes (matrix D)	MP Biomedicals Germany GmbH, Eschwege, Germany

#### 4.1.3 Chemicals and buffers

Unless stated otherwise, chemicals were purchased from Merck (Darmstadt, Germany), Roth (Karlsruhe, Germany) or Sigma-Aldrich (St. Louis, MO, USA). All buffers and solutions were prepared using double distilled water.

Buffers and Solutions	Composition
PBS	150 mM NaCl

	<p>10 mM Na<sub>2</sub>HPO<sub>4</sub>  2 mM KH<sub>2</sub>PO<sub>4</sub>  pH 7.4 adjusted with 5 N NaOH</p>
PBS (cell culture)	Dulbecco's PBS without Ca <sub>2</sub> <sup>+</sup> /Mg <sub>2</sub> <sup>+</sup> (PAA)
FACS Buffer	<p>PBS  2% FCS</p>
MACS Buffer	<p>PBS  0.5 % FCS, 2 mM EDTA</p>
ACK Lysis Buffer	<p>8.29 g NH<sub>4</sub>Cl  1 g KHCO<sub>3</sub>  37.2 mg Na<sub>2</sub>EDTA  H<sub>2</sub>O add 1 lt  pH 7.2-7.4 adjusted with HCl  sterilized by 0.2 µm filtration</p>
10x Gitocher Buffer	<p>670 mM Tris, pH 8.8  166 mM ammonium sulfate  65 mM MgCl<sub>2</sub>  0.1 % Gelatin</p>
5x Cresol Red Buffer	<p>250 mM KCL  50 mM Tris/HCL pH 8.3  43 % glycerol  2 mM Cresol-red  7.5 mM MgCl<sub>2</sub></p>
50x TAE Buffer	<p>242 g Tris  57.1 ml 100 % acetic acid  100 ml 0.5 M EDTA (pH 8.0), H<sub>2</sub>O add 1 lt</p>
SDS Running Buffer	<p>192 mM Glycin  25 mM Tris  0.1 % SDS</p>
Separating Gel 12%	<p>H<sub>2</sub>O (6.6 ml)  30 % acrylamide mix (8 ml)  1.5 M Tris/HCL, pH 8.8 (5 ml)  10 % SDS (200 µl)  10 % ammonia persulphate (200 µl)  TEMED (20 µl)</p>
Stacking Gel 5%	<p>H<sub>2</sub>O (2.1 ml)  30 % acrylamide mix (500 µl)</p>

	1 M Tris/HCL, pH 6.8 (380 $\mu$ l) 10 % SDS (30 $\mu$ l) 10 % ammonia persulphate (30 $\mu$ l) TEMED (3 $\mu$ l)
Cell culture medium	DMEM Medium (GIBCO) 10 % FCS 100 U/ml Penicillin
RIPA Lysis buffer	1M NaCl 1% Nonident P-40 0.5% Sodium deoxycholate 0.1% SDS 50 mM Tris, pH 7.4
Transfer buffer	192 mM Glycine 25 mM Tris 20 % Methanol 0.002 % SDS
Stripping buffer	62.5 mM Tris pH 6.7 adjusted with HCL 100 mM $\beta$ -mercaptoethanol 2 % SDS
10x TBS	0.2 M Tris base 1.5 M NaCl pH 7.4 adjusted with HCl
Washing buffer	1x TBS, 0.1% Tween-20

#### 4.1.3.1 Immunofluorescence

Buffers	Composition
Fixation buffer	4% PFA in 1x PBS
Blocking buffer	4% BSA in 1x PBS
Permeabilizing Buffers (Based on antibody compatibility)	100% Methanol 0.1% TRITON-X in 1x PBS 0.05% Saponin in blocking buffer 0.1% Saponin in blocking buffer

#### 4.1.3.2 Proteomics buffers

Buffers	Composition
Lysis buffer 1	100 mM TRIS, pH 7.6 6 M urea 2 M thiourea 30 mM DTT Phosphatase inhibitor (Roche)
Lysis buffer 2	100 mM TRIS, pH 7.6 20 mM Iodoacetamide 2 mM CaCl <sub>2</sub> 25 mM NaCl

#### 4.1.4 FACS antibodies

Epitope	Conjugate	Clone	Supplier
CD3e	PE	145-2C11	e-Bioscience
CD19	FITC	1D3	BD Pharmingen
CD45R	FITC	30-F11	Biolegend
CD16/32	unconjugated	2.4G2	BD Bioscience
CD11b	APC-Cy7	M1/70	e-Bioscience
F4/80	APC	BM8	e-Bioscience
MFGE8	Biotin	-	Novus Biologicals
Streptavidin	APC	-	BD Bioscience

#### 4.1.5 Western blot antibodies

Specificity	Host	Dilution	Supplier
DNASE2A	Rabbit	1:1000	LS Biosciences
$\beta$ -ACTIN	Rabbit	1:1000	CST
$\beta$ -TUBULIN	Mouse	1:1000	CST
IRF3	Rabbit	1:1000	Abcam
pIRF3	Rabbit	1:1500	CST
TBK1	Rabbit	1:1000	Abcam
pTBK1	Rabbit	1:1000	CST
STING	Rabbit	1:1000	Abcam
Anti-rabbit HRP	Donkey	1:2500	Jackson Lab
Anti-rat HRP	Donkey	1:2500	Cell Signaling
Anti-mouse HRP	Donkey	1:2500	Jackson Lab
Anti-goat HRP	Donkey	1:2500	Jackson Lab

#### 4.1.6 Immunohistochemistry antibodies

Specificity	Host	Dilution	Supplier
RAB5	Rabbit	1:100	CST
LAMP1	Rat	1:1000	BD Biosciences
LysoTracker DND-99	-	1:3000	Molecular Probes
DAPI	-	1:1000	Bio Legend
TFEB	Rabbit	1:200	BioMol
Anti-rabbit IgG(H+L)	-	1:600	Molecular probes
Anti-rat IgG (H+L)	-	1:600	Molecular probes
Anti-mouse IgG (H+L)	-	1:600	Molecular probes

### **4.1.7 Mouse strains**

C1q-KO (C1qa<sup>tm1Mjw</sup>) were bred on a (129x1/SvJ), F2 mixed background. B6129 (C57BL/6 x 129) were used as wild-type for all experiments. All mice were analyzed in sex and age-matched groups of 12-16 weeks of age. The SPF-status of the facility was tested according to the Federation for Laboratory Animal Science Association (FELASA) recommendations. Animal experiment permissions were granted by the animal ethics committee of the Regierung von Oberbayern, Munich, Germany. All mice were bred and maintained at the animal facility of the Institute for Immunology, Ludwig-Maximilians-Universität Munich.

## **4.2 Methods**

### **4.2.1 Immunological and cell biology methods**

#### **4.2.1.1 Harvest of blood and organs**

Animals were euthanized in a CO<sub>2</sub> chamber for harvesting pMPs and thymus. For harvest of spleens mice were euthanized by cervical dislocation after they had been sedated using isoflurane. Organs were removed using scissors and fine tweezers following which they were placed in FACS Buffer. For harvesting pMPs, a small incision in the center of the skin overlying the peritoneal wall is made. Afterwards 10-12 ml of PBS was injected into the peritoneum using a 20 ml syringe with a 25 g needle. After a brief massage for approximately 20 seconds a syringe with 20 g needle is inserted into the peritoneal membrane avoiding insertion into gut, fat or mesentery regions. About 8-10 ml fluid is recovered from each mouse and placed on ice. Spleens were removed from mice and smashed through a 100 µm cell strainer and washed with ice cold FACS buffer. Red blood cells were lysed using 1 ml of ACK buffer for 5 min at room temperature. Samples were washed once again, counted with CASY-counter (OMNI Life science, Bremen, Germany) and stored on ice for further analysis.

#### **4.2.1.2 Flow cytometry – Fluorescence activated cell sorting (FACS)**

Flow cytometry is a method used for the evaluation of various characteristics of single cells based on size, granularity and molecular markers. Cells are stained with fluorochrome coupled antibodies against cell surface or intracellular antigens. When cells pass in a fluid stream through a laser beam and several detectors certain information is obtained which can be further used for identification of distinct cell populations from a heterogenous mixture of cells. Data acquisition was performed using FACS Canto.

An improvement to classical flow cytometry is cell sorter (FACSAria, BD) in which the cell population of interest is defined and further collected by electrostatic droplet deflection. These sorted cells were further used for further analysis. Another additional improvement to flow cytometry is Image stream flow cytometry which combines features of flow cytometry and microscopy. The output files obtained can be used to categorize each cell types and also microscopic images of cell type at the same time. ImageStreamX Mark-II (Amnis Corporation, Seattle, WA, USA) is equipped with 5 lasers (405 nm, 488 nm, 561 nm, 642 nm and 785 nm) and is also capable of detecting side scatter and bright field. The raw data is obtained by Amnis INSPIRE and further analyzed by IDEAS software. The different cell populations are discriminated based on several features such as size, shape and fluorescent intensities.

For flow cytometric analysis equal cell numbers were plated onto a 96 well plate. Cells were washed once with 200  $\mu$ l FACS buffer and stained for 25 min at 4° C in dark using 100  $\mu$ l of antibody mix prepared in FACS buffer. Every antibody has been titrated before use and an antibody with minimal signal to noise ratio is chosen for further experiments. After incubation cells are washed thrice with 200  $\mu$ l FACS buffer and used for FACS acquisition immediately. For AMNIS acquisition cells were fixed with Cytofix/Cytoperm (BD Biosciences) for 20 min followed by washing twice in 1x Perm Wash Buffer (BD Biosciences). Cells were stained for intracellular markers followed by fixation and permeabilization in some cases. Data analysis was performed using FlowJo version 9 or 10 (TreeStar, Ashland, OR, USA).

#### **4.2.1.3 Magnetic cell sorting (MACS)**

MACS is a technique used to separate cell populations based on their surface markers using magnetic beads linked to monoclonal antibodies. This technique can be used either for depleting or enriching required cell type. Cells are incubated with respective magnetic beads (CD3e Biotin, CD19, CD11b) followed by washing with MACS buffer to remove unbound beads. After labelling, cells are loaded onto the respective magnetic column (Depletion – LD Columns and Enrichment – LS Columns). Labeled cells are retained in the magnetic columns while unlabeled cells (negative fraction) pass through the column which is also collected. The positive fraction is collected by applying pressure with the help of a provided plunger. In either case columns are rinsed thrice for collecting respective fractions. This technique was used for depleting T cells (CD3), B cells (CD19) from spleen and enriching MPs (CD11b) from the peritoneum. All procedures were performed according to manufacturer instructions without any modifications.

#### **4.2.1.4 Immunofluorescence staining**

For immunostaining, the flushed out pMPs were cultured on an 8-well chambered glass slides (ThermoScientific) for 3 hours at 37°C, 5% CO<sub>2</sub> which allows the MPs to adhere better. The cells were then washed with 1x PBS for three times to remove non-adherent cells. The samples were later fixed for 15 minutes with 4% paraformaldehyde followed by washing with 1x PBS thrice. The samples were permeabilized using 0.1% Triton-x for 10 min (RAB5), 0.05% Saponin for 30 minutes (LAMP-1) and 100% Methanol for 5 minutes (TFEB) followed by washing thrice with 1x PBS. All samples are blocked using 1x Blocking buffer (4% BSA in 1x PBS) for 1 hr. Without any washing steps cells were incubated overnight at 4°C with respective primary antibody resuspended in 1x Blocking Buffer. The samples were washed four times with 1x PBS and incubated for 1hr at room temperature with corresponding secondary antibody. The samples are taken for mounting after washing four times with 1x PBS. All staining was performed in a moist chamber and at dark conditions. Slides were mounted with Prolong gold-antifade reagent (Thermo Fisher Scientific) and viewed at 22°C on a ZEISS confocal laser-scanning LSM 780 microscope equipped with 100x (NA 1.46 oil) objective. Pictures were

acquired using Leica software (ZEN 2010) and processed, merged and gamma adjusted in ImageJ (version 10.2).

#### **4.2.1.5 Apoptosis induction**

HeLa spinner cells and mcherry tagged to Histone (H2B) HeLa cells were used as a source of apoptotic material for all experiments. mCherry-H2B HeLa cells were provided by Andreas Ladurner Lab [185], Department of Physiological Chemistry, LMU. These cells were cultured using DMEM supplemented with 10% FCS and Penstrap antibiotics grown in T75/T175 cell culture flasks (37°C, 5% CO<sub>2</sub>). Adherent cells are recovered from confluent flasks using 1x PBS supplemented with 2mM EDTA. Apoptosis is induced by adding Staurosporine (1 µg/ml) and incubating cells for three hours. Cells are washed thrice in 1x PBS and later used as apoptotic material to inject mice.

#### **4.2.1.6 *in vivo* Phagocytosis assay**

Apoptotic cells ( $8 \times 10^6$  –  $10 \times 10^6$ ) prepared as above is injected intraperitoneally (*i.p*) to experimental mice. pMPs were harvested following 3 hours, 6 hours and 12 hours following apoptotic cell injection. The cells are later stained and fixed for flow cytometry acquisition. For analyzing mRNA expression, flushed out peritoneal cells were CD11b<sup>+</sup> enriched using MACS and further stored in TRIzol.

### **4.2.2 Molecular Biology**

#### **4.2.2.1 mRNA isolation and cDNA conversion**

Tissue samples and cells (MACS depleted or enriched) were lysed in 1.5 ml of TRIzol (SIGMA) and RNA was isolated using Phenol-Chloroform extraction twice followed by precipitation of RNA with isopropyl alcohol. Next 1 µg of total RNA was transcribed to cDNA using Reverse transcription kit (Qiagen) and later used for qPCR analysis.

#### **4.2.2.2 Quantitative PCR (qPCR)**

qPCR is used to quantify the changes at gene level and is performed using the SYBr green SensiMix (Bioline) on a CFX96 Touch Real-Time PCR detection system (BioRad).

GAPDH was used as the house keeping gene for normalization. In a 96 well plate 10  $\mu$ l of cDNA (1:100) was mixed with 12.5  $\mu$ l 2x-concentrated SensiMix, 0.125  $\mu$ l of forward and reverse primer (100  $\mu$ M) and 2.25  $\mu$ l RNase free water. The SensiMix master mix containing StarTaq DNA Polymerase, SYBr Green I dye, reaction buffer and nucleotides (dATP, dCTP, dGTP, dUTP). All samples were amplified in triplicates.

The cycling conditions were as follows:

- Step 1: Denaturation at 95°C for 10 minutes
- Step 2: 95°C for 10 seconds
- Step 3: Primer annealing at 60°C for 10 seconds
- Step 4: Extension at 72°C for 10 seconds
- Step 2 – 4: Repeated 40 cycles

The qPCR raw data obtained were quantified using 2<sup>n</sup> technique by normalizing the gene expression of housekeeping GAPDH gene. The list of primers used in this study is listed in Appendix 9.3.

#### **4.2.2.3 SDS PAGE and western blot**

Cells for western blot were washed once with 1x PBS to remove extracellular proteins, pelleted and resuspended at a concentration of 1x10<sup>6</sup> cells per 10  $\mu$ l of RIPA Lysis buffer. To prepare spleen lysates for western blot, weight of spleen is measured and RIPA lysis buffer in the presence of protease (Roche) and phosphatase inhibitors (CST) according to tissue weight was added in a vial containing Matrix-D beads. The tissue samples were homogenized in a homogenizer at 6 M/s for 40 seconds. The supernatant from both cases is freeze thawed thrice using liquid nitrogen and centrifuged at 12000 rpm at 4°C to remove cellular any debris present. The protein concentration of cell lysates was quantified using BCA assay (Pierce). Equal amounts of protein were then denatured using sodium dodecyl sulfate (SDS) at 95°C for 5 minutes and further used for SDS-PAGE.

Equal amounts of protein were loaded onto a 12% SDS gel prepared and proteins are separated by gel electrophoresis for 2 hours at 80-100 V. PageRuler™ prestained marker was used to confirm the approximate size for the protein of interest. Separated proteins were later

transferred onto a nitrocellulose membrane (Amersham) using a wet transfer system (BIO-RAD) at 80 V for 90 minutes. Membranes were blocked in 5% milk powder in TBS supplemented with 0.5% Tween-20 (Blocking buffer) for 1 hour at room temperature with gentle shaking. Membranes were later washed once with 1X TBST followed by incubation with primary antibody overnight resuspended in 5% BSA resuspended in 1x TBST. Membranes were washed for (4x10 minutes each) in 1x TBST followed by incubation in corresponding secondary antibody resuspended in blocking buffer for 90 minutes. Once again membranes were washed for (4x10 minutes each) in 1x TBST. Membranes were developed using enhanced chemiluminescence (ECL) western blot substrate (PerkinElmer Inc., MA, USA) followed by exposure to Amersham Hyperfilm™ (GE Healthcare). The relative protein expression was quantified by normalizing either to  $\beta$ -actin or  $\beta$ -tubulin as mentioned in figure legends. The quantification was performed using the free online tool ImageJ.

#### **4.2.2.4 Sample preparation for proteomics**

##### **4.2.2.4.1 Spleen**

To induce germinal center responses 6-8 weeks mice were immunized intravenously with  $2 \times 10^8$  sheep red blood cells (SRBC), a T cell dependent antigen, in PBS on day 0 and analyzed on day 7. Spleen from SRBC immunized mice with four biological replicates. Depletion of B cells and T cells was performed using magnetic anti-CD19 and anti-CD3 microbeads (MACS Miltenyi Biotech). Samples were analyzed on an LC-MS/MS setup coupling a Proxeon Easy nLC11 to a Q-Exactive mass spectrometer. In-house packed 25 cm emitter columns and a bilinear 120 min gradient was applied for peptide separation. Eluted peptides were fractionated using the StagTip-based SAX fractionation technique into three fractions with pH 11, 6 and 3. For protein identification and quantification, the MaxQuant software suite was used and data was obtained by relative quantitation of ion-peak intensity. The expression levels of protein were computed as the mean of the LFQ values for all the proteins from WT spleens. The LFQ values from the C1q-KO mice were divided by this mean of the WT spleen samples for the respective protein to scale the knock-out LFQ values. The

proteomics was performed by Bastian Dislich from Stefan Lichtenthalers's group at the DZNE Munich.

#### **4.2.2.4.2 pMPs**

pMPs are flushed as mentioned before in section and stained for CD19, CD11b and F4/80 surface markers followed by FACS sorting of CD19<sup>-</sup>F4/80<sup>+</sup> CD11b<sup>+</sup> cells. Cells were disrupted using 50  $\mu$ l of Lysis buffer1 (recipe in 4.1.3) by sonicating in a covaries sonicator using cycles of 30 sec pulse and 30 sec cooling for 10 minutes. Subsequently, samples were incubated at 28°C for 1h to allow the disulfide bond reduction. For initial digestion of proteins at 28°C, 3  $\mu$ g LysC was used with slow agitation for 4 hrs. Subsequently, sample was diluted with 250  $\mu$ l of Lysis buffer2 (recipe in 4.1.3) and to ensure complete proteolytic digestion, 10  $\mu$ g trypsin was added and incubated for 12 hrs with slow agitation at 900 rpm. Samples were acidified by adding formic acid (FA) containing 10% trifluoroacetic acid to a final concentration of 4% FA, pH 2 to 3. Eluting peptides were ionized in a NanoESI source and detected on an QExactive HF mass spectrometer (ThermoFisher Scientific). The mass spectrometer was operated in a TOP10 method with positive ionization mode, detecting eluting peptide ions in the m/z range from 300 to 1600 and performing MS/MS analysis of up to 10 precursor ions per cycle. Peptide ion masses were acquired at a resolution of 60000 (200 m/z); higher-energy collision-induced dissociation (HCD) MS/MS spectra were acquired at a resolution of 15000 (at 200 m/z). The proteomics was performed by Andreas Schmidt from Axel Imhof group at the Protein analysis unit, Biomedical Center Munich.

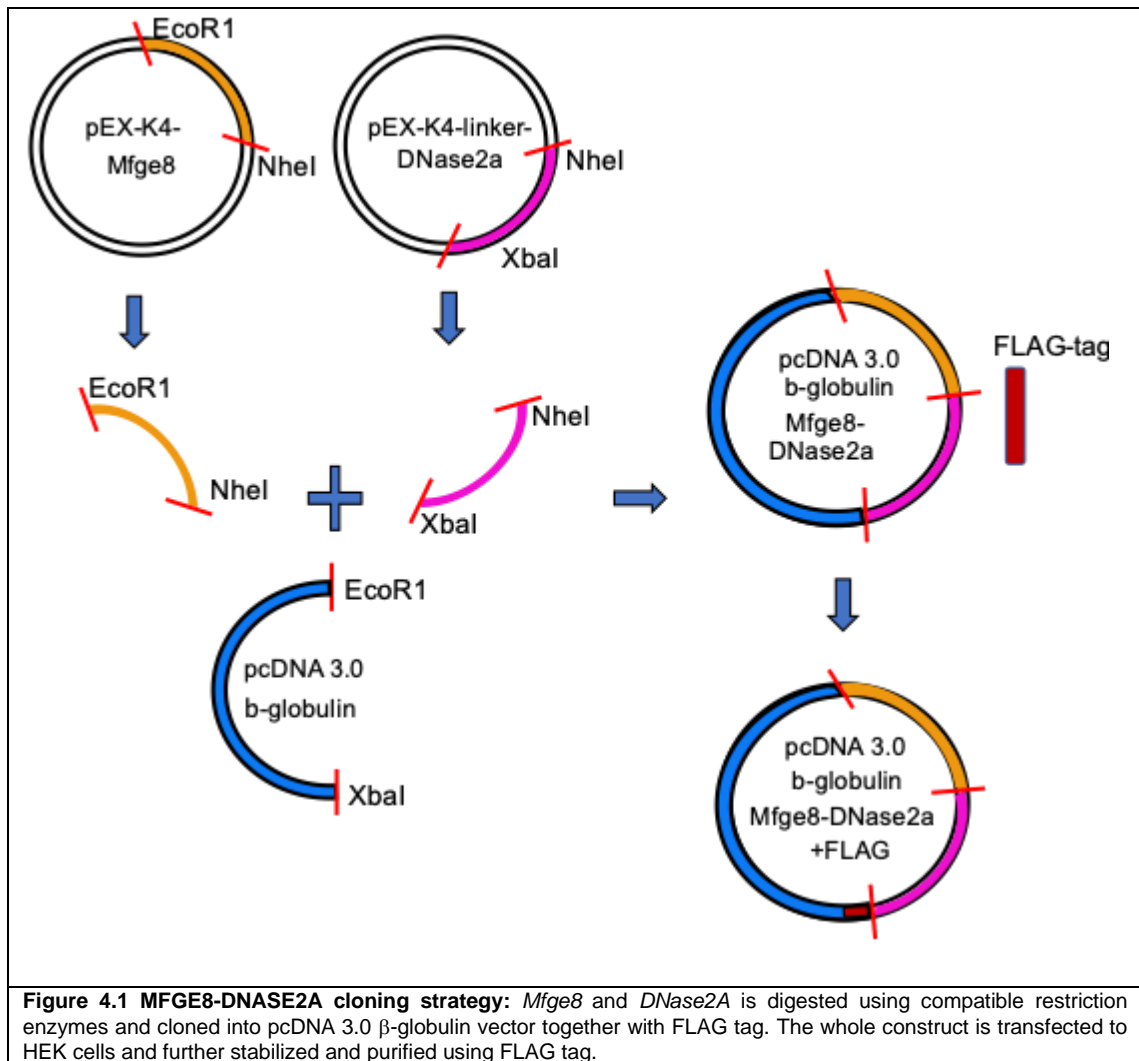
#### **4.2.2.5 Label-free quantification**

All MS raw data were searched against a combined forward/reversed protein database of *Mus musculus* by the Andromeda search engine within the Max Quant (vs. 1.5.5.1) software suit. For peptides the mass accuracy was set to 20 ppm for the first search, 5 ppm for the main search, 20 ppm for fragment ions was applied. Peptides with a maximum of 2 missed cleavages for Trypsin/P, a minimal score of 10 for unmodified peptides and 35 when carrying post-translational modifications were considered. Carbamidomethylation of Cys was set as a

fixed modification, putative variable modifications were oxidation (M), acetylation (Protein N-term), and phosphorylation (STY). These peptide spectrum matches were filtered for 1% FDR rate and the resulting protein hits were again filtered for 2% detection of reversed sequences. Proteins were quantified and considered for further analysis only when at least 2 peptides were detected. The resulting intensity values were converted to iBAQ values to compensate for protein sequence differences. LFQ intensities were  $\log_2$  transformed and compared between WT and C1q-KO using a modified student's t-test. In order to correct for multiple hypothesis testing, an FDR rate of 5% calculated by sample permutation was applied.

#### **4.2.2.6 Cloning and Protein purification**

Murine MFGE8-DNASE2A was produced from stably transfected HEK293 cells. Cells were grown in a Labfors Bioreactor (Infors, Switzerland) in serum-free medium (Ex-Cell 293, Sigma) for 5 days. Cells were removed from the cell culture supernatant (SN) by centrifugation (300g, 10 minutes). 0.1% Triton-X 100 was used to solubilize membrane proteins. SN was incubated under agitation for 1 hr. Debris was cleared by high-speed centrifugation (40.000g, 60 min) and filtration (0.2  $\mu$ m). MFGE8-DNASE2A was then purified by FLAG affinity chromatography using M2-FLAG agarose beads (Sigma). Bound protein was eluted using a FLAG-peptide (Genscript, China). The eluate was concentrated using spin columns with a cutoff of 30-kDa (Sartorius).



#### 4.2.2.7 Agarose gel electrophoresis

Agarose gel is used to visualize, and separate DNA fragments based on size. The agarose gel was prepared by dissolving 1-1.5% (w/v) agarose in TAE buffer, depending on the molecular size of the fragment of interest. As a reference and to predict the fragment size either a 100 bp or a 1 kb ladder was used (New England Biolabs, Ipswich, MA, USA). Loading buffer (10% glycerol, Xylene cyanol FF) was added before loading the sample to the gel. DNA samples were visualized using ethidium bromide (0.5  $\mu\text{g}/\text{mL}$ ) that was added during agarose gel preparation followed by visualization and documentation in Gel Doc<sup>TM</sup> (BIO-RAD).

#### 4.2.2.8 Statistics

Significance was performed using PRISM Software (GraphPad Software, La Jolla, CA, USA). All bar graphs are represented as average  $\pm$  standard error of the mean (SEM) from

single or combined experiments as indicated in the figure legends. The significance was analyzed using the students t-test and defined as follows: \*p = 0.01 - 0.05, \*\*p = 0.001 – 0.01 and \*\*\*p < 0.001.

## 5 RESULTS

### 5.1 Does C1q deficiency affect phagocytosis pathways?

#### 5.1.1 *in vivo* tracking of apoptotic cells

It has been reported earlier that peritoneal macrophages (pMPs) from C1q-KO mice have an early uptake defect of apoptotic cells *in vitro* [186]. To investigate the influence of C1q on phagocytosis, apoptotic HeLa cells were injected into wild-type (WT) and C1q-KO mice. The peritoneal cavity is an ample source of macrophages (MPs), thus ideally suited to study phagocytosis pathways *in vivo*. The tracking of injected mcherry-HeLa cells is possible, as the H2B-histones of HeLa cells are fluorescently labelled with mCherry. This allows us to visualize non-degraded nuclear material inside MPs. The apoptotic cells were administered intraperitoneally (i.p.) and pMPs were harvested following 3 hours, 6 hours and 12 hours (Fig. 5.1A). For imaging flow cytometric analysis, pMPs containing engulfed apoptotic mCherry-labelled HeLa cells are defined as B220<sup>-</sup>CD19<sup>-</sup>CD11b<sup>+</sup>mCherry<sup>int</sup> cells and unengulfed apoptotic cells as B220<sup>-</sup>CD19<sup>-</sup>CD11b<sup>-</sup>mCherry<sup>high</sup> cells (Fig. 5.1B).

We found no significant difference between WT and C1q-KO mice in the frequencies of CD11b<sup>+</sup>mCherry<sup>int</sup> after 3 hours of phagocytosis. However, we observed that the frequency of CD11b<sup>+</sup>mCherry<sup>int</sup> cells was significantly increased at least by three-fold in C1q-KO mice as compared to WT mice after 6 hours of phagocytosis ( $p = 0.01$ ). Similarly, there was a two-fold increase in the frequency of CD11b<sup>+</sup>mCherry<sup>int</sup> cells in C1q-KO mice compared to WT after 12 hours of phagocytosis ( $p = 0.09$ ) (Fig. 5.1B, upper panel). The total frequency of CD11b<sup>+</sup>mCherry<sup>int</sup> cells in WT and C1q-KO mice following 3 hours, 6 hours and 12 hours of phagocytosis is quantified and shown (Fig. 5.1C, left panel). The persistence of phagocytosed material inside the MPs of WT and C1q-KO mice upon 6 hours of phagocytosis was also confirmed by images obtained from imaging flow cytometry (Fig. 5.1D).

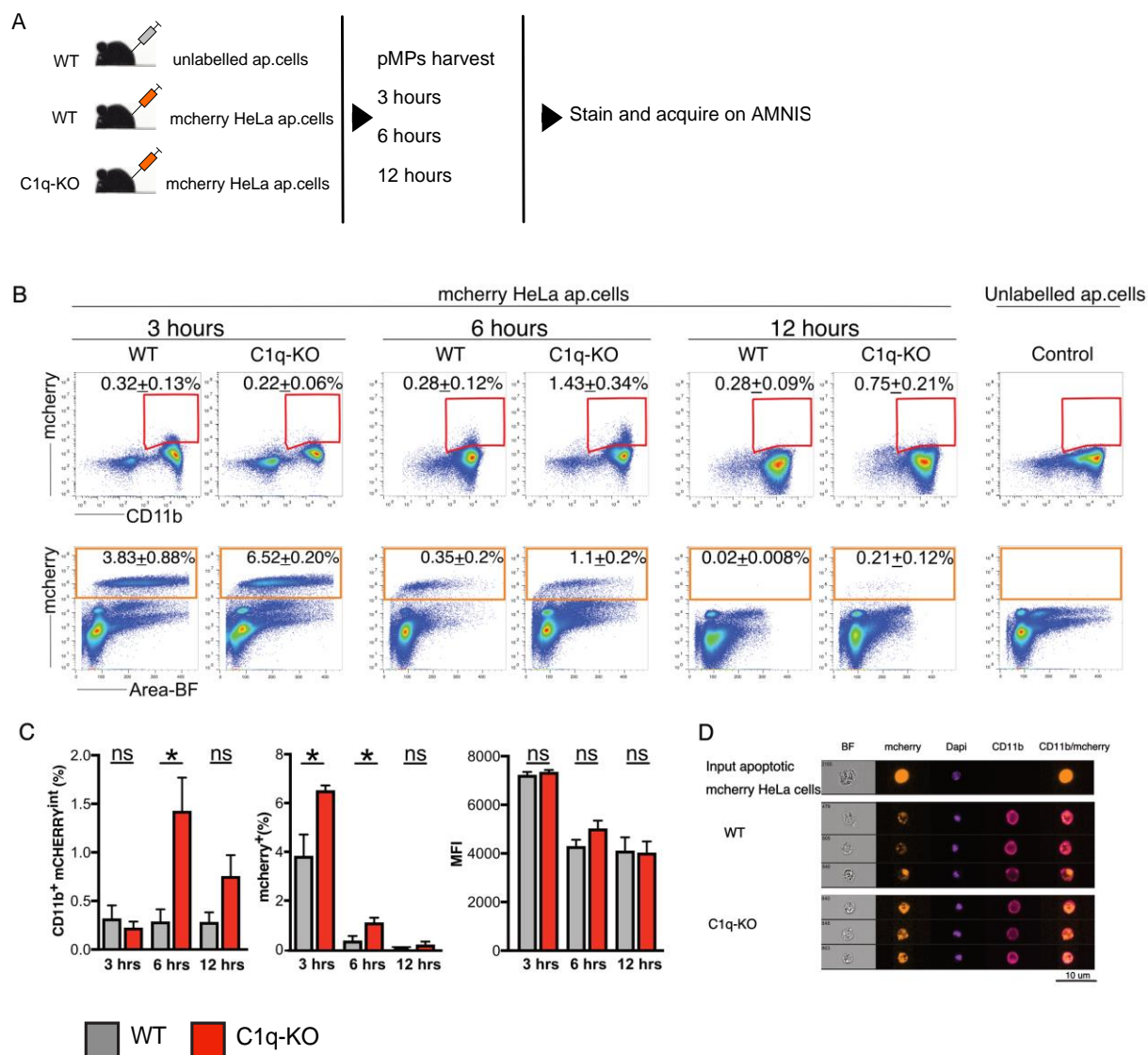


**Figure 5.1 *in vivo* phagocytosis assay WT and C1q-KO mice**

- A. WT (n = 4) and C1q-KO mice (n = 4) were injected with apoptotic mCherry HeLa cells. In addition, WT (n=1) was injected with unlabelled HeLa cells as control. pMPs were flushed following 3 hours, 6 hours and 12 hours of *in vivo* phagocytosis assay. Single cell suspension of harvested peritoneal washes was stained and fixed for acquisition on image stream flow cytometry.
- B. The upper panel shows representative FACS plots for CD11b<sup>+</sup>mCherry<sup>int</sup> pMPs which have taken up mCherry tagged apoptotic cells following 3 hours, 6 hours and 12 hours of *in vivo* phagocytosis. Cells are gated on live B220<sup>+</sup>CD19<sup>-</sup> cells. The lower panel shows representative FACS plots for mCherry<sup>high</sup> cells (unengulfed cells) gated on all cells. The FACS plots of one out of two independent experiments (n = 4 animals per group) is shown.
- C. The frequency of CD11b<sup>+</sup> mCherry<sup>int</sup> (left panel), MFI of CD11b<sup>+</sup> mCherry<sup>+</sup> (right panel) and mCherry<sup>+</sup> as unengulfed cells (middle panel) is quantified and shown. Statistically significant differences between WT and C1q-KO mice: \*p < 0.05, not significant (ns).
- D. Representative Imagestream flow cytometric images showing the co-localization of mCherry-labelled HeLa cells within CD11b<sup>+</sup> pMPs upon six hours of *in vivo* phagocytosis in WT and C1q-KO mice. Scale bar for all images is 10  $\mu$ m and 40x magnification.

The unengulfed CD11b<sup>-</sup>mCherry<sup>+</sup> cells represent the injected apoptotic mCherry HeLa cells which were not taken up by the MPs (Fig. 5.1B, lower panel). There was a significant increase in the frequencies of CD11b<sup>-</sup>mCherry<sup>high</sup> unengulfed cells after 3 hours ( $p = 0.04$ ) and 6 hours ( $p = 0.02$ ) indicating a delayed uptake of apoptotic cells in C1q-KO mice (Fig. 5.1B, lower panel, 3 hours). A very small percentage of unengulfed cells (CD11b<sup>-</sup>mCherry<sup>high</sup>)

persisted after 12 hours in C1q-KO mice which further supported the notion that there was an uptake defect of apoptotic cells (Fig. 5.1B, lower panel, 12 hours). The frequencies of mCherry<sup>high</sup> unengulfed cells following 3 hours, 6 hours and 12 hours is quantified and shown (Fig. 5.1C, right panel). Taken together these results not only confirm the previously reported uptake defect of apoptotic cells seen from the pMPs of C1q-KO mice [186], but also indicate an impaired degradation of nuclear material derived from phagocytosed apoptotic cells.

## **5.1.2 An unbiased proteomics screen**

Having confirmed the phagocytosis defect and having identified a previously undescribed degradation defect of engulfed nuclear material in C1q-KO pMPs, we sought to identify factors responsible for the observed defects caused by C1q deficiency. Therefore, we analyzed the whole protein content (proteome) of WT and C1q-KO MPs by performing an unbiased label-free proteomics screen.

### **5.1.2.1 Spleen Proteomics**

For this, we enriched for phagocytic cell populations of spleens from sheep red blood cells (SRBC) immunized WT and C1q-KO mice by depleting B cells and T cells using magnetic anti-CD3 and anti-CD19 beads (Fig. 5.2A). SRBC immunization was performed to enhance germinal centre responses in the spleen as described earlier [187]. WT and C1q-KO samples were analysed separately from each other and resulting data sets were combined for label-free quantification as described in chapter 4.2.2.4.1.

From these proteomic analyses, 3738 proteins with at least two unique peptides were selected. The fold change values for each identified protein as a ratio of C1q-KO/WT showed which proteins were up- or downregulated in cells from C1q-KO mice. About 40 proteins were identified as being significantly upregulated, while 50 proteins were downregulated by >30% in C1q-KO mice compared to the WT group. To determine differentially regulated proteins, an increase, or decrease in the protein level at least by 1.2-fold and a p-value according to student's t-test below 0.05 was chosen (Fig. 5.2B).

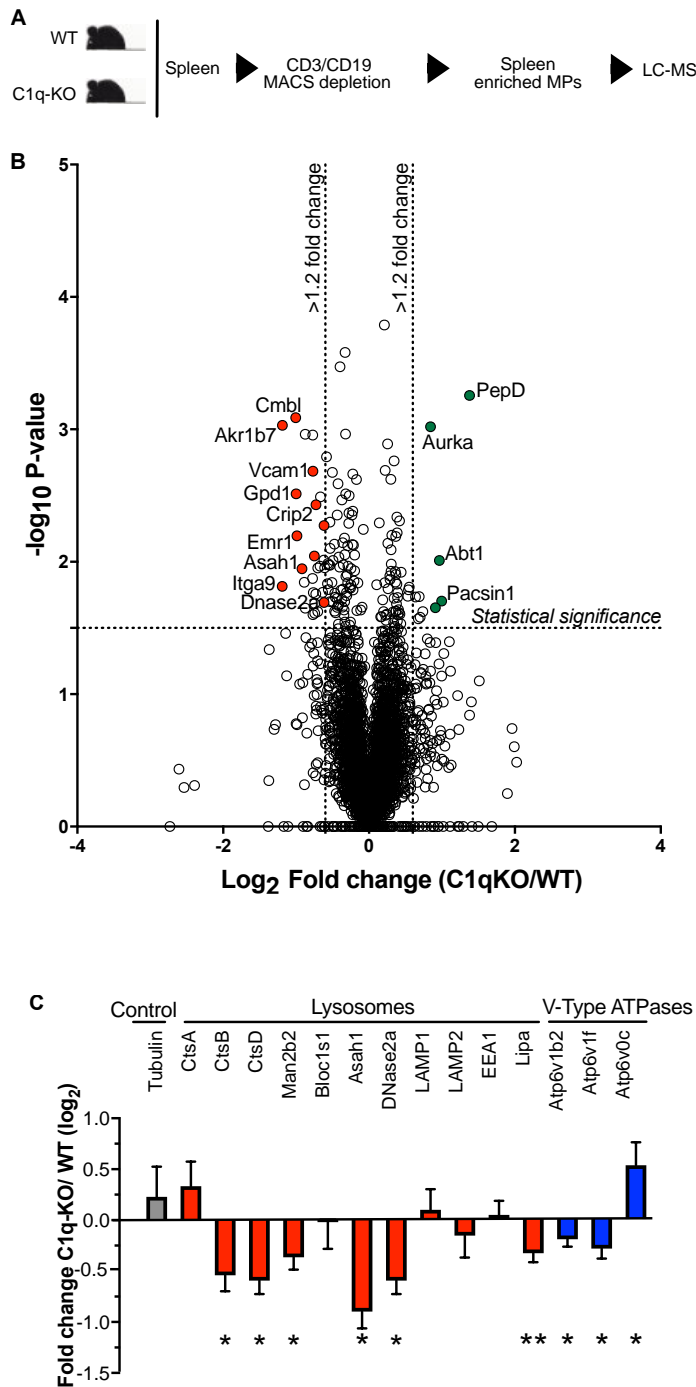


**Figure 5.2 Label free proteomics for identifying differentially regulated proteins in C1q-KO spleen enriched MPs**

- Spleen cells of SRBC immunized WT ( $n = 4$ ) and C1q-KO mice ( $n = 4$ ) were depleted of T and B cells to enrich phagocytic cells, followed by label-free proteomics.
- The differentially regulated proteins in C1q-KO mice are shown by volcano plot where the p-value (in  $\log_{10}$  scale) on the y-axis is plotted against the ratio of protein levels (in  $\log_2$  scale) on the x-axis. The protein candidates marked red are downregulated and green are upregulated by 1.2-fold change.
- The bar graph shows fold change values (C1q-KO/WT)  $\pm$  SEM of selected protein candidates in lysosomal compartments and V-Type ATPases. Tubulin was used as a housekeeping protein for normalization. Proteins marked with an asterisk are significantly regulated candidates.

Within the differentially regulated proteins, we observed a significant downregulation of lysosomal hydrolases such as DNASE2A, ASAH1, CTSB and CTSD in splenic MPs of C1q-KO mice, which also exhibited a significant reduction in V-ATPase hydrolases such as

ATP6v1b2 and ATP6v1f (Fig. 5.2C). The list of regulated candidates is provided in Appendix 9.1.

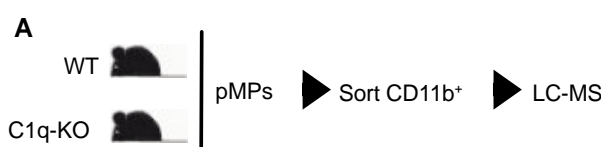
### 5.1.2.2 pMP Proteomics

We have identified some of the most important lysosomal hydrolases to be significantly reduced in a cell suspension enriched for C1q-KO MPs from spleen. Next, we wanted to confirm these results from less complex samples and therefore performed an additional proteomics screen, using pure pMPs from WT and C1q-KO mice.

To obtain pure pMPs, cells were stained with anti-CD11b antibodies, purified by FACS sorting on an AriaXY and further processed for label-free proteomics (Fig. 5.3A). The purity of pMPs obtained following sorting was typically around 93-95%. WT and C1q-KO samples were analysed separately from each other and resulting data sets were combined for label-free quantification as described in chapter 4.2.2.4.2.

From these proteomic analyses, 2044 proteins with at least two unique peptides were selected. LFQ intensities were  $\log_2$  transformed and compared between WT and C1q-KO using a modified student's t-test. To distinguish the differentially regulated proteins, an increase, or decrease in the protein level at least by 3- fold and p-value according to student's t-test below 0.05 was chosen (Fig. 5.3B).

Again, many lysosomal and endosomal proteins were downregulated in C1q-KO mice, such as LAMP1 & LAMP2 and the endosomal trafficking proteins VAMP7 & VAMP8. It was also evident that proteins from Rab-GTPases family such as RAB5B, RAB9A, RASSF2 and RAB11FIP1 were significantly downregulated in C1q-KO pMPs. In this analysis, we did not observe any significant differences in lysosomal hydrolases as we observed in splenic MPs (Fig. 5.2). The changes in lysosomal protein composition were obvious in C1q-KO pMPs as compared to WT and the list of regulated candidates is provided in the Appendix 9.2.



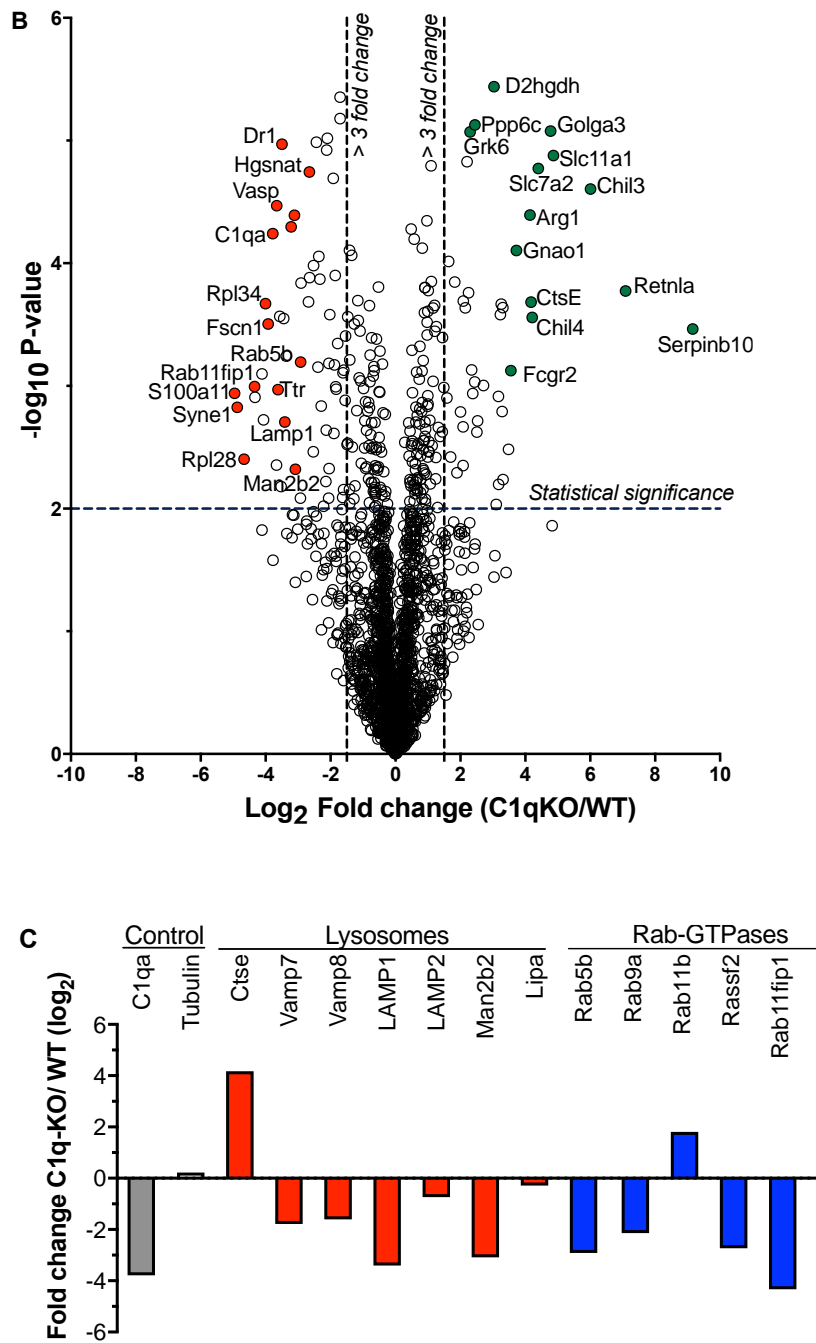


**Figure 5.3 Label free proteomics for identifying differentially regulated proteins in C1q-KO pMPs**

- CD11b<sup>+</sup> pMPs of WT (n = 4) and C1q-KO mice (n = 4) were FACS sorted and processed for label-free proteomics.
- Differentially regulated proteins in C1q-KO mice are shown by volcano plot where the p-value (in  $\log_{10}$  scale) on the y-axis is plotted against the ratio of protein levels (in  $\log_2$  scale) on the x-axis. The proteins shown in red are downregulated and proteins shown in green are upregulated by 3-fold change.
- The bar graph shows fold change values (C1q-KO/WT) of selected protein candidates in lysosomal compartments and Rab-GTPases. Tubulin was used as a housekeeping protein for normalization.

The downregulation of proteins in the endo-lysosomal compartment in C1q-KO MPs corroborates the fact that C1q-KO MPs exhibit an uptake defect as published previously. Furthermore, such a defect might contribute to the delayed degradation of phagocytosed nuclear material observed in this study (Fig. 5.1). The accumulation of nuclear material in C1q-

KO MPs could be a direct consequence of the reduced DNASE2A levels we detected in the spleen of C1q-KO mice. DNASE2A is ubiquitously expressed in lysosomes and exhibits activity over a low pH 4.5-5.5 [188]. DNASE2A deficient MPs are unable to digest the DNA from apoptotic cells, which thereby accumulates in their lysosomes and activates the production of interferons [189],[190]. Since C1q-KO mice exhibit impaired phagocytosis, further investigation of DNASE2A levels in these phagocytic cells could provide an insight into disease development in C1q-KO mice. Also, studies have shown the importance of RAB5 in establishing a stable endo-lysosomal system in phagocytes [191]. Thereby from these two proteomic screen DNASE2A, RAB5B and LAMP1 were chosen as potential candidates for further analysis which could possibly have a major role in SLE development.

### 5.1.3 Confirmation of the proteomics screen

#### 5.1.3.1 *DNase2a* expression in WT and C1q-KO spleen enriched MPs and pMPs

Next, *Dnase2a* expression levels in C1q-KO mice were quantified at gene levels by qPCR and detected by Western blot in spleen enriched MPs and pMPs. The *Dnase2a* gene expression was more than two-fold reduced in C1q-KO MPs enriched from spleen ( $p = 0.0003$ ) and pMPs ( $p = 0.0009$ ) (Fig. 5.4).

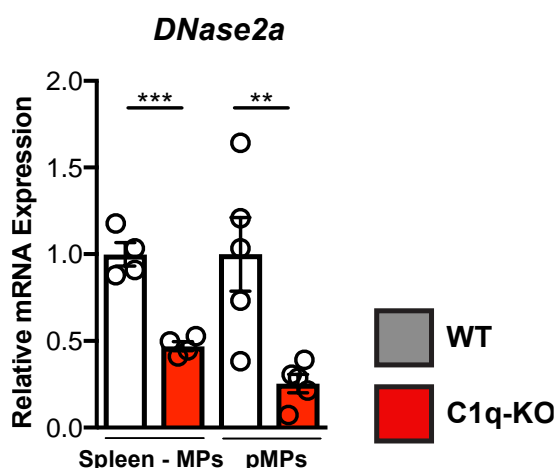


**Figure 5.4 Gene expression of *DNase2a* in WT and C1q-KO mice**

WT (n = 4) and C1q-KO mice (n = 4) was used for quantifying *DNase2a* expression in enriched MPs from spleen (CD3<sup>+</sup>CD19<sup>-</sup>). WT (n = 5) and C1q-KO mice (n = 5) was used for quantifying *DNase2a* expression in CD11b enriched pMPs. Statistically significant differences between WT and C1q-KO mice: \*\*( $p < 0.01$ ), \*\*\*( $p < 0.05$ ). Data shown here are from one representative experiment out of two independent experiments.

Having confirmed reduced *DNase2a* mRNA levels in C1q-KO MPs, next we analyzed DNASE2A expression in pMPs and splenic enriched MPs. It was interesting to analyze MFGE8-KO mice because it has been previously shown to exhibit impaired uptake of apoptotic cells and develop lupus like autoimmune disease [92], [192]. In addition, we also investigated DNASE2A levels in C3-KO because the complement factor C3 acts downstream of C1q even though it has been shown earlier that they do not render a protective role against SLE development [193].

The expression of DNASE2A protein was diminished in pMPs (Fig. 5.5A) and enriched MPs from C1q-KO spleen compared to WT (Fig. 5.5B). We detected normal protein levels of DNASE2A in enriched MPs from C3-KO and MFGE8-KO spleens. However, the DNASE2A expression in total splenocytes remained unchanged in C1q-KO mice (Fig. 5.5C). Therefore, above results indicate that the reduction in DNASE2A levels, an important lysosomal hydrolase might be specific to C1q-KO MPs. Also, these experiments indicate C1q deficiency leads to substantial and significant decrease of DNASE2A protein and *DNase2a* gene expression which warrant further investigation. The reduced DNASE2A expression in C1q-KO MPs corroborate with those findings of mice showing delayed degradation of phagocytosed apoptotic material as shown earlier (Fig. 5.1).

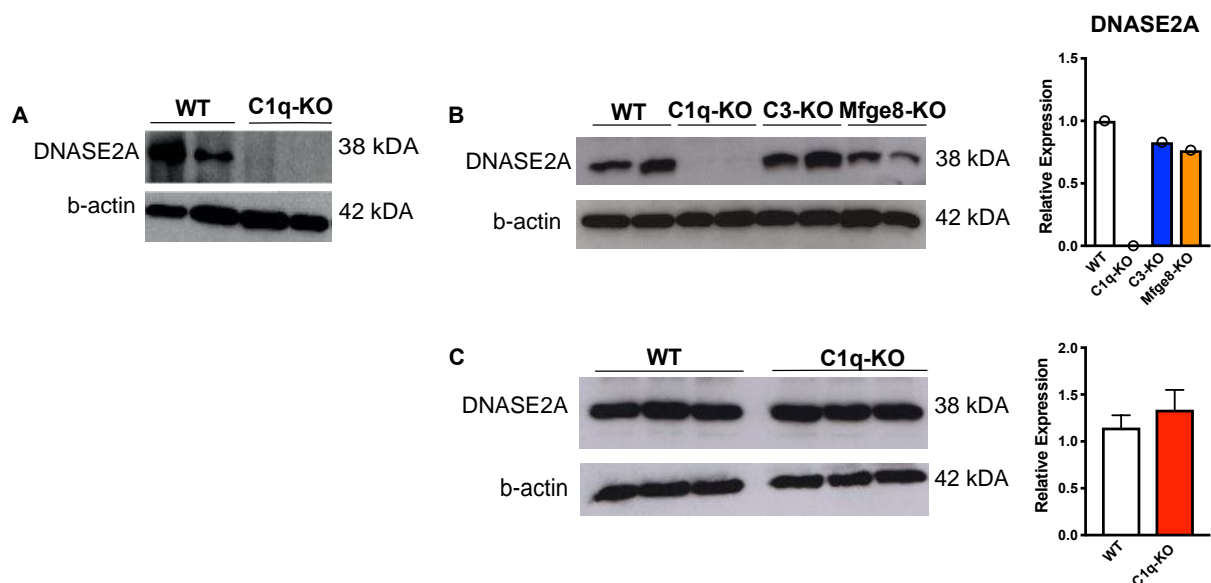


**Figure 5.5 Protein level Expression of DNASE2A in WT and C1q-KO mice**

A. Western blot showing DNASE2A expression in pMPs of WT (n = 6) and C1q-KO (n = 6) where isolates from three mice were pooled for each sample.

- B. Western blot showing DNASE2A expression levels in spleen enriched MPs of WT (n = 2), C1q-KO (n = 2), C3-KO (n = 2), Mfge8-KO (n = 2).
- C. Western blot showing DNASE2A expression levels in total splenocytes of WT (n = 3) and C1q-KO (n = 3).
- D. The relative expression is quantified with  $\beta$ -actin as housekeeping control. Bar graphs show one representative experiment out of two with similar trend.

### 5.1.3.2 Rab-GTPases in WT and C1q-KO spleen enriched MPs and pMPs

RAB5 is commonly used as a marker for early endosomes, RAB9 for recycling endosomes and LAMP1 as a marker for lysosomal compartments [194], [195]. As we found the levels of these proteins being decreased in C1q-KO pMPs, we next analyzed gene expression by qPCR. While MPs enriched from spleen did not show any significant regulation of these genes, pMPs from C1q-KO mice showed more than two-fold down-regulation of *Rab5*- and *Rab9*-expression, but strong upregulation of *Lamp1* (Fig. 5.6).

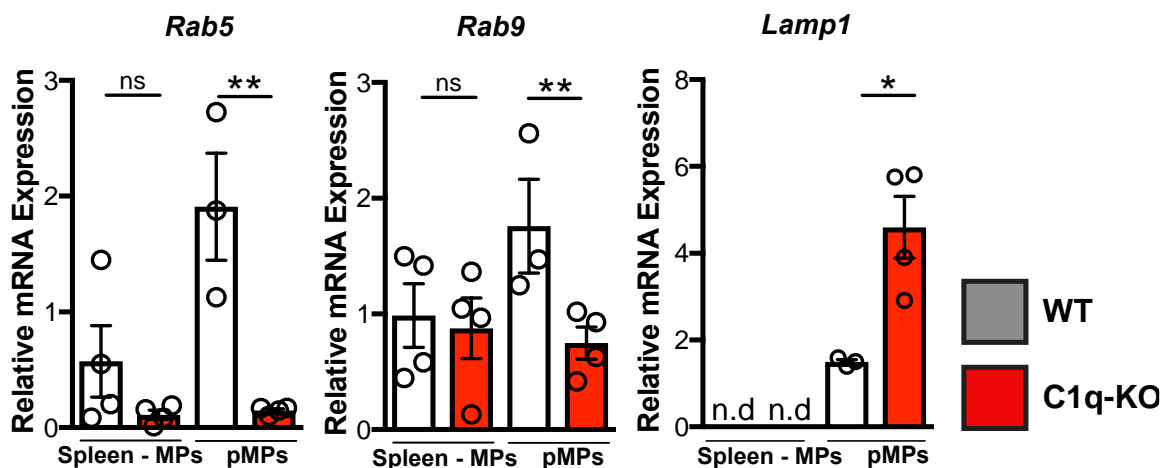


**Figure 5.6 Gene expression of *Rab5*, *Rab7*, *Rab9* and *Lamp1* in WT and C1q-KO mice**

WT (n = 4) and C1q-KO mice (n = 4) were used for quantifying *Rab5*, *Rab9* and *LAMP1* mRNA expression in spleen enriched MPs (CD3<sup>+</sup>CD19<sup>+</sup>) and in CD11b-enriched pMPs. Statistically significant difference between WT and C1q-KO mice: \*(p < 0.05), \*\*\*(p < 0.001), ns – non-significant. Data shown here are from one representative experiment performed with triplicates.

RAB5 has been known to have an important role in establishing a stable endo-lysosomal system and in phagosomal maturation [108], [191]. Since, we see a strong reduction of *Rab5* expression at gene level, the protein levels were further quantified by immunofluorescence using the respective antibodies in pMPs from WT and C1q-KO mice. Although western blots to investigate RAB5 protein expression levels would give us an information about the total protein levels, further investigations by immunofluorescence may provide additional insights about the sub cellular localization in the pMPs.

RAB5<sup>+</sup> early endosomes (green) were seen as brightly stained vesicles and located more towards the periphery of pMPs. Though we see a reduction in RAB5<sup>+</sup> early endosomes in C1q-KO pMPs (Fig. 5.7A, lower panel) compared to WT pMPs (Fig. 5.7A, upper panel), manual counting of these vesicles would give us biased results. Therefore, to enumerate RAB5<sup>+</sup> endosomal vesicles in an automated fashion, we employed customized macros for endosomal counting in ImageJ as discussed previously [196]. About 30-40 individual pMPs from WT and C1q-KO mice were used for quantification. As a result, it is clearly seen that the number of early endosomes ( $p < 0.001$ ) is significantly reduced in C1q-KO pMPs (Fig. 5.7B).

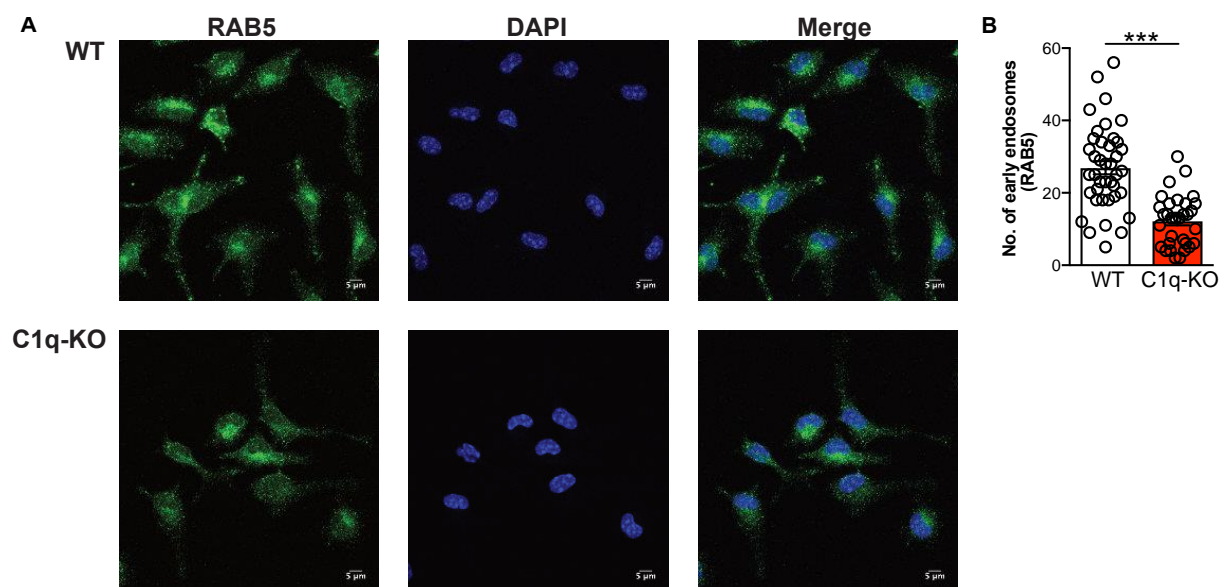


**Figure 5.7 RAB5 expression in WT and C1q-KO mice pMPs**

- A. RAB5 expression was detected by immunofluorescence in pMPs. The immunofluorescence images show RAB5 expression levels in pMPs of WT and C1q-KO mice. Scale for all images is 5 μm. Shown here are representative images from one experiment out of three independent experiments.
- B. The RAB5<sup>+</sup> vesicles were quantified by applying the automated macros to at least 30-40 cells per sample. The number of RAB5<sup>+</sup> vesicles are counted and quantified and shown as MFI ± SEM (n = 30 cells). Bar graphs show data from one representative experiment out of three with similar trend. Statistically significant difference between WT and C1q-KO mice: \*( $p < 0.05$ ), \*\*( $p < 0.01$ ), \*\*\*( $p < 0.001$ ).

Therefore, above results demonstrate that key proteins such as RAB5, which are required for establishing a functional phagocytic machinery, are affected by C1q-deficiency. This is in line with reduced lysosomal DNASE2A expression in the C1q-KO MPs. Thus, the delayed uptake and digestion of apoptotic material observed in C1q-KO MPs could be due to a disturbed endo-lysosomal system in MPs.

### 5.1.4 Does C1q-KO pMPs exhibit an acidification defect?

Since we saw a reduction in most of the lysosomal hydrolases (Fig. 5.2, Fig. 5.3), it was also interesting to see if the C1q-KO pMPs have an acidification defect in the lysosomal compartments. To analyze this by flow cytometry, single cell suspension from peritoneum of WT and C1q-KO mice were analyzed with LysoTracker to stain acidic compartments (Fig. 5.8). We did not see any significant differences between WT and C1q-KO mice in the LysoTracker intensities for F4/80<sup>+</sup>CD11b<sup>+</sup> pMPs (Fig. 5.8). This data suggests there is no substantial lysosomal acidification defect in C1q-KO pMPs.

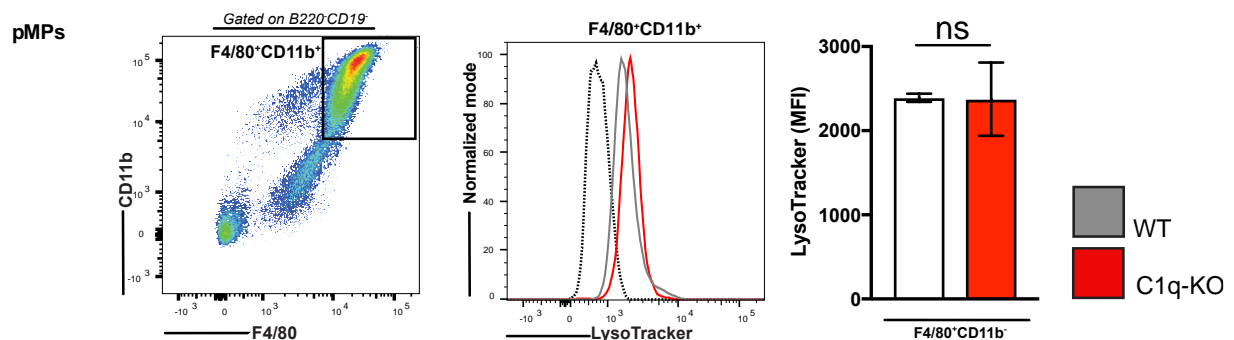


**Figure 5.8 LysoTracker staining of pMPs from WT and C1q-KO mice**

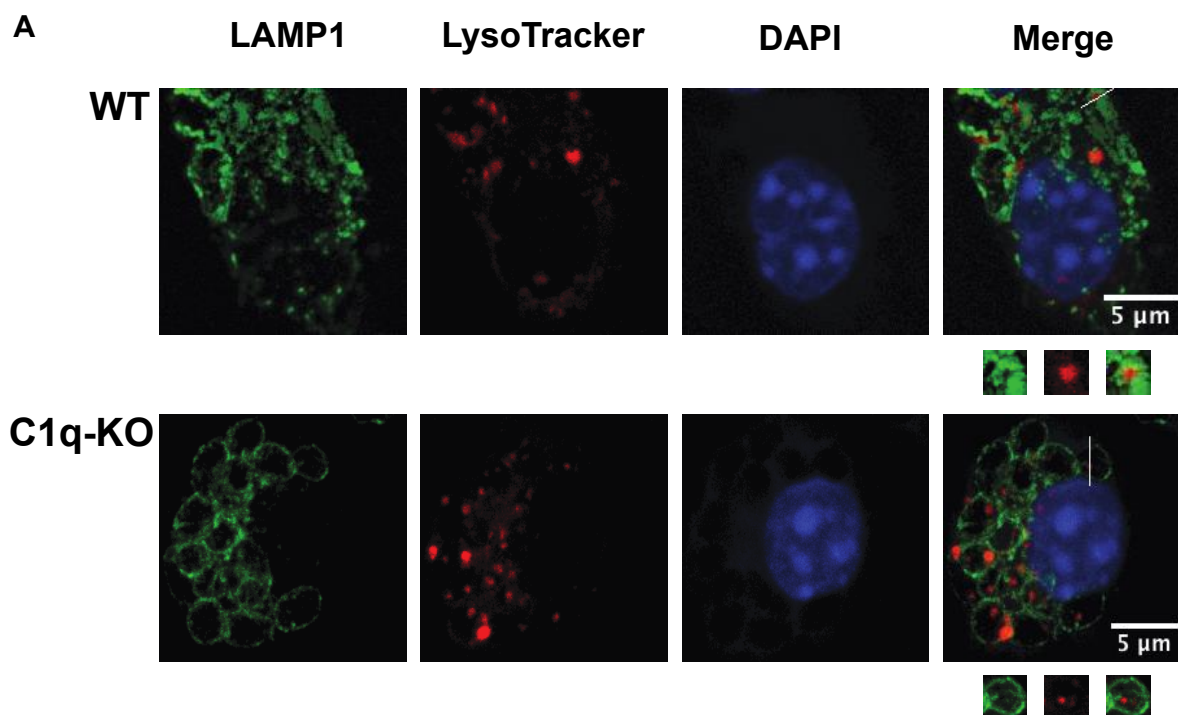
WT (n = 3) and C1q-KO (n = 3) was used for quantifying LysoTracker expression in F4/80<sup>+</sup>CD11b<sup>+</sup> pMPs using flow cytometry. All cells were gated on B220<sup>-</sup> CD19<sup>-</sup> population. LysoTracker MFI intensities are quantified and shown as MFI ± SEM (n = 3). Statistically significant difference between WT and C1q-KO mice: \*(p < 0.05), \*\*(p < 0.01), \*\*\*(p < 0.001), ns – non-significant. Data shown here are from one representative experiment out of three.

Nevertheless, it was important to see if the acidification would occur in the lysosomal compartment, since the intensities obtained from flow cytometry only indicated the overall acidification in cells. To visualize the acidification inside of lysosomes of C1q-KO pMPs we used immunofluorescence microscopy. To this end, WT and C1q-KO pMPs were stained with anti-LAMP1 antibodies and LysoTracker to visualize the lysosomes [197] and acidification [198], respectively. The co-localization extent of LAMP1 and LysoTracker was quantified by fluorescence line scanning analysis similar to earlier studies [199], [200].

We observed that there was a significant increase by two-fold in the size of LysoTracker<sup>+</sup>LAMP1<sup>+</sup> compartments in C1q-KO pMPs (Fig. 5.9A, Fig. 5.9C). In order, to quantify the extent of co-localization between LAMP1 and LysoTracker fluorescence line

scanning analysis was performed as described previously [201]. It was evident that there was a reduction in the co-localization efficiency of LysoTracker with lysosomes (Fig. 5.9A, Fig. 5.9B) in C1q-KO pMPs. The co-localization efficiency correlates to the overlap of LAMP1<sup>+</sup> and LysoTracker<sup>+</sup> peaks. So, closer the overlap better is the co-localization of LysoTracker within LAMP1<sup>+</sup> compartments (Fig. 5.9B).

Taken together, this data suggests that the acidification of lysosomes is impaired in C1q-KO pMPs. This data provides yet another line of evidence for the disturbed endo-lysosomal system in C1q-KO MPs. A stable endo-lysosomal system is required to create optimal conditions for the activity of lysosomal hydrolases such as DNASE2A to degrade phagocytosed apoptotic material. Thus, the failure to establish these conditions supports the notion of defective phagocytosis in C1q-KO mice.



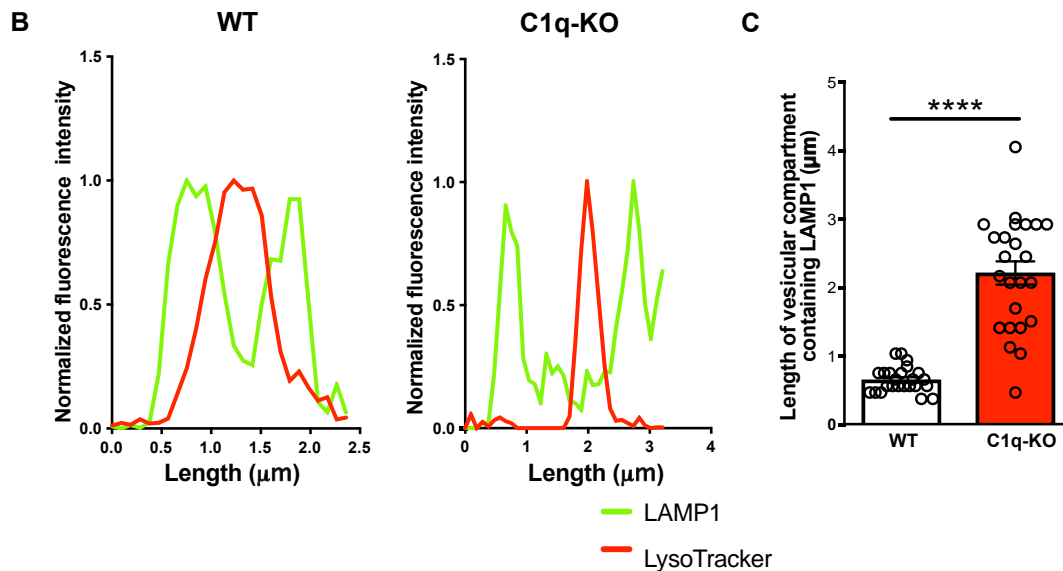


**Figure 5.9 Lysosomes in WT and C1q-KO pMPs**

- A. LAMP1 expression was detected by immunofluorescence microscopy in pMPs. The immunofluorescence images show LAMP1 expression levels in pMPs of WT and C1q-KO mice. The LysoTracker<sup>+</sup> (red) LAMP1<sup>+</sup> vesicles (green) were selected for further line scanning analysis (solid white line). One representative image of LysoTracker co-localization with LAMP1<sup>+</sup> vesicle is shown. Scale for all images is 5  $\mu\text{m}$ .
- B. Fluorescence line scanning analysis was performed for at least 20-23 cells per sample. Each raw data of LAMP1 (green) or LysoTracker (red) intensity was normalized to the highest intensity value in the region of interest (ROI). The normalized fluorescence intensity on the y-axis is plotted against the length ( $\mu\text{m}$ ) on the x-axis. Closer overlap between two peaks indicate better co-localization of LAMP1 with LysoTracker.
- C. The length of LAMP1<sup>+</sup> vesicles is quantified and shown. Statistically significant difference between WT and C1q-KO mice: \*( $p < 0.05$ ), \*\*( $p < 0.01$ ), \*\*\*( $p < 0.05$ ), \*\*\*\*( $p < 0.0001$ ). One representative out of two independent experiments is shown here.

#### 5.1.4 Why is the phagocytic machinery disturbed in C1q-KO mice?

Since we see a reduction in the early endosomes (RAB5<sup>+</sup>), an impairment in lysosomal acidification and enlarged lysosomal compartments in C1q-KO pMPs, we wanted to investigate if the known master regulator of lysosomal biogenesis Transcription factor EB (TFEB) [202] is affected in C1q-KO mice. *Tfeb* gene expression was quantified by qPCR in enriched spleen MPs and pMPs. It was found to be reduced approximately two-fold in C1q-KO but did not reach statistical significance ( $p = 0.08$ ) (Fig. 5.10).

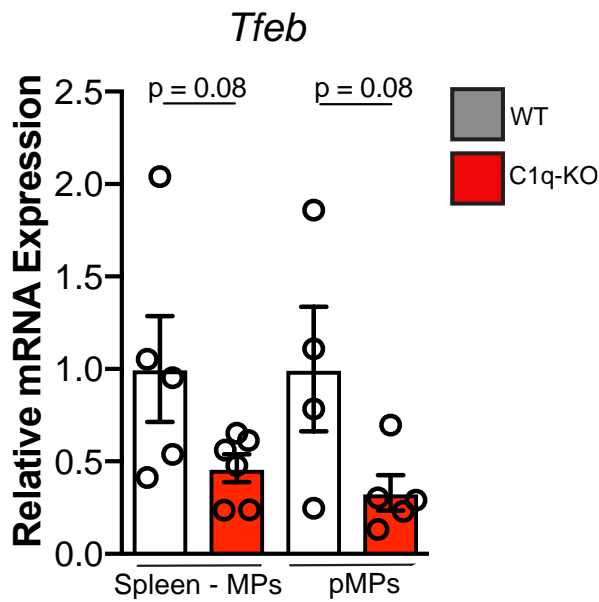


**Figure 5.10 Gene expression of *Tfeb* in WT and C1q-KO mice**  
mRNA from enriched spleen MPs (CD3<sup>+</sup>CD19<sup>+</sup>) and pMPs from WT and C1q-KO mice was used to quantify *Tfeb* gene expression (n = 4-5). No statistically significant difference was observed between WT and C1q-KO mice. Data shown here is from a single experiment out of two independent experiments.

In order to further investigate TFEB expression, immunofluorescence analysis with TFEB-specific antibody was performed in the pMPs. We could observe a very strong reduction in TFEB intensity in C1q-KO pMPs (Fig. 5.11, lower panel) compared to WT (Fig. 5.11, upper panel). This quantification of MFI showed that TFEB protein levels were significantly reduced in C1q-KO pMPs (Fig. 5.11, right panel). Due to the important role of TFEB in controlling the lysosomal biogenesis [203], [204], it might be responsible for the phagocytosis defects observed in MPs of C1q-KO mice.

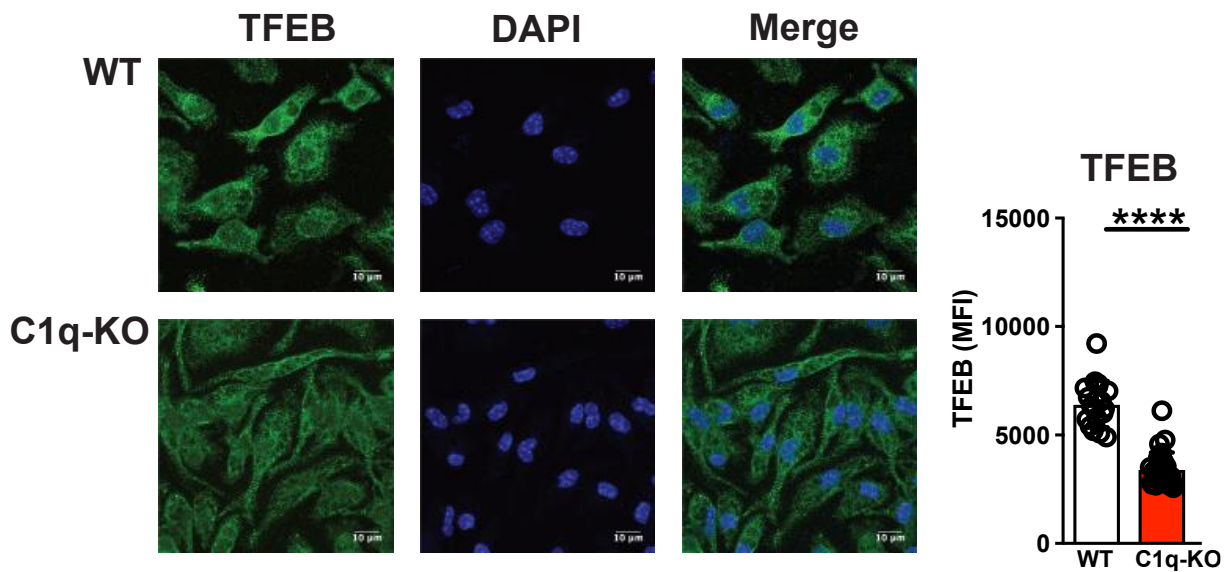


**Figure 5.11 TFEB expression in WT and C1q-KO pMPs**

TFEB expression was detected by immunofluorescence in pMPs. The immunofluorescence images show TFEB expression levels in pMPs of WT and C1q-KO mice. The MFI of TFEB<sup>+</sup> vesicles is quantified and shown. Statistically significant difference between WT and C1q-KO mice: \*(p < 0.05), \*\*(p < 0.01), \*\*\*(p < 0.001), \*\*\*\*(p < 0.0001). Scale for all images is 10 μm. One representative image out of two independent experiments is shown.

## 5.2 Do phagocytosis defects trigger inflammatory pathways in C1q-KO mice?

Since we found that C1q-KO MPs express diminished levels of several key proteins required to establish a stable phagocytic machinery, the next interesting question was to look for other effects from delayed degradation of phagocytosed apoptotic material in C1q-KO MPs. Though C1q-KO MPs take up and digest apoptotic material at a slower rate than WT MPs, it was interesting to test if the increased load of accumulating apoptotic material inside and outside of MPs act as a trigger for inflammatory cytokine production. Due to a delay in degradation of phagocytosed DNA, cytosolic DNA sensing pathways inside these MPs could be activated and lead to the production of inflammatory cytokines such as IL-1 $\beta$ , IL-18, CXCL10, TNF- $\alpha$ , IL-6 and IFN- $\alpha/\beta$  [205], [206].

To investigate this, apoptotic HeLa cells were injected to WT and C1q-KO mice. Since we observed a maximum accumulation of ingested apoptotic material at 6 hours (see Fig. 5.1), pMPs were harvested 6-7 hours after the injection of apoptotic cells. cDNA from CD11b<sup>+</sup> pMPs enriched by MACS was used to quantify gene expression of inflammatory markers. These results show that at steady state we do observe a slight increase in cytokine production of *Cxcl10*, *Il18*, *Il1 $\beta$* , and *Tnf $\alpha$*  which was however, never significant in C1q-KO MPs. Nevertheless, when exposed to apoptotic material gene expression of inflammatory cytokines *Il1b* ( $p = 0.04$ ), *Il18* ( $p = 0.003$ ) and *Cxcl10* ( $p = 0.02$ ) in C1q-KO pMPs were significantly upregulated in comparison to WT pMPs (Fig. 5.12). *Tnf $\alpha$*  was the only inflammatory mediator which was not significantly altered (Fig. 5.12). *Ifn- $\alpha/\beta$*  mRNA levels could not be detected in these samples by qPCR.

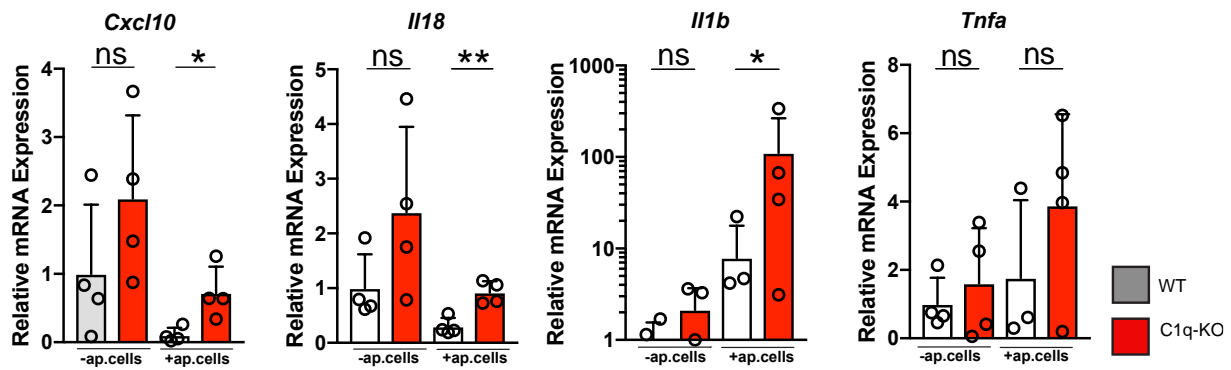


**Figure 5.12 Inflammatory cytokine gene expression in the WT and C1q-KO pMPs at steady state and following *in vivo* phagocytosis.**

pMPs were enriched using anti-CD11b microbeads and subsequently were used for quantifying the mRNA expression of pro-inflammatory cytokines. WT (n = 4) and C1q-KO mice (n = 3-4) were used for quantifying *Cxcl10*, *Il18*, *Il1b* and *Tnfa* expression in CD11b enriched pMPs. All bar graphs represent mean  $\pm$  standard error mean (SEM). Statistical significance was analyzed using a student's t-test with \*: p < 0.05, \*\* p < 0.01, \*\*\* p < 0.001. Shown here are data from one representative out of two independent experiments.

These results support the notion that the impaired clearance of phagocytosed material results in a significant upregulation of inflammatory cytokines in C1q-KO pMPs. Since we found an increase in the mRNA levels of inflammatory cytokines, we next wanted to identify the signaling pathways involved.

As we observe an accumulation of non-degraded DNA due to the DNASE2A deficiency in C1q-KO MPs there was potential involvement of the Stimulator of interferon genes protein (STING) pathway, which could be responsible for elevated inflammatory response. Once self or foreign DNA is sensed in the cytosol, STING recruits Tank binding kinase (TBK1) to endoplasmic reticulum to form STING signalosome followed by activation of Interferon Regulatory factor (IRF3) resulting in elevated inflammation [207].

In order to confirm this hypothesis, apoptotic HeLa cells were injected to WT and C1q-KO mice. After 6h cDNA from CD11b<sup>+</sup> pMPs was used for quantifying the levels of TBK1, pTBK1 and STING in order to monitor a potential activation of the STING pathway by Western blot.

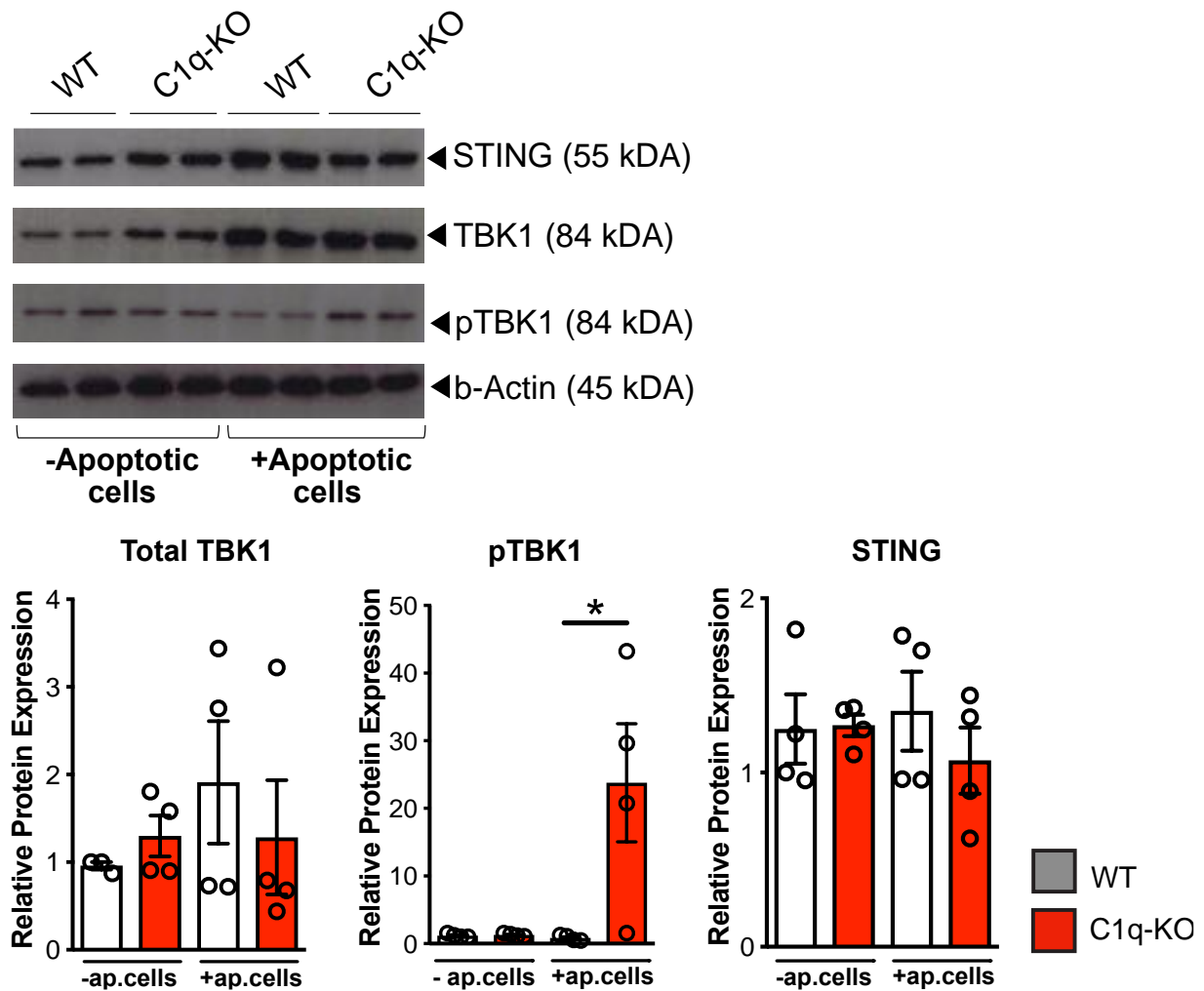


**Figure 5.13 Protein expression of TBK1, pTBK1 and STING in WT and C1q-KO mice**

TBK1, pTBK1 and STING expression was detected by Western blot in CD11b<sup>+</sup> enriched pMPs from WT (n = 2) and C1q-KO mice (n = 2) at steady state and following *in vivo* phagocytosis conditions. The relative expression is quantified with  $\beta$ -actin as housekeeping control. All bar graphs represent mean  $\pm$  standard error mean (SEM). Statistical significance was analyzed using a student's t-test with \*: p < 0.05, \*\* p < 0.01, \*\*\* p < 0.001. Shown here is one representative western blot out of two independent experiments. The bar graphs show pooled data from two independent experiments (n = 2).

At steady-state there was a no significant difference in expression levels of TBK1, pTBK1 and STING in C1q-KO pMPs. However, when C1q-KO mice receive apoptotic cells we do see a significant increase in pTBK1 expression which is accompanied by a slight reduction in STING expression levels as the latter is utilized for TBK1 phosphorylation (Fig. 5.13). C1q-KO pMPs exhibit a delayed degradation of nuclear material derived from phagocytosed apoptotic cells. Consequently, they show elevated levels of factors from the STING-pathway, which is activated by recognition of cytosolic DNA and can trigger inflammation.

### 5.3 Can MFGE8-DNASE2A restore the DNA degradation?

In an attempt to restore DNA degradation in C1q-KO MPs, we tried to target rDNASE2A specifically to the lysosome by attaching it to dying cells. For this, we fused DNASE2A to the PS-binding protein MFGE8, which has been shown to bind to apoptotic cells [91], [208]. The MFGE8-DNASE2A - opsonized dying cells are recognized by MPs and taken up together with MFGE8-DNASE2A, thereby delivering DNASE2A to the phagolysosomes. Briefly, MFGE8-DNASE2A fusion protein was generated and further tested for its efficacy in recovering the phagocytosis defects observed in C1q-KO mice.

#### 5.3.1 Generation of MFGE8-DNASE2A fusion protein

*Mfge8-DNase2a* construct was cloned into pcDNA3.1. Expression is driven by the Cytomegalovirus (CMV) promoter. MFGE8-DNASE2A was produced from stably transfected HEK 293T cells. MFGE8-DNASE2A fusion protein was purified from the supernatant by FLAG affinity chromatography. Expression was confirmed by Western blot. MFGE8 was detected around 55 kDA while MFGE8-DNASE2A fusion protein showed the expected molecular weight of 110 kDA (Fig. 5.14).

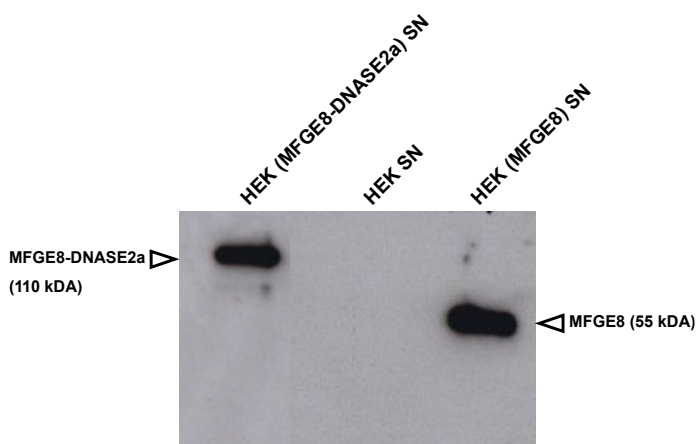


**Figure 5.14 Confirmation of MFGE8-DNASE2A by western blot**

The supernatant obtained from a large-scale protein production was loaded on to an SDS-Gel and protein of interest was detected with anti-MFGE8 antibodies. Lane 1 – Supernatant (SN) from HEK cells transfected with MFGE8-DNASE2A; Lane 2 – Supernatant (SN) HEK cells only; Lane 3 – Supernatant (SN) HEK cells transfected with MFGE8. Arrows indicate the presence of respective protein. Shown here is one representative western blot for one MFGE8-DNASE2A fusion protein production out of two independent production.

#### 5.3.2 Enzymatic activity of MFGE8-DNASE2A fusion protein

In order to test if MFGE8-DNASE2A fusion protein is enzymatically active, genomic DNA obtained was digested. We used equimolar concentration of rDNASE2A and rMFGE8-DNASE2A to digest DNA. rDNASE2A serves as positive control and undigested DNA serves

as the negative control. Indeed, MFGE8-DNASE2A was enzymatically active and degraded the DNA seen with a clear DNA smearing pattern however less efficiently compared to rDNASE2A. The undigested control shows a clear band of intact DNA (Fig. 5.15). These results confirm that MFGE8-DNASE2A fusion protein maintained its DNASE2A activity.

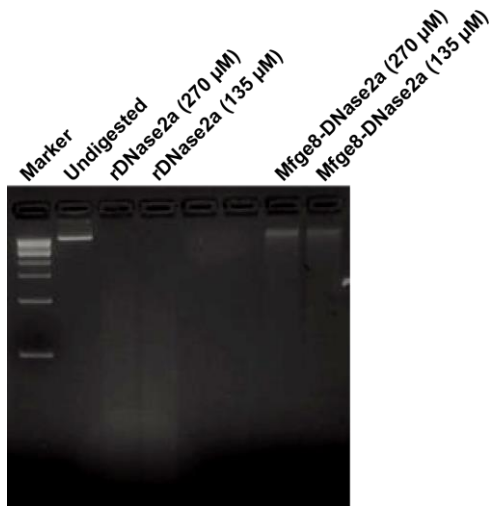


**Figure 5.15 Enzymatic activity of MFGE8-DNASE2A**

1 pg mouse tail DNA was incubated with 270 $\mu$ M or 130 $\mu$ M of rDNASE2A or MFGE8-DNASE2A fusion protein for 2.5h at 37°C at a pH of 5.7. Samples were loaded onto a 2% agarose gel. Shown here is one representative agarose gel for one MFGE8-DNASE2A fusion protein production out of two independent protein production.

### 5.3.3 Functional activity of MFGE8-DNASE2A fusion protein

To further investigate if MFGE8-DNASE2A is functionally active, apoptotic HeLa cells were used. Briefly, apoptotic cells were incubated with equimolar concentration of rMFGE8 and MFGE8-DNASE2A followed by staining with anti-MFGE8 (Fig. 5.16). MFGE8-DNASE2A binds apoptotic cells with same efficiency as rMFGE8 as compared to uncoated cells, which served as a control (Fig. 5.16). These results confirm that MFGE8-DNASE2A has maintained its PS-binding activity and can be used for further investigations.

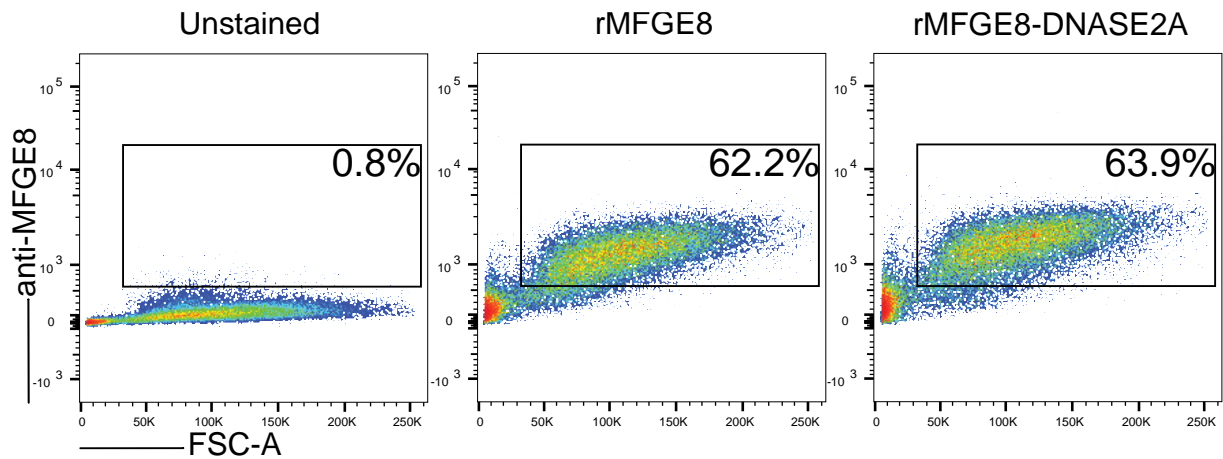


**Figure 5.16 Functional activity of MFGE8-DNASE2A**

$1 \times 10^6$  apoptotic HeLa cells were incubated with equimolar concentration of rMFGE8 or MFGE8-DNASE2A fusion protein for 30 minutes at  $4^\circ\text{C}$ . Samples were then stained with anti-MFGE8 for 30 minutes at  $4^\circ\text{C}$ . Shown here are one representative FACS plots for one fusion protein production out of two independent production.

### 5.3.4 Efficacy of MFGE8-DNASE2A to recover phagocytosis defect

To investigate if MFGE8-DNASE2A can be used to recover the phagocytosis defect in C1q-KO mice an *in vivo* phagocytosis assay was performed. Briefly, apoptotic H2b-mCherry HeLa cells were coated with equimolar concentrations of either rMFGE8 or MFGE8-DNASE2A or left uncoated before injection into WT and C1q-KO. The peritoneal lavage was harvested after 7 hours and stained for CD11b and live cell markers for imaging flow cytometric analysis (Fig. 5.17A).

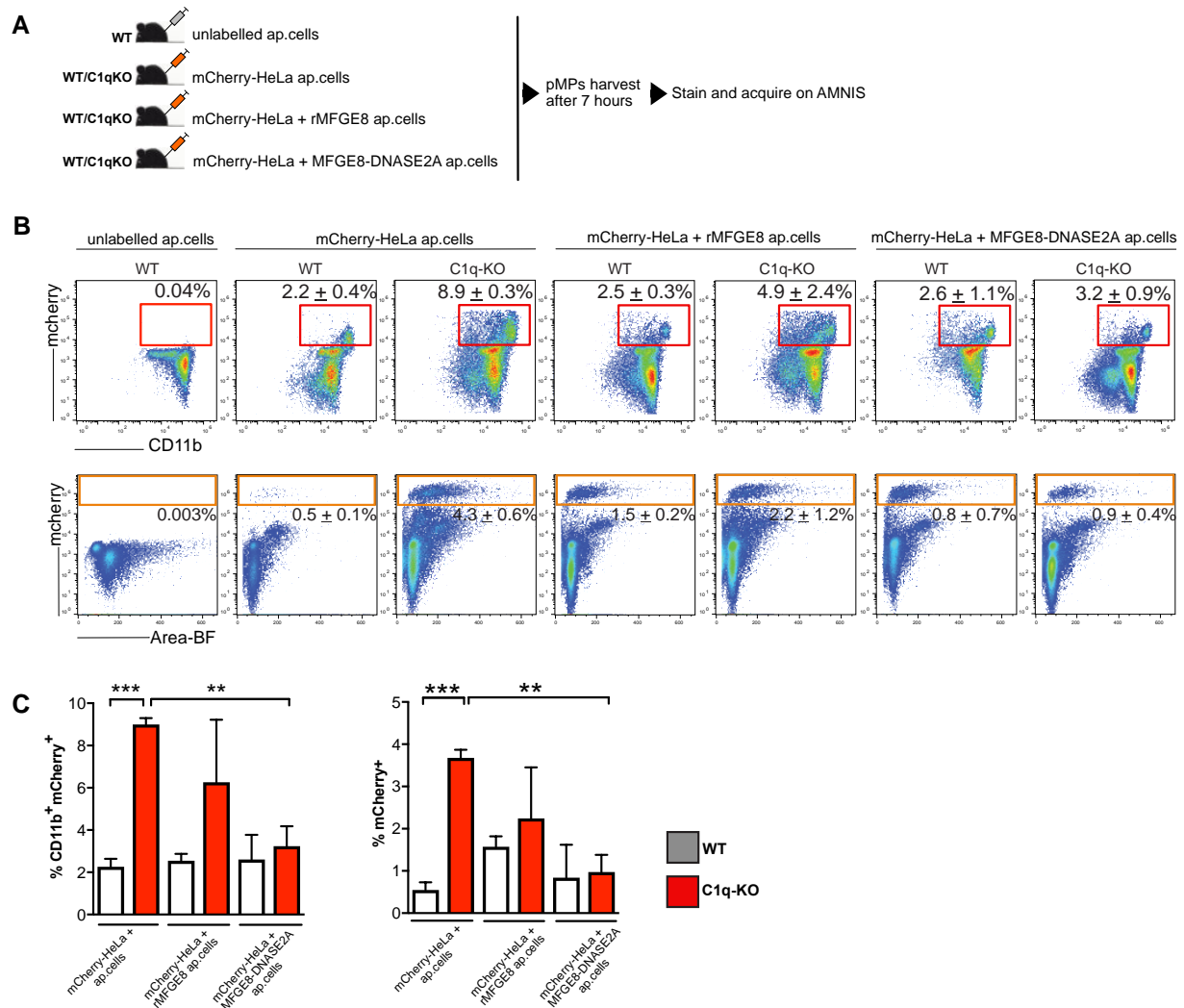


**Figure 5.17 MFGE8-DNASE2A restores delayed degradation of nuclear material in C1q-KO mice**

- A.  $10 \times 10^6$  apoptotic mCherry HeLa cells were incubated with equimolar concentration of rMFGE8 or MFGE8-DNASE2A fusion protein for 30 minutes at 4°C.  $10 \times 10^6$  apoptotic mCherry HeLa cells were injected either as uncoated, rMFGE8 coated or MFGE8-DNASE2A coated in separate groups to WT and C1q-KO mice. WT (n = 3) and C1q-KO (n = 3) for each group was injected with apoptotic mCherry HeLa cells and WT (n = 1) injected with apoptotic unlabelled HeLa cells as control. pMPs from WT and C1q-KO mice were flushed following 7 hours of *in vivo* phagocytosis. Single cell suspension was stained and fixed for acquisition on image stream flow cytometry.
- B. The upper panel shows representative FACS plots for CD11b<sup>+</sup>mCherry<sup>+</sup> MPs which have taken up mCherry tagged apoptotic cells following 7 hours of *in vivo* phagocytosis. Cells are gated on live cells. The lower panel shows representative FACS plots for mCherry<sup>+</sup> cells (unengulfed cells) where it is gated on all cells. The FACS plots of one out of two independent experiments with similar outcome (n = 3-4 animals per group) are shown.
- C. The frequency as percentage of CD11b<sup>+</sup> mCherry<sup>+</sup> (left panel) and mCherry<sup>+</sup> (right panel) is quantified and shown. Statistically significant differences between WT and C1q-KO mice: \*\* (p < 0.01), \*\*\* (p < 0.05).

The frequency of CD11b<sup>+</sup>mCherry<sup>+</sup> cells was significantly increased at least by four-fold in C1q-KO mice compared to WT following 7 hours of *in vivo* phagocytosis (p = 0.001). When C1q-KO mice received MFGE8-coated apoptotic cells, the frequency of CD11b<sup>+</sup>mCherry<sup>+</sup> cells were decreased by 2-fold. Importantly, however, when C1q-KO mice received MFGE8-DNASE2A coated apoptotic cells there was a further reduction of

CD11b<sup>+</sup>mCherry<sup>+</sup> cells to WT levels in comparison to C1q-KO mice injected with uncoated apoptotic cells ( $p = 0.004$ ) (Fig. 5.17B, upper panel and Fig. 5.17C, left panel).

The unengulfed cells represent the injected apoptotic H2b-mCherry HeLa cells which are not taken by the MPs and gated as CD11b<sup>+</sup>mcherry<sup>high</sup>. The frequency of unengulfed cells in C1q-KO mice which received uncoated apoptotic cells shows a significant increase by four-fold. However, we saw an almost two-fold reduction in the frequency of unengulfed cells in C1q-KO mice injected with MFGE8-coated apoptotic cells. In addition, we also observed a more striking significant reduction in the frequency of unengulfed cells in C1q-KO mice which received MFGE8-DNASE2A coated apoptotic cells ( $p = 0.003$ ) (Fig. 5.17B, lower panel and Fig. 5.17C, right panel).

Thus, from these observations it is evident that administration of MFGE8-DNASE2A coated apoptotic cells seems to increase the rate of phagocytosis and also promotes the apoptotic DNA degradation in C1q-KO mice. This strategy is more efficient in comparison to administration of MFGE8 coated apoptotic cells. Due to the higher efficiency of MFGE8-DNASE2A over MFGE8 in rectifying the delayed uptake and degradation of apoptotic cells we next investigated if this had an impact on the inflammation in C1q-KO mice.

### **5.3.5 Efficacy of MFGE8-DNASE2A to reduce inflammation in C1q-KO mice**

Since the administration of MFGE8-DNASE2A coated apoptotic cells helped to restore the delayed uptake and degradation of apoptotic material in C1q-KO mice, we expected an impact on the onset of inflammatory signals.

In order to address if MFGE8-DNASE2A has the capability to reduce the inflammatory responses induced by an elevated accumulation of phagocytosed material inside C1q-KO MPs, uncoated apoptotic cells, or apoptotic cells coated with equimolar concentration of rMFGE8 or MFGE8-DNASE2A were injected into WT and C1q-KO mice. The peritoneal lavage was then harvested and analyzed for inflammatory parameters both at gene and protein level (Fig. 5.18A).

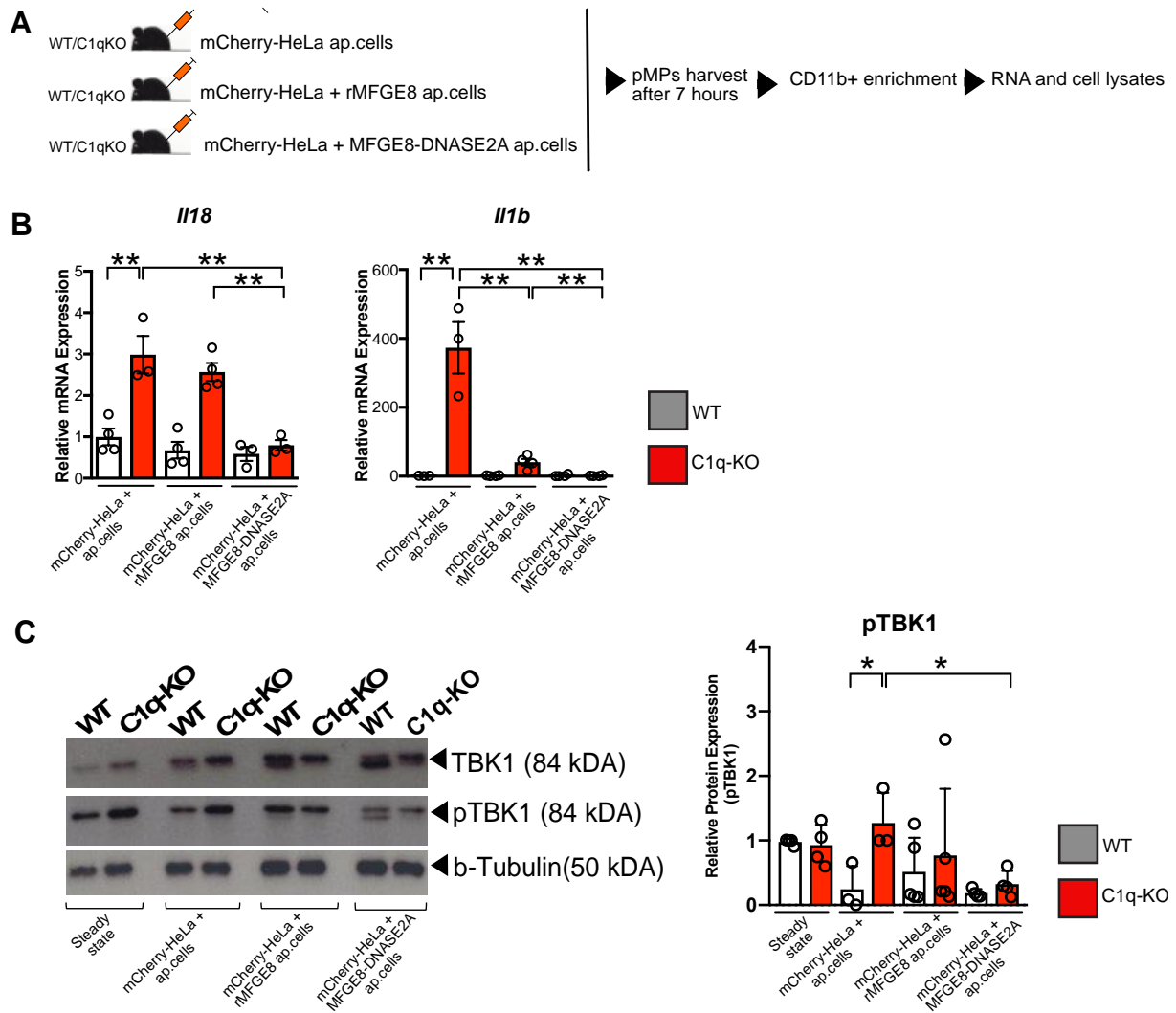


**Figure 5.18 Inflammation induced by impaired degradation is reduced by MFGE8-DNASE2A in C1q-KO mice:**

- A.  $10 \times 10^6$  apoptotic HeLa cells were incubated with equimolar concentration of rMFGE8 or MFGE8-DNASE2A fusion protein for 30 minutes at 4°C.  $10 \times 10^6$  apoptotic mcherry HeLa cells were injected either as uncoated or MFGE8-coated or MFGE8-DNASE2A-coated in separate groups to WT and C1q-KO mice. WT (n = 3-4) and C1q-KO (n = 3-4) for each group were injected with apoptotic mCherry HeLa cells. pMPs from WT and C1q-KO mice were flushed following 7 hours of *in vivo* phagocytosis and enriched for CD11b<sup>+</sup> pMPs by MACS.
- B. 1 µg of RNA from the enriched CD11b<sup>+</sup> pMPs was reverse transcribed and used for quantifying mRNA levels of *IL18* and *IL1b*. Shown data are relative expression quantified with GAPDH as housekeeping control. All bar graphs represent mean ± standard error mean (SEM). Statistical significance was analyzed using a student's t-test with \*: p < 0.05, \*\* p < 0.01, \*\*\* p < 0.001. Shown here are data from one representative experiment out of two.
- C. Western blot showing TBK1 and pTBK1 levels in pMPs of WT (n = 2) and C1q-KO (n = 2) at steady state and following *in vivo* phagocytosis with each treatment. The relative expression is quantified with b-tubulin as housekeeping control. Shown western blot is a one representative out of three experiments and data for bar graphs is pooled from two independent experiments.

cDNA from CD11b<sup>+</sup> pMPs was used for quantification of inflammatory markers at mRNA level. C1q-KO mice that received uncoated apoptotic cells, showed a significant increase in gene expression of *Il18* (p = 0.006) compared to WT mice. However, C1q-KO mice that received rMFGE8-coated apoptotic cells showed no significant difference in the gene

expression of *Il18* as compared to these mice administered with uncoated apoptotic cells. Nevertheless, upon administration of MFGE8-DNASE2A coated apoptotic cells there is a significant reduction in the *Il18* expression between C1q-KO mice exposed to either uncoated ( $p = 0.0094$ ) or rMFGE8 coated apoptotic cells ( $p = 0.0014$ ) at gene level (Fig. 5.18B, left panel). Next, C1q-KO mice exposed to uncoated apoptotic cells, showed a significant increase in gene expression of *IL1b* ( $p = 0.0077$ ) compared to WT mice. In addition, administration of rMFGE8 coated apoptotic cells to C1q-KO mice significantly reduced the gene expression of *Il1b* compared to these mice that received uncoated apoptotic cells ( $p = 0.0034$ ). However, administration of MFGE8-DNASE2A coated apoptotic cells to C1q-KO mice resulted in significant reduction in *IL1b* expression compared to either uncoated ( $p = 0.0019$ ) or rMFGE8 coated apoptotic cells ( $p = 0.0073$ ) at gene level (Fig. 5.18B, right panel).

These results support the idea that MFGE8-DNASE2A is successful in eliminating the excess accumulation of phagocytosed apoptotic material inside the MPs thereby reducing inflammatory cytokine production in C1q-KO mice. Since these inflammatory cytokines are induced via STING pathway it was also important to see if MFGE8-DNASE2A treatment had an impact on STING pathway. Protein lysates from CD11b<sup>+</sup> pMPs enriched by MACS were used for quantifying the levels of TBK1 and pTBK1 to in order to identify the activation status of STING pathway. Western blots showed that administration of uncoated apoptotic cells to C1q-KO MPs resulted in increased TBK1 phosphorylation, corroborating our previous findings (Fig. 5.13, middle panel). However, when rMFGE8 coated apoptotic cells were administered, TBK1 phosphorylation was reduced (Fig. 5.18C). Application of the fusion protein MFGE8-DNASE2A to apoptotic cells could reduce TBK1-phosphorylation even further (Fig. 5.18C), a phenomenon, which was observed not only in C1q-KO, but also in WT pMPs (Fig. 5.18C). A low molecular weight faint protein band observed on western blot in some of the protein samples might be due to unknown post-translational modifications. These results confirm that MFGE8-DNASE2A has a positive impact on promoting phagocytosis and degradation of nuclear material thereby reducing the inflammation via STING pathway in (Fig. 5.18C).

## 6 DISCUSSION

The clearance of apoptotic cells by phagocytosis plays an important role in protecting tissues from exposure to inflammatory and harmful contents of dying cells. There are a number of complementary receptor-ligand systems identified to facilitate phagocytosis [209]. Though the role of the complement system has been shown by many studies in phagocytosis of apoptotic cells the precise cellular mechanism of how C1q deficiency results in SLE development is unclear. The reports available so far indicate C1q can have a dual role, both protective and a detrimental in SLE pathogenesis. This study was aimed to investigate the possible mechanisms of how C1q deficiency contributes towards lupus pathogenesis using a homozygous knockout of C1q on a mixed background. We observed a delayed degradation of nuclear material derived from apoptotic cells in C1q-KO mice. This is due to the DNASE2A deficiency in C1q-KO MPs. Due to this longer retention of nuclear material inside the cytosol, STING pathway is triggered which is responsible for inducing inflammatory phenotype in C1q-KO mice. We also observed disturbances in endo-lysosomal system of C1q-KO MPs. Nevertheless, it is still unclear why C1q-KO mice exhibit these lysosomal defects.

### 6.1 C1q-KO mice exhibit a phagocytosis defect

C1q has been shown to bind directly to the surface blebs of apoptotic cells *in vitro* [163], [210], [211], indicating that it promotes their clearance thereby preventing further activation of immune system by autoantigens. In order to investigate the influence of C1q on phagocytosis an *in vivo* phagocytosis assay was performed. We have shown that C1q-KO MPs phagocytose apoptotic material slower than control mice *in vivo*. In addition, an unexpected finding was a significant increase in the frequency of MPs with non-degraded apoptotic nuclear material in C1q-KO mice (Fig.

5.1). The uptake defect in C1q-KO mice observed in our study is in agreement with a previous study wherein it was shown that homozygous C1q deficiency on a mixed background mouse develop glomerulonephritis by a C3-independent pathway. These mice had significantly higher amounts of autoantibodies and uncleared apoptotic cells in the kidneys which implicate a phagocytosis defect [169]. In addition, a similar uptake defect was also observed in lupus prone MRL/Mp or NZB/W resident pMPs both *in vivo* and *in vitro* [212]. However, up to now an impaired degradation of phagocytosed material in C1q-KO mice and other lupus prone mice has never been reported. Nevertheless, MFGE8-deficient mice on a C57Bl/6x129 genetic background developed lupus due to defective uptake as well as an altered intracellular processing which results in enhanced self-antigen presentation [213]. It has been shown that an appropriate time point is important while investigating the differences in apoptotic cell uptake by MPs [186]. Unlike the previous studies in our experiments we analysed the apoptotic cell uptake following 3 hours to 16 hours *in vivo* which gave us information regarding not only the uptake, but also the degradation of engulfed apoptotic cells. So far it was hypothesized that during C1q deficiency unengulfed apoptotic cells act as a trigger for interferon (IFN) production. Therefore, we followed to study the consequences for the longer retention of nuclear material inside C1q-KO MPs.

## **6.2 Inflammation is a consequence of phagocytosis defect in C1q-KO mice**

Our proteome analysis revealed that C1q-KO splenic enriched MPs exhibit reduced expression of lysosomal hydrolases and other proteases. We observed that DNASE2A, an important lysosomal hydrolase was significantly downregulated in C1q-deficient splenic enriched MPs both at gene and protein level. DNASE2A has been previously shown to degrade the nuclei expelled from the erythroid precursors or DNA

following the engulfment of apoptotic cells by MPs [214]. In addition, it was also shown that many MPs containing undigested DNA accumulates in the fetal liver of DNASE2A deficient embryos [215],[216]. From earlier studies it was evident that DNASE2A<sup>-/-</sup> embryos die *in utero* late in embryogenesis due to high levels of type-1 IFN [189]. In addition, conditional ablation of DNASE2A and IFNAR in mice leads to the production of inflammatory cytokines such as *IL6*, *TNF $\alpha$* , *CXCL10*, *IL1 $\beta$*  and other type-1 IFNs. These mice eventually succumb to autoimmune disease associated with polyarthritis [217]. Therefore, we speculated that a delay in degradation of nuclear material observed in C1q-KO mice might be due to DNASE2A deficiency.

We could show that following an *in vivo* phagocytosis, C1q-KO mice show elevated pro-inflammatory cytokine levels such as *IL1 $\beta$* , *CXCL10*, *IL18* and *TNF $\alpha$*  (Fig. 5.12) which is in concordance with these previous studies. The secretion of pro-inflammatory cytokines such as *IFN $\alpha$* , *IL1 $\beta$* , *IL18*, *TNF $\alpha$*  has been shown to promote tissue damage in SLE patients [218]–[221]. As a consequence, circulating immune complex deposits in organs and joints resulting in complement system activation which in turn attracts many innate immune cells thereby promoting local inflammation. In addition, pDCs are activated by immune complex deposits which also favours IFN- $\alpha$  secretion. As a result of a persistent inflammatory milieu, irreversible organ damage occurs thereby turning into a vicious cycle by increasing the load of apoptotic cells [80], [222]. Unfortunately, in our experiments *IFN $\beta$*  or *IFN $\alpha$*  levels by qPCR could not be detected and further investigations using a high sensitivity ELISA is required to confirm these results.

Furthermore, the STING pathway was activated causing elevated expression of TBK1 and pTBK1 in C1q-KO mice during an *in vivo* phagocytosis assay. This implies that non-degraded DNA inside the MPs is sensed by cGAS which further activates the STING pathway and results in an inflammatory phenotype in C1q-KO mice. This is in

line with a previous finding which demonstrates the role of STING by transplanting DNASE2A deficient bone marrow to WT mice. Following transplantation, these mice developed inflammatory arthritis similar to systemic-onset juvenile idiopathic arthritis [190]. However, the ablation of STING resulted in reversal of the inflammatory phenotype and improved the survival rate which further indicates the importance of STING [205].

Apart from STING there are other cytosolic sensing mechanisms through which inflammation is induced such as absent in melanoma (AIM2). AIM2 acts independent of the STING pathway. This was shown with the triple deficient DNASE2A<sup>-/-</sup>/IFNAR<sup>-/-</sup>/STING<sup>-/-</sup> mice which exhibit autoantibody production [223]. At this point, it was evident that DNASE2A also regulates inflammation and autoimmunity through other mechanisms. However, deletion of UNC93B1, a major adaptor for TLR7 and TLR9, on a DNase2a<sup>-/-</sup>/IFNAR<sup>-/-</sup> background blocked autoantibody production but fails to confer protection from arthritis [224]. In addition, DNase2a<sup>-/-</sup>AIM2<sup>-/-</sup> mice were lethal supporting the notion that AIM2 is not a pathway responsible for triggering inflammation in DNASE2A deficient mice [223]. Thus, from above studies it is evident that DNASE2A plays multiple critical roles in regulating or preventing DNA-driven inflammation.

Taken together, due to DNASE2A deficiency in C1q-KO MPs the nuclear material is retained longer in its cytosol. Furthermore, this longer retention of DNA triggers the cytosolic sensing pathways via cGAS-STING axis and results in an inflammatory phenotype in C1q-KO. Moreover, autoantibodies detected in SLE patients are mostly against DNA and nuclear material. Our results so far may indicate that the undegraded material may escape cells as self-antigens and thereby trigger autoantibody production.

### **6.3 C1q-KO mice exhibit a dysfunctional phagocytic machinery**

Our proteome analysis also revealed that C1q-KO pMPs exhibit a significant reduction in important RAB-GTPases such as RAB5, RAB9 AND RAB11FIP1. RAB5 has been demonstrated to regulate tethering and fusion of early endosomes thereby playing a critical role in phagosome maturation. RAB5 is also required for the recruitment of RAB7 which regulates the phagosome fusion with late endosomes to facilitate the elimination of apoptotic cells [101], [194]. More recently it was shown that reduction of RAB5 in hepatocytes results in loss of the endo-lysosomal pathway by almost 80% accompanied by a reduction in lysosomes and recycling endosomes [191]. Consistent with this notion, our results indicate that the RAB5 reduction in C1q-KO MPs destabilizes the endo-lysosomal pathway required for effective degradation of phagocytosed apoptotic material. This further correlates with an accumulation of enlarged lysosomes as seen in C1q-KO MPs which is essential for efficient degradation of ingested apoptotic cells. LAMP1 and LAMP2 dysfunctional MPs exhibit an arrested phagosomal maturation although these MPs phagocytosed particles normally [225]. In addition, these lysosomes have an impaired ability to move towards the microtubule organizing centre which further hinders the interaction with other phagosomal compartments [225]. Our results strongly suggest that C1q-KO MPs fail to establish a functional phagocytic machinery causing reduced lysosomal DNASE2A levels.

Furthermore, our proteomic screen showed a reduction in V-ATPases such as ATP6v1f and ATP6v1b2 in C1q-KO splenic MPs. Vacuolar H<sup>+</sup>-ATPase (v-ATPase) is a multimeric proton pump involved in pH homeostasis, membrane trafficking and protein degradation [226]. It is required for the acidification of lysosomes, late endosomes, autophagic and phagocytic vesicles [227], [228]. Therefore, it is likely that C1q-KO MPs have an acidification defect due to a reduction in important V-ATPases.

However, from LysoTracker staining of pMPs no substantial differences between WT and C1q-KO mice in the LysoTracker intensities were seen (Fig. 5.8). This might indicate that acidic compartments are functional in C1q-KO mice. Nevertheless, when investigated by immunofluorescence, surprisingly, we could observe a reduced co-localization of LysoTracker with the lysosomal compartments in C1q-KO MPs (Fig. 5.9). This suggests that acidification inside the lysosomes could be impaired in C1q-KO mice. It has been shown from previous studies that proper lysosomal acidification is required for optimal degradative activity of lysosomal hydrolases [229]. Furthermore, it has been reported that impaired lysosomal acidification contributes to lysosomal storage disorders (LSDs) such as Batten disease [230]–[232]. In addition, defective lysosomal acidification regulation has been reported in Alzheimer and Parkinson diseases [233]–[235]. The reduction of lysosomal acidification in MPs could be also an underlying reason for DNASE2A reduction in C1q-KO MP since it is shown that DNASE2A functional activity requires an optimal acidic pH inside the lysosomal compartment [236].

#### **6.4 Diminished TFEB expression in C1q-KO MPs**

The biogenesis and further functioning of endosomal-lysosomal pathway is controlled by the transcription factor EB (TFEB) which regulates almost 471 genes that constitute the CLEAR gene network (coordinated lysosomal expression and regulation). The CLEAR network includes numerous lysosomal hydrolases, membrane proteins and acidification proteins [204], [237]. It has also been shown that TFEB overexpression results in an elevated number of lysosomes and higher levels of lysosomal enzymes thereby subsequently increases the lysosomal catabolic activity [202].

To this end, TFEB expression was quantified by immunofluorescence and we could observe that the TFEB expression was reduced in C1q-KO pMPs at steady state.

Therefore, the diminished expression of TFEB could be a reason for the impaired lysosomal biogenesis seen in C1q-KO mice. From earlier studies, it was shown that TFEB overexpression favours MHC-II dependent antigen presentation by enhancing lysosome hydrolytic activity and preserving exogeneous antigens [238]. Moreover, recently it was identified that Fc $\gamma$  receptor activation during phagocytosis promotes TFEB translocation to nucleus. In addition, upregulation in TFEB expression occurs during phagosomal maturation with the help of lysosomal Ca<sup>2+</sup> release [239]. Indeed, it was also shown that TFEB overexpression helps to resolve some defects in lysosomal storage disorders [240], [241].

In summary, C1q-KO mice exhibit multiple defects in the endo-lysosomal machinery. Defects in lysosomal acidification together with the inability to establish a stable phagocytic machinery in C1q-KO pMPs could be a plausible explanation for the reduced DNASE2A levels. Moreover, C1q-KO pMPs also show reduced TFEB expression which is a major transcription factor for lysosomal biogenesis.

## **6.5 MFGE8-DNASE2A administration does have a therapeutic potential**

Our data suggest that MFGE8-DNASE2A fusion protein is efficient not only to restore DNA degradation but also to improve uptake of apoptotic cells in C1q-KO mice. MFGE8 was previously implicated in regulating phagocytosis through its interaction with Crk-DOCK180-Rac1 pathway. Rac1 aggregates at the cell membrane which further promotes the formation of protrusion thereby facilitating phagocytosis [242]. The inflammatory phenotype observed in C1q-KO following *in vivo* phagocytosis was resolved when MFGE8-DNASE2A coated apoptotic cells were administered. In addition, administration of MFGE8-DNASE2A coated apoptotic cells were more efficient compared apoptotic cells coated with rMFGE8 only in resolving phagocytosis defects as well as inflammation (Fig 5.18). In the context of previously reported findings, we noticed that rMFGE8 promotes phagocytosis and partially compensates

for the uptake defect observed in C1q-KO mice. MFGE8 has been known to inhibit the release of pro-inflammatory cytokines such as IL-1 $\beta$ , TNF- $\alpha$  and IL-6 by suppressing MAPK, NF- $\kappa$ B, ERK1/2 activation, thus plays an important role in anti-inflammation [243]–[245]. However, surprisingly we saw that there was no reduction in the *IL18* levels in C1q-KO mice when they were administered rMFGE8 coated apoptotic cells. We speculate at this point that rMFGE8 promotes phagocytosis and given the inability of C1q-KO MPs to degrade DNA the high load of cytosolic DNA might favour IL18 production. Taken together, the fusion of MFGE8 to DNASE2A provides a tool for increasing the amount of DNASE2A inside the C1q-KO MPs thereby providing a promising tool for the treatment of autoimmune disorders associated with aberrant recognition of self-DNA.

## 7 GRAPHICAL ABSTRACT

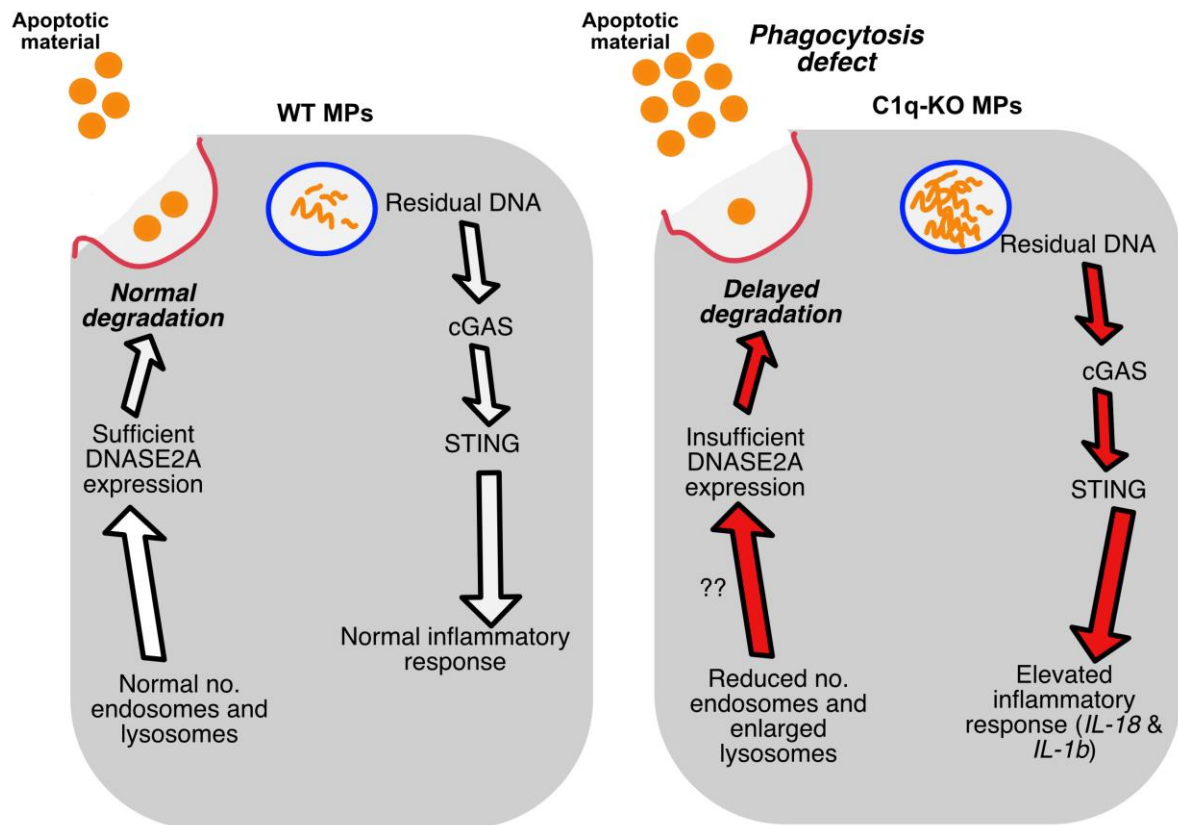


**Figure 7.1 Model for generation of autoimmunity in C1q-KO mice**

WT MPs (left) take up apoptotic cells (orange) and degrade them inside the lysosomal compartments. WT MPs exhibit normal endo-lysosomal system with sufficient DNASE2A expression inside the lysosomes. The residual DNA inside the lysosomes is sufficient to activate STING pathway and results in normal inflammatory responses.

C1q-KO MPs (right) take up apoptotic cells (orange) and degrade slowly compared to WT. C1q-KO MPs disturbed endo-lysosomal system with insufficient DNASE2A expression inside the lysosomes. The load of residual DNA inside the lysosomes is more compared to WT MPs. This increased residual DNA leads to aberrant activation of STING pathway (red arrows) and results in elevated inflammatory responses.

## 8 OUTLOOK

SLE is a complex disease with great heterogeneity in symptoms. Novel immunotherapies under development include targeting co-stimulatory molecules, cytokines or its respective receptors, cell based and peptide therapies. However, there is a need to explore the wide array of immunotherapies due to its high failure rate in clinical trials. Our *in vivo* results from mouse models are promising and it is important to investigate DNASE2A expression in lupus patients. To achieve this, in future studies monocytes from lupus patients will be used to quantify *DNase2a* on RNA and protein level, respectively. Our strategy to restore DNASE2A function in MPs by fusing DNASE2A to the apoptotic-cell binding protein MFGE8 could lead to novel therapeutic approaches for the treatment of lupus patients.

## 9 APPENDIX

### 9.1 Spleen enriched MPs proteomics

<b>Downregulated (1.2 fold)</b>	
<b>Gene Name</b>	<b>Protein Name</b>
Cmb1	Carboxymethylenebutenolidase homolog
Akr1b7	Aldo-Keto Reductase Family 1 Member B7
Vcam1	Vascular cell adhesion protein 1
Gpd1	Glycerol-3-Phosphate Dehydrogenase 1
Crip2	Cysteine-rich protein 2
Emr1	Adhesion G protein-coupled receptor E1
Asah1	Acid ceramidase
Itga9	Integrin $\alpha$ - 9
DNase2a	Deoxyribonuclease-2-alpha
C3	Complement C3
CtsB	Cathepsin B
CtsD	Cathepsin D
Man2b2	Epididymis-specific alpha-mannosidase
Bloc1s1	Biogenesis of Lysosomal Organelles Complex 1 Subunit 1
LAMP2	Lysosomal-associated membrane protein 2
Lipa	Lysosomal acid lipase
ATP6v1b2	ATPase H <sup>+</sup> Transporting V1 Subunit B2
ATP6v1f	ATPase H <sup>+</sup> Transporting V1 Subunit F

<b>Upregulated (1.2 fold)</b>	
<b>Gene Name</b>	<b>Protein Name</b>
PepD	Peptidase D
Aurka	Aurora Kinase A
Abt1	Activator Of basal Transcription 1
Pacsin1	Protein Kinase C And Casein Kinase Substrate In Neurons 1
CtsA	Cathepsin A
Lamp1	Lysosomal - associated membrane protein 1
ATP6v0c	ATPase H <sup>+</sup> Transporting V0 Subunit C

## 9.2 pMPs proteomics

<b>Downregulated candidates (3 - fold)</b>	
<b>Gene Name</b>	<b>Protein Name</b>
C1qa	Complement subunit A
Ctse	Cathepsin A
Dr1	Protein Dr1
Fscn1	Ficolin-1
Hgsnat	Heparan-alpha-glucosaminide N-acetyltransferase
Vamp7	Vesicle-associated membrane protein 7
Vamp8	Vesicle-associated membrane protein 8
Lamp1	Lysosomal-associated membrane protein 1
Lamp2	Lysosomal-associated membrane protein 2
Lipa	Lysosomal acid lipase
Man2b2	Mannosidase Alpha Class 2B Member 2
Rab5b	Ras-related protein Rab-5B
Rab9a	Ras-related protein Rab-9a
Rab11b	Ras-related protein Rab-11b
Rassf2	Ras Association Domain Family Member 2
Rab11fip1	RAB11 Family Interacting Protein 1
Rpl28	60S ribosomal protein L34
Rpl34	60S ribosomal protein L34
S100a11	S100 Calcium Binding Protein A11
Syne1	Spectrin Repeat Containing Nuclear Envelope Protein 1
Vasp	Vasodilator Stimulated Phosphoprotein

<b>Upregulated candidates (3 - fold)</b>	
<b>Gene Name</b>	<b>Protein Name</b>
Fcgr2	Low affinity immunoglobulin gamma Fc region receptor II
Serpinb10	Serpin peptidase inhibitor, clade B (ovalbumin), member 10
Retnla	Resistin-like alpha
CtsE	Cathepsin E
Chil4	Chitinase-like protein 4
Gna01	Guanine nucleotide-binding protein G(o) subunit alpha
Arg1	Arginase-1
Slc7a2	Cationic amino acid transporter 2
Chil3	Chitinase-like protein 3
Slc11a1	Natural resistance-associated macrophage protein 1
Golga3	Golgin subfamily A member 3
Grk6	G protein-coupled receptor kinase 6
Ppp6c	Serine/threonine-protein phosphatase 6 catalytic subunit
D2hgdh	D-2-hydroxyglutarate dehydrogenase, mitochondrial

### 9.3 Primer sequences

Gene	FP (5' – 3')	RP (5' – 3')	Annealing Temperature
<i>DNase2a</i>	TGGAAGGCTTCTTCGCTCAG	CTGGACCTGTAGGTTGGTGC	56
<i>Rab5</i>	CCAACGGGCCAAATACTGGA	ACCGTTCTTGACCAGCTGTA	56
<i>Rab9</i>	GGACAACGGCGACTATCCTT	GAGTTTGGCTTGGGCTTTTCG	56
<i>Lamp1</i>	CCTACGAGACTGCGAATGGT	CCACAAGAACTGCCATTTTTTC	56
<i>Tfeb</i>	GCATCAGAAGGTTTCGGGAGT	CGGGGTTGGAGCTGATATGT	56
<i>Cxcl10</i>	GCCGTCATTTTCTGCCTCATC	TAGGCTCGCAGGGATGATTTTC	56
<i>Il18</i>	GGCTGCCATGTCAGAAGACTC	GTGAAGTCGGCCAAAGTTGT	56
<i>Il1β</i>	CAGGCAGGCAGTATCACTCA	AGCTCATATGGGTCCGACAG	56
<i>Tnfα</i>	GAACTGGCAGAAGAGGCACT	AGGGTCTGGGCCATAGAACT	56
<i>Gapdh</i>	GGGTTCTATAAATACGGACTGC	CCATTTTGTCTACGGGACGA	56

## 10 REFERENCES

- [1] M. Stebegg, K. Saumya, S. Alyssa, R. Valter, A. Michelle, and G. Luis, "Regulation of the Germinal Center response," *Front. Immunol.*, vol. 9, no. October, pp. 1–13, 2018.
- [2] R. Van Furth, "Current View on the Mononuclear Phagocyte System," *Immunobiology*, vol. 161, no. 3–4, pp. 178–185, 1982.
- [3] R. van Furth, Z. A. Cohn, J. G. Hirsch, J. H. Humphrey, W. G. Spector, and H. L. Langevoort, "The mononuclear phagocyte system: a new classification of macrophages, monocytes, and their precursor cells.," *Bull. World Health Organ.*, vol. 46, no. 6, pp. 845–852, 1972.
- [4] L. C. Davies, S. J. Jenkins, J. E. Allen, and P. R. Taylor, "Tissue-resident macrophages," *Nat. Immunol.*, vol. 14, no. 10, pp. 986–995, 2013.
- [5] A. Mildner and S. Jung, "Development and function of dendritic cell subsets," *Immunity*, vol. 40, no. 5, pp. 642–656, 2014.
- [6] C. D. Mills, K. Kincaid, J. M. Alt, M. J. Heilman, and A. M. Hill, "M-1/M-2 Macrophages and the Th1/Th2 Paradigm," *J. Immunol.*, vol. 164, no. 12, pp. 6166–6173, 2000.
- [7] L. M. Stuart and R. A. B. Ezekowitz, "Phagocytosis: Elegant complexity," *Immunity*, vol. 22, no. 5, pp. 539–550, 2005.
- [8] Y. Lavin, D. Winter, R. Blecher-Gonen, E. David, H. Keren-Shaul, M. Merad, S. Jung, and I. Amit, "Tissue-Resident Macrophage Enhancer Landscapes Are Shaped by the Local Microenvironment," *Cell*, vol. 159, no. 6, pp. 1312–1326, 2014.
- [9] K. Takahashi, F. Yamamura, and M. Naito, "Differentiation, maturation, and proliferation of macrophages in the mouse yolk sac: A light-microscopic, enzyme-cytochemical, immunohistochemical, and ultrastructural study," *J. Leukoc. Biol.*, vol. 45, no. 2, pp. 87–96, 1989.
- [10] C. Schulz, E. G. Perdiguero, L. Chorro, H. Szabo-Rogers, N. Cagnard, K. Kierdorf, M. Prinz, B. Wu, S. E. W. Jacobsen, J. W. Pollard, J. Frampton, K. J. Liu, and F. Geissmann, "A Lineage of Myeloid Cells Independent of Myb and Hematopoietic Stem Cells," *Science (80-. )*, vol. 336, no. 6077, pp. 86–90, 2012.
- [11] F. Ginhoux, M. Greter, M. Leboeuf, S. Nandi, P. See, M. F. Mehler, S. J. Conway, L. G. Ng, E. R. Stanley, M. Igor, and M. Merad, "Fate Mapping Analysis Reveals That Adult Microglia Derive from Primitive Macrophages," *Science (80-. )*, vol. 330, no. 6005, pp. 841–845, 2010.
- [12] M. Naito, K. Takahashi, and S. Nishikawa, "Development, differentiation, and maturation of macrophages in the fetal mouse liver.," *J. Leukoc. Biol.*, vol. 48, no. 1, pp. 27–37, 1990.
- [13] G. Hoeffel, Y. Wang, M. Greter, P. See, P. Teo, B. Malleret, M. Leboeuf, D. Low, G. Oller, F. Almeida, S. H. Y. Choy, M. Grisotto, L. Renia, S. J. Conway, E. R. Stanley, J.

- K. Y. Chan, L. G. Ng, I. M. Samokhvalov, M. Merad, and F. Ginhoux, "Adult Langerhans cells derive predominantly from embryonic fetal liver monocytes with a minor contribution of yolk sac-derived macrophages," *J. Exp. Med.*, vol. 209, no. 6, pp. 1167–1181, 2012.
- [14] M. Guilliams, I. De Kleer, S. Henri, S. Post, L. Vanhoutte, S. De Prijck, K. Deswarte, B. Malissen, H. Hammad, and B. N. Lambrecht, "Alveolar macrophages develop from fetal monocytes that differentiate into long-lived cells in the first week of life via GM-CSF," *J. Exp. Med.*, vol. 210, no. 10, pp. 1977–1992, 2013.
- [15] S. Epelman, K. J. Lavine, A. E. Beaudin, D. K. Sojka, J. A. Carrero, B. Calderon, T. Brija, E. L. Gautier, S. Ivanov, T. Ansuman, J. D. Schilling, R. Schwendener, I. Sergin, B. Razani, C. Forsberg, W. Yokoyama, E. R. Unanue, M. Colonna, J. Gwendalyn, and D. L. Mann, "Embryonic and adult-derived resident cardiac macrophages are maintained through distinct mechanisms at steady state and during Inflammation," *Immunity*, vol. 40, no. 1, pp. 91–104, 2014.
- [16] A. Dahdah, G. Gautier, T. Attout, F. Fiore, E. Lebourdais, R. Msallam, M. Daëron, R. C. Monteiro, M. Benhamou, N. Charles, J. Davoust, U. Blank, B. Malissen, and P. Launay, "Mast cells aggravate sepsis by inhibiting peritoneal macrophage phagocytosis," *J. Clin. Invest.*, vol. 124, no. 10, pp. 4577–4589, 2014.
- [17] S. Pavlou, L. Wang, H. Xu, and M. Chen, "Higher phagocytic activity of thioglycollate-elicited peritoneal macrophages is related to metabolic status of the cells," *J. Inflamm. (United Kingdom)*, vol. 14, no. 1, pp. 12–17, 2017.
- [18] E. E. B. Ghosn, A. A. Cassado, G. R. Govoni, T. Fukuhara, Y. Yang, D. M. Monack, K. R. Bortoluci, S. R. Almeida, L. A. Herzenberg, and L. A. Herzenberg, "Two physically, functionally, and developmentally distinct peritoneal macrophage subsets," *Proc. Natl. Acad. Sci.*, vol. 107, no. 6, pp. 2568–2573, 2010.
- [19] S. Yona, K.-W. Kim, Y. Wolf, A. Mildner, D. Varol, M. Breker, D. S. Ayali, S. Viukov, M. Guilliams, A. Misharin, D. A. Hume, H. Perlman, B. Malissen, E. Zelzer, and S. Jung, "Fate mapping reveals origins and dynamics of monocytes and tissue macrophages under homeostasis," *Immunity*, vol. 38, no. 1, pp. 79–91, 2013.
- [20] J. M. M. Den Haan and G. Kraal, "Innate immune functions of macrophage subpopulations in the spleen," *J. Innate Immun.*, vol. 4, no. 5–6, pp. 437–445, 2012.
- [21] M. Knutson and M. Wessling-Resnick, "Iron metabolism in the reticuloendothelial system," *Crit. Rev. Biochem. Mol. Biol.*, vol. 38, no. 1, pp. 61–88, 2003.
- [22] T. B. H. Geijtenbeek, P. C. Groot, M. A. Nolte, S. J. Van Vliet, S. T. Gangaram-Panday, G. C. F. Van Duijnhoven, G. Kraal, A. J. M. Van Oosterhout, and Y. Van Kooyk, "Marginal zone macrophages express a murine homologue of DC-SIGN that captures blood-borne antigens in vivo," *Blood*, vol. 100, no. 8, pp. 2908–2916, 2002.
- [23] Y.-S. Kang, J. Y. Kim, S. a Bruening, M. Pack, A. Charalambous, A. Pritsker, T. M.

- Moran, J. M. Loeffler, R. M. Steinman, and C. G. Park, "The C-type lectin SIGN-R1 mediates uptake of the capsular polysaccharide of *Streptococcus pneumoniae* in the marginal zone of mouse spleen.," *Proc. Natl. Acad. Sci. U. S. A.*, vol. 101, pp. 215–220, 2004.
- [24] R. E. Mebius and G. Kraal, "Structure and function of the spleen," *Nat. Rev. Immunol.*, vol. 5, no. 8, pp. 606–616, 2005.
- [25] M. Ato, H. Nakano, T. Kakiuchi, and P. M. Kaye, "Localization of Marginal Zone Macrophages Is Regulated by C-C Chemokine Ligands 21/19," *J. Immunol.*, vol. 173, no. 8, pp. 4815–4820, 2004.
- [26] A. P. Heikema, M. P. Bergman, H. Richards, P. R. Crocker, M. Gilbert, J. N. Samsom, W. J. B. Van Wamel, H. P. Endtz, and A. Van Belkum, "Characterization of the specific interaction between sialoadhesin and sialylated *Campylobacter jejuni* lipooligosaccharides," *Infect. Immun.*, vol. 78, no. 7, pp. 3237–3246, 2010.
- [27] H. Veninga, E. G. F. Borg, K. Vreeman, P. R. Taylor, H. Kalay, Y. van Kooyk, G. Kraal, L. Martinez-Pomares, and J. M. M. den Haan, "Antigen targeting reveals splenic CD169+macrophages as promoters of germinal center B-cell responses," *Eur. J. Immunol.*, vol. 45, no. 3, pp. 747–757, 2015.
- [28] E. R. Winkelmann, D. G. Widman, J. Xia, A. J. Johnson, N. van Rooijen, P. W. Mason, N. Bourne, and G. N. Milligan, "Subcapsular sinus macrophages limit dissemination of West Nile virus particles after inoculation but are not essential for the development of West Nile virus-specific T cell responses," *Virology*, vol. 450–451, pp. 278–289, 2014.
- [29] D. van Dinther, H. Veninga, S. Iborra, E. G. F. Borg, L. Hoogterp, K. Olesek, M. R. Beijer, S. T. T. Schetters, H. Kalay, J. J. Garcia-Vallejo, K. L. Franken, L. B. Cham, K. S. Lang, Y. van Kooyk, D. Sancho, P. R. Crocker, and J. M. M. den Haan, "Functional CD169 on Macrophages Mediates Interaction with Dendritic Cells for CD8+T Cell Cross-Priming," *Cell Rep.*, vol. 22, no. 6, pp. 1484–1495, 2018.
- [30] L. L. Chen, J. C. Adams, and R. M. Steinman, "Anatomy of germinal centers in mouse spleen, with special reference to 'follicular dendritic cells,'" *J. Cell Biol.*, vol. 77, no. 1, pp. 148–164, 1978.
- [31] J. Kranich, N. J. Krautler, E. Heinen, M. Polymenidou, C. Bridel, A. Schildknecht, C. Huber, M. H. Kosco-Vilbois, R. Zinkernagel, G. Miele, and A. Aguzzi, "Follicular dendritic cells control engulfment of apoptotic bodies by secreting Mfge8," *J. Exp. Med.*, vol. 205, no. 6, pp. 1293–1302, 2008.
- [32] T. N. Khan, E. B. Wong, C. Soni, and Z. S. Rahman, "Prolonged apoptotic cell accumulation in germinal centers of Mer-deficient mice causes elevated B cell and CD4+helper T cell responses leading to autoantibody production," *J. Immunol.*, vol. 190, no. 4, pp. 1433–1446, 2013.
- [33] R. A. Lockshin and Z. Zakeri, "Programmed cell death and apoptosis: origins of the

- theory,” *Nat Rev Mol Cell Biol*, vol. 2, no. 7, pp. 545–550, 2001.
- [34] G. Kroemer, L. Galluzzi, P. Vandenabeele, J. Abrams, E. Alnemri, E. Baehrecke, M. Blagosklonny, W. El-Deiry, P. Golstein, D. Green, M. Hengartner, R. Knight, S. Kumar, S. a Lipton, W. Malorni, G. Nuñez, M. Peter, J. Tschopp, J. Yuan, M. Piacentini, B. Zhivotovsky, and G. Melino, “Classification of Cell Death 2009,” *Cell Death Differ.*, vol. 16, no. 1, pp. 3–11, 2009.
- [35] A. Mahajan, M. Herrmann, and L. E. Muñoz, “Clearance Deficiency and Cell Death Pathways : A Model for the Pathogenesis of SLe,” vol. 7, no. February, pp. 1–12, 2016.
- [36] A. Saraste and K. Pulkki, “Morphologic and biochemical hallmarks of apoptosis,” *Cardiovasc. Res.*, vol. 45, no. 3, pp. 528–537, 2000.
- [37] S. Elmore, “Apoptosis: A Review of Programmed Cell Death,” *Toxicol. Pathol.*, vol. 35, no. 4, pp. 495–516, 2007.
- [38] Y. L. P. Ow, D. R. Green, Z. Hao, and T. W. Mak, “Cytochrome c: Functions beyond respiration,” *Nat. Rev. Mol. Cell Biol.*, vol. 9, no. 7, pp. 532–542, 2008.
- [39] C. Loreto, G. La Rocca, R. Anzalone, R. Caltabiano, G. Vespasiani, S. Castorina, D. J. Ralph, S. Celtek, G. Musumeci, S. Giunta, R. Djinic, D. Basic, and S. Sansalone, “The role of intrinsic pathway in apoptosis activation and progression in Peyronie’s disease,” *Biomed Res. Int.*, vol. 2014, 2014.
- [40] S. Nagata, “Apoptosis by death factor,” *Cell*, vol. 88, no. 3, pp. 355–365, 1997.
- [41] P. H. Krammer, “CD95’s deadly mission in the immune system,” *Nature*, vol. 407, no. October, pp. 789–795, 2000.
- [42] A. Strasser, P. J. Jost, and S. Nagata, “The many roles of FAS receptor signaling in the immune system,” *Immunity*, vol. 30, no. 2, pp. 180–192, 2009.
- [43] T. Vanden Berghe, A. Linkermann, S. Jouan-Lanhouet, H. Walczak, and P. Vandenabeele, “Regulated necrosis: The expanding network of non-apoptotic cell death pathways,” *Nat. Rev. Mol. Cell Biol.*, vol. 15, no. 2, pp. 135–147, 2014.
- [44] C. J. Kearney and S. J. Martin, “An Inflammatory Perspective on Necroptosis,” *Mol. Cell*, vol. 65, no. 6, pp. 965–973, 2017.
- [45] D. Vercaemmen, R. Beyaert, G. Denecker, V. Goossens, G. Van Loo, W. Declercq, J. Grooten, W. Fiers, and P. Vandenabeele, “Inhibition of Caspases Increases the Sensitivity of L929 Cells to Necrosis Mediated by Tumor Necrosis Factor,” *J. Exp. Med.*, vol. 187, no. 9, pp. 1477–1485, 1998.
- [46] N. Holler, R. Zaru, O. Micheau, M. Thome, A. Attinger, S. Valitutti, J. L. Bodmer, P. Schneider, B. Seed, and J. Tschopp, “Fas triggers an alternative, caspase-8-independent cell death pathway using the kinase RIP as effector molecule,” *Nat. Immunol.*, vol. 1, no. 6, pp. 489–495, 2000.
- [47] Y. Cho, S. Challa, D. Moquin, R. Genga, T. Dutta, M. Guildford, and F. K. Chan,

- “Phosphorylation-Driven Assembly of RIP1-RIP3 Complex Regulates Programmed Necrosis and Virus-Induced Inflammation,” *Cell*, vol. 137, no. 6, pp. 1112–1123, 2009.
- [48] D. Zhang, J. Shao, J. Lin, N. Zhang, B. Lu, S. Lin, M. Dong, and J. Han, “RIP3, an Energy Metabolism Regulator That Switches TNF-Induced Cell Death from Apoptosis to Necrosis,” *Science (80-. )*, vol. 325, no. July, pp. 332–336, 2009.
- [49] S. He, L. Wang, L. Miao, T. Wang, F. Du, L. Zhao, and X. Wang, “Receptor Interacting Protein Kinase-3 Determines Cellular Necrotic Response to TNF- $\alpha$ ,” *Cell*, vol. 137, no. 6, pp. 1100–1111, 2009.
- [50] L. Sun, H. Wang, Z. Wang, S. He, S. Chen, D. Liao, L. Wang, J. Yan, W. Liu, X. Lei, and X. Wang, “Mixed lineage kinase domain-like protein mediates necrosis signaling downstream of RIP3 kinase,” *Cell*, vol. 148, no. 1–2, pp. 213–227, 2012.
- [51] C. J. Kearney, S. P. Cullen, G. A. Tynan, C. M. Henry, D. Clancy, E. C. Lavelle, and S. J. Martin, “Necroptosis suppresses inflammation via termination of TNF-or LPS-induced cytokine and chemokine production,” *Cell Death Differ.*, vol. 22, no. 8, pp. 1313–1327, 2015.
- [52] N. Borregaard, “Neutrophils, from Marrow to Microbes,” *Immunity*, vol. 33, no. 5, pp. 657–670, 2010.
- [53] A. Mantovani, M. A. Cassatella, C. Costantini, and S. Jaillon, “Neutrophils in the activation and regulation of innate and adaptive immunity,” *Nat. Rev. Immunol.*, vol. 11, no. 8, pp. 519–531, 2011.
- [54] T. A. Fuchs, U. Abed, C. Goosmann, R. Hurwitz, I. Schulze, V. Wahn, Y. Weinrauch, V. Brinkmann, and A. Zychlinsky, “Novel cell death program leads to neutrophil extracellular traps,” *J. Cell Biol.*, vol. 176, no. 2, pp. 231–241, 2007.
- [55] S. Sangaletti, C. Tripodo, C. Chiodoni, C. Guarnotta, B. Cappetti, P. Casalini, S. Piconese, M. Parenza, C. Guiducci, C. Vitali, and M. P. Colombo, “Neutrophil extracellular traps mediate transfer of cytoplasmic neutrophil antigens to myeloid dendritic cells toward ANCA induction and associated autoimmunity,” *Blood*, vol. 120, no. 15, pp. 3007–3018, 2012.
- [56] F. L. van de Veerdonk, M. G. Netea, C. A. Dinarello, and L. A. B. Joosten, “Inflammasome activation and IL-1 $\beta$  and IL-18 processing during infection,” *Trends Immunol.*, vol. 32, no. 3, pp. 110–116, 2011.
- [57] N. Hu, J. Westra, and C. G. M. Kallenberg, “Dysregulated neutrophil-endothelial interaction in antineutrophil cytoplasmic autoantibody (ANCA)-associated vasculitides: Implications for pathogenesis and disease intervention,” *Autoimmun. Rev.*, vol. 10, no. 9, pp. 536–543, 2011.
- [58] A. Schreiber and R. Kettritz, “The neutrophil in antineutrophil cytoplasmic autoantibody-associated vasculitis,” *J. Leukoc. Biol.*, vol. 94, no. 4, pp. 623–31, 2013.
- [59] J. Dieker, J. Tel, E. Pieterse, A. Thielen, N. Rother, M. Bakker, J. Fransen, H. B. P. M.

- Dijkman, J. H. Berden, J. M. De Vries, L. B. Hilbrands, and J. Van Der Vlag, "Circulating Apoptotic Microparticles in Systemic Lupus Erythematosus Patients Drive the Activation of Dendritic Cell Subsets and Prime Neutrophils for NETosis," *Arthritis Rheumatol.*, vol. 68, no. 2, pp. 462–472, 2016.
- [60] G. C. Brown, A. Vilalta, and M. Fricker, "Phagoptosis - Cell Death By Phagocytosis - Plays Central Roles in Physiology, Host Defense and Pathology.," *Curr. Mol. Med.*, vol. 15, no. 9, pp. 842–51, 2015.
- [61] D. G. Russell, "Mycobacterium tuberculosis and the intimate discourse of a chronic infection," *Immunol. Rev.*, vol. 240, no. 1, pp. 252–268, 2011.
- [62] S. Gordon, "Phagocytosis: An Immunobiologic Process," *Immunity*, vol. 44, no. 3, pp. 463–475, 2016.
- [63] S. Arandjelovic and K. S. Ravichandran, "Phagocytosis of apoptotic cells in homeostasis," *Nat Immunol*, vol. 16, no. 9, pp. 907–917, 2015.
- [64] S. Uderhardt, M. Herrmann, O. V. Oskolkova, S. Aschermann, W. Bicker, N. Ipseiz, K. Sarter, B. Frey, T. Rothe, R. Voll, F. Nimmerjahn, V. N. Bochkov, G. Schett, and G. Krönke, "12/15-Lipoxygenase Orchestrates the Clearance of Apoptotic Cells and Maintains Immunologic Tolerance," *Immunity*, vol. 36, no. 5, pp. 834–846, 2012.
- [65] W. Wood, M. Turmaine, R. Weber, V. Camp, R. A. Maki, S. R. McKercher, and P. Martin, "Mesenchymal cells engulf and clear apoptotic footplate cells in macrophageless PU.1 null mouse embryos," *Development*, vol. 127, no. 24, pp. 5245–5252, 2000.
- [66] M. R. Elliot, S. Zheng, D. Park, R. I. Woodson, M. A. Reardon, I. J. Juncadella, J. M. Kinchen, J. Zhang, J. J. Lysiak, and K. S. Ravichandran, "Unexpected requirement for ELMO1 in apoptotic germ cell clearance in vivo Michael," *Nature*, vol. 467, no. 7313, pp. 333–337, 2010.
- [67] T. Burstyn-Cohen, E. D. Lew, P. G. Traves, P. G. Burrola, J. C. Hash, and G. Lemke, "Genetic dissection of TAM receptor-ligand interaction in retinal pigment epithelial cell phagocytosis," *Neuron*, vol. 76, no. 6, pp. 1123–1132, 2012.
- [68] M. R. Elliott and K. S. Ravichandran, "The Dynamics of Apoptotic Cell Clearance," *Dev. Cell*, vol. 38, no. 2, pp. 147–160, 2016.
- [69] S. Nagata, R. Hanayama, and K. Kawane, "Autoimmunity and the Clearance of Dead Cells," *Cell*, vol. 140, no. 5, pp. 619–630, 2010.
- [70] D. R. Gude, S. E. Alvarez, S. W. Paugh, P. Mitra, J. Yu, R. Griffiths, S. E. Barbour, S. Milstien, and S. Spiegel, "Apoptosis induces expression of sphingosine kinase 1 to release sphingosine-1-phosphate as a 'come-and-get-me' signal," *FASEB J.*, vol. 22, no. 8, pp. 2629–2638, 2008.
- [71] L. Truman, C. Ford, M. Pasikowska, and Jd, "CX3CL1/fractalkine is released from apoptotic lymphocytes to stimulate macrophage chemotaxis," *Blood*, vol. 112, no. 13,

- pp. 5026–5036, 2008.
- [72] M. R. Elliott, F. B. Chekeni, P. C. Trampont, E. R. Lazarowski, A. Kadl, S. F. Walk, D. Park, R. I. Woodson, P. Sharma, J. J. Lysiak, T. K. Harden, and K. S. Ravichandran, “Nucleotides released by apoptotic cells act as a find-me signal for phagocytic clearance Michael,” *Nature*, vol. 461, no. 7261, pp. 282–286, 2009.
- [73] K. Lauber, S. G. Blumenthal, M. Waibel, and S. Wesselborg, “Clearance of apoptotic cells: Getting rid of the corpses,” *Mol. Cell*, vol. 14, no. 3, pp. 277–287, 2004.
- [74] K. Balasubramanian and A. J. Schroit, “Aminophospholipid Asymmetry: A Matter of Life and Death,” *Annu. Rev. Physiol.*, vol. 65, no. 1, pp. 701–734, 2003.
- [75] V. A. Fadok, D. R. Voelker, P. A. Campbell, J. J. Cohen, D. L. Bratton, and P. M. Henson, “Exposure of phosphatidylserine on the surface of apoptotic lymphocytes triggers specific recognition and removal by macrophages,” *J. Immunol.*, vol. 148, no. 7, pp. 2207–2216, 1992.
- [76] K. M. Kodigepalli, K. Bowers, A. Sharp, and M. Nanjundan, “Roles and regulation of phospholipid scramblases,” *FEBS Lett.*, vol. 589, no. 1, pp. 3–14, 2015.
- [77] S. Krahling, M. K. Callahan, P. Williamson, and R. A. Schlegel, “Exposure of phosphatidylserine is a general feature in the phagocytosis of apoptotic lymphocytes by macrophages,” *Cell Death Differ.*, vol. 6, no. 2, pp. 183–189, 1999.
- [78] K. Asano, M. Miwa, K. Miwa, R. Hanayama, H. Nagase, S. Nagata, and M. Tanaka, “Masking of Phosphatidylserine Inhibits Apoptotic Cell Engulfment and Induces Autoantibody Production in Mice,” *J. Exp. Med.*, vol. 200, no. 4, pp. 459–467, 2004.
- [79] K. Tada, M. Tanaka, R. Hanayama, K. Miwa, A. Shinohara, A. Iwamatsu, and S. Nagata, “Tethering of apoptotic cells to phagocytes through binding of CD47 to Src homology 2 domain-bearing protein tyrosine phosphatase substrate-1,” *J. Immunol.*, vol. 171, no. 11, pp. 5718–5726, 2003.
- [80] L. E. Muñoz, K. Lauber, M. Schiller, A. A. Manfredi, and M. Herrmann, “The role of defective clearance of apoptotic cells in systemic autoimmunity,” *Nat. Rev. Rheumatol.*, vol. 6, no. 5, pp. 280–289, 2010.
- [81] V. Le Cabec, S. Carreno, A. Moisand, C. Bordier, and I. Maridonneau-Parini, “Complement Receptor 3 (CD11b/CD18) Mediates Type I and Type II Phagocytosis During Nonopsonic and Opsonic Phagocytosis, Respectively,” *J. Immunol.*, vol. 169, no. 4, pp. 2003–2009, 2002.
- [82] R. S. Flannagan, V. Jaumouillé, and S. Grinstein, “The Cell Biology of Phagocytosis,” *Annu. Rev. Pathol. Mech. Dis.*, vol. 7, no. 1, pp. 61–98, 2012.
- [83] M. Klaas and P. R. Crocker, “Sialoadhesin in recognition of self and non-self,” *Semin. Immunopathol.*, vol. 34, no. 3, pp. 353–364, 2012.
- [84] I. M. Dambuza and G. D. Brown, “C-type lectins in immunity: Recent developments,” *Curr. Opin. Immunol.*, vol. 32, pp. 21–27, 2015.

- [85] A. Pluddemann, S. Mukhopadhyay, and S. Gordon, "Innate immunity to intracellular pathogens: Macrophage receptors and responses to microbial entry," *Immunol. Rev.*, vol. 240, no. 1, pp. 11–24, 2011.
- [86] J. Canton, D. Neculai, and S. Grinstein, "Scavenger receptors in homeostasis and immunity," *Nat. Rev. Immunol.*, vol. 13, no. 9, pp. 621–634, 2013.
- [87] R. Hanayama and S. Nagata, "Impaired involution of mammary glands in the absence of milk fat globule EGF factor 8," *Proc. Natl. Acad. Sci.*, vol. 102, no. 46, pp. 16886–16891, 2005.
- [88] R. Hanayama, M. Tanaka, and K. Miyasaka, "Autoimmune Disease and Impaired Uptake of Apoptotic Cells in MFG-E8 – Deficient Mice," *Science (80-. )*, vol. 1147, no. 2004, pp. 1147–1150, 2007.
- [89] K. Miyasaka, R. Hanayama, M. Tanaka, and S. Nagata, "Expression of milk fat globule epidermal growth factor 8 in immature dendritic cells for engulfment of apoptotic cells," *Eur. J. Immunol.*, vol. 34, no. 5, pp. 1414–1422, 2004.
- [90] H. Yamaguchi, J. Takagi, T. Miyamae, S. Yokota, T. Fujimoto, S. Nakamura, S. Ohshima, T. Naka, and S. Nagata, "Milk fat globule EGF factor 8 in the serum of human patients of systemic lupus erythematosus," *J. Leukoc. Biol.*, vol. 83, no. 5, pp. 1300–1307, 2008.
- [91] R. Hanayama, M. Tanaka, K. Miwa, A. Shinohara, A. Iwamatsu, and S. Nagata, "Identification of a factor that links apoptotic cells to phagocytes," *Nature*, vol. 417, no. 6885, pp. 182–187, 2002.
- [92] R. Hanayama, K. Miyasaka, M. Nakaya, and S. Nagata, "MFG-E8-Dependent Clearance of Apoptotic Cells, and Autoimmunity Caused by Its Failure," *Curr. Dir Autoimmun.*, vol. 9, pp. 162–172, 2006.
- [93] M. Miyanishi, K. Tada, M. Koike, Y. Uchiyama, T. Kitamura, and S. Nagata, "Identification of Tim4 as a phosphatidylserine receptor," *Nature*, vol. 450, no. 7168, pp. 435–439, 2007.
- [94] D. Park, A. C. Tosello-Tramont, M. R. Elliott, M. Lu, L. B. Haney, Z. Ma, A. L. Klibanov, J. W. Mandell, and K. S. Ravichandran, "BAI1 is an engulfment receptor for apoptotic cells upstream of the ELMO/Dock180/Rac module," *Nature*, vol. 450, no. 7168, pp. 430–434, 2007.
- [95] G. Lemke, "Biology of the TAM receptors," *Cold Spring Harb. Perspect. Biol.*, vol. 5, no. 11, pp. 1–17, 2013.
- [96] D. Park, A. Hochreiter-Hufford, and K. S. Ravichandran, "The Phosphatidylserine Receptor TIM-4 Does Not Mediate Direct Signaling," *Curr. Biol.*, vol. 19, no. 4, pp. 346–351, 2009.
- [97] N. Kobayashi, P. Karisola, V. Peña-cruz, D. M. Dorfman, S. E. Umetsu, M. J. Butte, H. Nagumo, I. Chernova, A. H. Sharpe, S. Ito, G. Dranoff, G. G. Kaplan, M. Jose, D. T.

- Umetsu, R. H. Dekruyff, and G. J. Freeman, "T cell Immunoglobulin Mucin Protein (TIM)-4 binds phosphatidylserine and mediates uptake of apoptotic cells Norimoto," *Immunity*, vol. 27, no. 6, pp. 617–632, 2009.
- [98] M. Nakayama, H. Akiba, K. Takeda, Y. Kojima, M. Hashiguchi, M. Azuma, H. Yagita, and K. Okumura, "Tim-3 mediates phagocytosis of apoptotic cells and cross-presentation," *Blood*, vol. 113, no. 16, pp. 3821–3830, 2009.
- [99] J. M. Kinchen and K. S. Ravichandran, "Phagosome maturation: Going through the acid test," *Nat. Rev. Mol. Cell Biol.*, vol. 9, no. 10, pp. 781–795, 2008.
- [100] M. Desjardins, L. A. Huber, R. G. Parton, and G. Griffiths, "Biogenesis of phagolysosomes proceeds through a sequential series of interactions with the endocytic apparatus," *J. Cell Biol.*, vol. 124, no. 5, pp. 677–688, 1994.
- [101] O. V. VIEIRA, R. J. BOTELHO, and S. GRINSTEIN, "Phagosome maturation: aging gracefully," *Biochem. J.*, vol. 366, no. 3, pp. 689–704, 2002.
- [102] J. Boulais, M. Trost, C. R. Landry, R. Dieckmann, E. D. Levy, T. Soldati, S. W. Michnick, P. Thibault, and M. Desjardins, "Molecular characterization of the evolution of phagosomes," *Mol. Syst. Biol.*, vol. 6, no. 423, 2010.
- [103] H. Stenmark, "Rab GTPases as coordinators of vesicle traffic," *Nat. Rev. Mol. Cell Biol.*, vol. 10, no. 8, pp. 513–525, 2009.
- [104] P. M. Mangahas, X. Yu, K. G. Miller, and Z. Zhou, "The small GTPase Rab2 functions in the removal of apoptotic cells in *Caenorhabditis elegans*," *J. Cell Biol.*, vol. 180, no. 2, pp. 357–373, 2008.
- [105] X. Yu, N. Lu, and Z. Zhou, "Phagocytic receptor CED-1 initiates a signaling pathway for degrading engulfed apoptotic cells," *PLoS Biol.*, vol. 6, no. 3, pp. 0581–0600, 2008.
- [106] P. Guo, T. Hu, J. Zhang, S. Jiang, and X. Wang, "Sequential action of *Caenorhabditis elegans* Rab GTPases regulates phagolysosome formation during apoptotic cell degradation," *Proc. Natl. Acad. Sci. U. S. A.*, vol. 107, no. 42, pp. 18016–18021, 2010.
- [107] B. He, X. Yu, M. Margolis, X. Liu, X. Leng, Y. Etzion, F. Zheng, N. Lu, F. A. Quiocho, D. Danino, and Z. Zhou, "Live-Cell Imaging in *Caenorhabditis elegans* Reveals the Distinct Roles of Dynamin Self-Assembly and Guanosine Triphosphate Hydrolysis in the Removal of Apoptotic Cells," *Mol. Biol. Cell*, vol. 21, no. 22, pp. 610–629, 2010.
- [108] M. Kitano, M. Nakaya, T. Nakamura, S. Nagata, and M. Matsuda, "Imaging of Rab5 activity identifies essential regulators for phagosome maturation," *Nature*, vol. 453, no. 7192, pp. 241–245, 2008.
- [109] K. W. Beyenbach and H. Wieczorek, "The V-type H<sup>+</sup> ATPase: molecular structure and function, physiological roles and regulation," *J. Exp. Biol.*, vol. 209, no. 4, pp. 577–589, 2006.
- [110] L. P. Erwig and P. M. Henson, "Immunological consequences of apoptotic cell

- phagocytosis," *Am. J. Pathol.*, vol. 171, no. 1, pp. 2–8, 2007.
- [111] G. Riemekasten and B. H. Hahn, "Key autoantigens in SLE," *Rheumatology*, vol. 44, no. 8, pp. 975–982, 2005.
- [112] B. L. Kotzin, "Systemic Lupus Erythematosus Review," *Cell*, vol. 85, pp. 303–306, 1996.
- [113] B. H. Hahn, "Antibodies to DNA," *N. Engl. J. Med.*, vol. 338, no. 19, pp. 1359–1368, 1998.
- [114] P. E. Lipsky, "Systemic lupus erythematosus: An autoimmune disease of B cell hyperactivity," *Nat. Immunol.*, vol. 2, no. 9, pp. 764–766, 2001.
- [115] G. S. Cooper, E. L. Treadwell, E. W. St.Clair, G. S. Gilkeson, and M. A. Dooley, "Sociodemographic associations with early disease damage in patients with systemic lupus erythematosus," *Arthritis Care Res.*, vol. 57, no. 6, pp. 993–999, 2007.
- [116] A. Samanta, J. Feehally, S. Roy, F. Nichok, P. Sheldon, and J. Walls, "High prevalence of systemic disease and mortality in Asian subjects with systemic lupus erythematosus," *Ann. Rheum. Dis.*, vol. 50, pp. 490–492, 1991.
- [117] G. Alarcon, A. Friedman, and K. Straaton, "Systemic lupus erythematosus in three ethnic groups: III A comparison of characteristics early in the natural history of the LUMINA cohort," *Lupus*, vol. 8, pp. 197–209, 1999.
- [118] G. J. Pons-Estel, G. Alarcon, L. Scofield, L. Reinlib, and G. S. Cooper, "Understanding the Epidemiology and Progression of Systemic Lupus Erythematosus," *Semin Arthritis Rheum*, vol. 39, no. 4, pp. 1–23, 2010.
- [119] M. Segasothy and P. A. Phillips, "Systemic lupus erythematosus in Aborigines and Caucasians in central Australia: A comparative study," *Lupus*, vol. 10, no. 6, pp. 439–444, 2001.
- [120] D. Bossingham, "Systemic lupus erythematosus in the far north of Queensland," *Lupus*, vol. 12, pp. 327–331, 2003.
- [121] S. Kamphuis and E. D. Silverman, "Prevalence and burden of pediatric-onset systemic lupus erythematosus," *Nat. Rev. Rheumatol.*, vol. 6, no. 9, pp. 538–546, 2010.
- [122] H. I. Brunner, J. Huggins, and M. S. Klein-Gitelman, "Pediatric SLE-towards a comprehensive management plan," *Nat. Rev. Rheumatol.*, vol. 7, no. 4, pp. 225–233, 2011.
- [123] Z. Liu and A. Davidson, "Taming lupus-a new understanding of pathogenesis is leading to clinical advances," *Nat. Med.*, vol. 18, no. 6, pp. 871–882, 2012.
- [124] M. Teruel and M. E. Alarcón-Riquelme, "The genetic basis of systemic lupus erythematosus: What are the risk factors and what have we learned," *J. Autoimmun.*, vol. 74, pp. 161–175, 2016.
- [125] C. M. Hedrich and G. C. Tsokos, "Epigenetic mechanisms in systemic lupus erythematosus and other autoimmune diseases," *Trends Mol Med*, vol. 17, no. 12, pp.

- 714–724, 2011.
- [126] D. M. Absher, X. Li, L. L. Waite, A. Gibson, K. Roberts, J. Edberg, W. W. Chatham, and R. P. Kimberly, “Genome-Wide DNA Methylation Analysis of Systemic Lupus Erythematosus Reveals Persistent Hypomethylation of Interferon Genes and Compositional Changes to CD4+ T-cell Populations,” *PLoS Genet.*, vol. 9, no. 8, 2013.
- [127] J. Bourré-Tessier, C. A. Peschken, S. Bernatsky, L. Joseph, A. E. Clarke, P. R. Fortin, C. Hitchon, S. Mittoo, C. D. Smith, M. Zummer, J. Pope, L. Tucker, M. Hudson, H. Arbillaga, J. Esdaile, E. Silverman, G. Chédeville, A. M. Huber, P. Belisle, and C. A. Pineau, “Association of Smoking With Cutaneous Manifestations in Systemic Lupus Erythematosus,” *Arthritis Care Res. (Hoboken)*, vol. 65, no. 8, pp. 1275–1280, 2013.
- [128] B. James, AJ Neas, “Systemic lupus erythematosus in adults is associated with previous Epstein- Barr virus exposure,” *Arthritis Rheum.*, vol. 44, no. 5, pp. 1122–1126, 2001.
- [129] C. G. Parks, G. S. Cooper, L. L. Hudson, M. A. Dooley, E. L. Treadwell, E. W. St.Clair, G. S. Gilkeson, and J. P. Pandey, “Association of Epstein-Barr virus with systemic lupus erythematosus: Effect modification by race, age, and cytotoxic T lymphocyte-associated antigen 4 genotype,” *Arthritis Rheum.*, vol. 52, no. 4, pp. 1148–1159, 2005.
- [130] I. Baumann, W. Kolowos, R. E. Voll, B. Manger, U. Gaipl, W. L. Neuhuber, T. Kirchner, J. R. Kalden, and M. Herrmann, “Impaired uptake of apoptotic cells into tingible body macrophages in germinal centers of patients with systemic lupus erythematosus Impaired Uptake of Apoptotic Cells Into Tingible Body Macrophages in Germinal Centers of Patients With Systemic Lupus Eryth,” *Arthritis Rheum.*, vol. 46, no. January, pp. 191–201, 2002.
- [131] D. V. Vlahakos, M. H. Foster, S. Adams, M. Katz, A. A. Ucci, K. J. Barrett, S. K. Datta, and M. P. Madaio, “Anti-DNA antibodies form immune deposits at distinct glomerular and vascular sites,” *Kidney Int.*, vol. 41, no. 6, pp. 1690–1700, 1992.
- [132] M. Herrmann, R. E. Voll, O. . Zoller, M. Hagenhofer, B. Ponner, and J. Kalden, “Impaired phagocytosis of apoptotic cell material by monocyte-derived macrophages from patients with systemic lupus erythematosus,” *Arthritis Rheum.*, vol. 41, no. 7, pp. 1241–1250, 1998.
- [133] L. E. Muñoz, R. A. Chaurio, U. S. Gaipl, G. Schett, and P. Kern, “MoMa from patients with systemic lupus erythematosus show altered adhesive activity,” *Autoimmunity*, vol. 42, no. 4, pp. 269–271, 2009.
- [134] L. E. Muñoz, B. Frey, U. Appelt, C. Janko, K. Sarter, R. E. Voll, P. Kern, M. Herrmann, and U. S. Gaipl, “Peripheral Blood Stem Cells of Patients with Systemic Lupus Erythema- tosus Show Altered Differentiation into Macrophages,” *Open Autoimmun. J.*, vol. 2, pp. 11–16, 2010.
- [135] H. M. Lorenz, M. Grünke, T. Hieronymus, M. Herrmann, A. Kühnel, B. Manger, and J.

- R. Kalden, "In vitro apoptosis and expression of apoptosis-related molecules in lymphocytes from patients with systemic lupus erythematosus and other autoimmune diseases.," *Arthritis Rheum.*, vol. 40, no. 2, pp. 306–317, 1997.
- [136] G. S. Garcia-romo, S. Caielli, B. Vega, J. Connolly, Z. Xu, M. Punaro, J. Baisch, C. Guiducci, L. Coffman, F. J. Barrat, J. Banchereau, and V. Pascual, "Netting Neutrophils Are Major Inducers of Type I IFN Production in Pediatric Systemic Lupus Erythematosus," *Sci Transl Med.*, vol. 3, no. 73, 2011.
- [137] V. Urbonaviciute and R. E. Voll, "High-mobility group box 1 represents a potential marker of disease activity and novel therapeutic target in systemic lupus erythematosus," *J. Intern. Med.*, vol. 270, no. 4, pp. 309–318, 2011.
- [138] S. Vordenbaumen, R. Fischer-Betz, D. Timm, O. Sander, G. Chehab, J. Richter, E. Bleck, and M. Schneider, "Elevated levels of human beta-defensin 2 and human neutrophil peptides in systemic lupus erythematosus.," *Lupus*, vol. 19, no. 14, pp. 1648–1653, 2010.
- [139] C. Y. Ma, Y. L. Jiao, J. Zhang, Q. R. Yang, Z. F. Zhang, Y. J. Shen, Z. J. Chen, and Y. R. Zhao, "Elevated plasma level of HMGB1 is associated with disease activity and combined alterations with IFN-alpha and TNF-alpha in systemic lupus erythematosus," *Rheumatol. Int.*, vol. 32, no. 2, pp. 395–402, 2012.
- [140] R. Lande, D. Ganguly, V. Facchinetti, L. Frasca, C. Conrad, J. Gregorio, S. Meller, G. Chamilos, V. Riccieri, R. Bassett, H. Amuro, and S. Fukuhara, "Neutrophils Activate Plasmacytoid Dendritic Cells by Releasing Self-DNA–Peptide Complexes in Systemic Lupus Erythematosus," *Sci. Transl. Med.*, vol. 3, no. 73, pp. 1–20, 2011.
- [141] D. Ganguly, G. Chamilos, R. Lande, J. Gregorio, S. Meller, V. Facchinetti, B. Homey, F. J. Barrat, T. Zal, and M. Gilliet, "Self-RNA–antimicrobial peptide complexes activate human dendritic cells through TLR7 and TLR8," *J. Exp. Med.*, vol. 206, no. 9, pp. 1983–1994, 2009.
- [142] M. J. Podolska, M. H. C. Biermann, C. Maueröder, J. Hahn, and M. Herrmann, "Inflammatory etiopathogenesis of systemic lupus erythematosus: An update," *J. Inflamm. Res.*, vol. 8, pp. 161–171, 2015.
- [143] M.-A. Dragon-Durey, P. Quartier, V. Fremeaux-Bacchi, J. Blouin, C. de Barace, A.-M. Prieur, L. Weiss, and W.-H. Fridman, "Molecular Basis of a Selective C1s Deficiency Associated with Early Onset Multiple Autoimmune Diseases," *J. Immunol.*, vol. 166, no. 12, pp. 7612–7616, 2001.
- [144] K. L. Rupert, J. M. Moulds, Y. Yang, F. C. Arnett, R. W. Warren, J. D. Reveille, B. L. Myones, C. A. Blanchong, and C. Y. Yu, "The Molecular Basis of Complete Complement C4A and C4B Deficiencies in a Systemic Lupus Erythematosus Patient with Homozygous C4A and C4B Mutant Genes," *J. Immunol.*, vol. 169, no. 3, pp. 1570–1578, 2002.

- [145] D. a Fraser and a J. Tenner, "Directing an appropriate immune response: the role of defense collagens and other soluble pattern recognition molecules.," *Curr. Drug Targets*, vol. 9, no. 2, pp. 113–122, 2008.
- [146] M. D. Galvan, M. C. Greenlee-Wacker, and S. S. Bohlson, "C1q and phagocytosis: the perfect complement to a good meal," *J. Leukoc. Biol.*, vol. 92, no. 3, pp. 489–497, 2012.
- [147] D. Spitzer, L. M. Mitchell, J. P. Atkinson, and D. E. Hourcade, "Properdin Can Initiate Complement Activation by Binding Specific Target Surfaces and Providing a Platform for De Novo Convertase Assembly," *J. Immunol.*, vol. 179, no. 4, pp. 2600–2608, 2007.
- [148] M. J. Walport, "Complement First of two parts," *N. Engl. J. Med.*, vol. 344, no. 14, pp. 1058–1066, 2001.
- [149] M. J. Walport, "Complement Second of two parts," *N. Engl. J. Med.*, vol. 344, no. 15, pp. 1140–1144, 2001.
- [150] K. B. Reid and R. R. Porter, "Subunit composition and structure of subcomponent C1q of the first component of human complement.," *Biochem. J.*, vol. 155, no. 1, pp. 19–23, 1976.
- [151] D. A. Fraser, K. Pisalyaput, and A. J. Tenner, "C1q enhances microglial clearance of apoptotic neurons and neuronal blebs, and modulates subsequent inflammatory cytokine production," *J. Neurochem.*, vol. 112, no. 3, pp. 733–743, 2010.
- [152] H. Paidassi, P. Delorme, V. Garlatti, C. Darnault, B. Ghebrehiwet, C. Gaboriaud, G. Arlaud, and P. Frchet, "C1q Binds Phosphatidylserine and Likely Acts as a Multiligand- Bridging Molecule in Apoptotic Cell Recognition," *J. Immunol.*, vol. 180, no. 4, pp. 2329–2338, 2008.
- [153] H. Jiang, B. Cooper, F. A. Robey, and H. Gewurz, "DNA binds and activates complement via residues 14-26 of the human C1q A chain," *J. Biol. Chem.*, vol. 267, no. 35, pp. 25597–25601, 1992.
- [154] T. G. Johns and C. C. A. Bernard, "Binding of complement component C1q to myelin oligodendrocyte glycoprotein: A novel mechanism for regulating CNS inflammation," *Mol. Immunol.*, vol. 34, no. 1, pp. 33–38, 1997.
- [155] A. R. Korotzer, J. Watt, D. Cribbs, A. J. Tenner, D. Burdick, C. Glabe, and C. W. Cotman, "Cultured rat microglia express C1q and receptor for C1q: Implications for amyloid effects on microglia," *Experimental Neurology*, vol. 134, no. 2, pp. 214–221, 1995.
- [156] G. Chen, C. S. Tan, B. K. Teh, and J. Lu, "Molecular mechanisms for synchronized transcription of three complement C1q subunit genes in dendritic cells and macrophages," *J. Biol. Chem.*, vol. 286, no. 40, pp. 34941–34950, 2011.
- [157] A. Tenner and N. Cooper, "Identification of types of cells in human peripheral blood

- that bind C1q.," *J. Immunol.*, vol. 126, pp. 1174–1179, 1981.
- [158] A. J. Tenner and N. R. Cooper, "Stimulation of a human polymorphonuclear leukocyte oxidative response by the C1q subunit of the first complement component.," *J. Immunol.*, vol. 128, no. 6, pp. 2547–2552, 1982.
- [159] L. E. Leigh, B. Ghebrehiwet, T. P. Perera, I. N. Bird, P. Strong, U. Kishore, K. B. Reid, and P. Eggleton, "C1q-mediated chemotaxis by human neutrophils: involvement of gC1qR and G-protein signalling mechanisms.," *Biochem. J.*, vol. 330, pp. 247–54, 1998.
- [160] Z. Bajtay, M. Józsi, Z. Bánki, S. Thiel, N. Thielens, and A. Erdei, "Mannan-binding lectin and C1q bind to distinct structures and exert differential effects on macrophages," *Eur. J. Immunol.*, vol. 30, no. 6, pp. 1706–1713, 2000.
- [161] Z. Vegh, R. R. Kew, B. L. Gruber, and B. Ghebrehiwet, "Chemotaxis of human monocyte-derived dendritic cells to complement component C1q is mediated by the receptors gC1qR and cC1qR," *Mol. Immunol.*, vol. 43, no. 9, pp. 1402–1407, 2006.
- [162] L. B. Klickstein, S. F. Barbashov, T. Liu, R. M. Jack, and A. Nicholson-Weller, "Complement receptor type 1 (CR1, CD35) is a receptor for C1q," *Immunity*, vol. 7, pp. 345–355, 1997.
- [163] R. W. Vandivier, C. A. Ogden, V. A. Fadok, P. R. Hoffmann, K. K. Brown, M. Botto, M. J. Walport, J. H. Fisher, P. M. Henson, and K. E. Greene, "Role of Surfactant Proteins A, D, and C1q in the Clearance of Apoptotic Cells In Vivo and In Vitro: Calreticulin and CD91 as a Common Collectin Receptor Complex," *J. Immunol.*, vol. 169, pp. 3978–3986, 2002.
- [164] A. P. Lillis, I. Mikhailenko, and D. K. Strickland, "Beyond endocytosis: LRP function in cell migration, proliferation and vascular permeability.," *J. Thromb. Haemost.*, vol. 3, pp. 1884–93, 2005.
- [165] B. T. Edelson, T. P. Stricker, Z. Li, S. K. Dickeson, V. L. Shepherd, S. A. Santoro, and M. M. Zutter, "Novel collectin/C1q receptor mediates mast cell activation and innate immunity," *Blood*, vol. 107, no. 1, pp. 143–150, 2006.
- [166] S. Bohlsón, M. Greenlee, and S. Sullivan, "CD93 and Related Family Members: Their Role in Innate Immunity," *Curr. Drug Targets*, vol. 9, pp. 130–138, 2008.
- [167] U. S. Gaipf, T. D. Beyer, P. Heyder, S. Kuenkele, A. Böttcher, R. E. Voll, J. R. Kalden, and M. Herrmann, "Cooperation between C1q and DNase I in the Clearance of Necrotic Cell-Derived Chromatin," *Arthritis Rheum.*, vol. 50, no. 2, pp. 640–649, 2004.
- [168] D. Santer, A. Wiedeman, T. Teal, P. Ghosh, and K. Elkon, "Plasmacytoid dendritic cells and C1q differentially regulate inflammatory gene induction by lupus immune complexes," *J. Immunol.*, vol. 188, no. 2, pp. 902–915, 2009.
- [169] M. Botto, C. Agnola, A. Bygrave, E. Thompson, H. Cook, F. Petry, M. Loos, P. Pandolfi, and M. J. Walport, "Homozygous C1q deficiency causes glomerulonephritis

- associated with multiple apoptotic bodies,” *Nat. Genet.*, vol. 19, pp. 56–59, 1998.
- [170] D. A. Mitchell, M. C. Pickering, J. Warren, L. Fossati-Jimack, J. Cortes-Hernandez, H. T. Cook, M. Botto, and M. J. Walport, “C1q Deficiency and Autoimmunity: The Effects of Genetic Background on Disease Expression,” *J. Immunol.*, vol. 168, no. 5, pp. 2538–2543, 2002.
- [171] A. P. Manderson, M. Botto, and M. J. Walport, “The Role of Complement in the Development of Systemic Lupus Erythematosus,” *Annu. Rev. Immunol.*, vol. 22, pp. 431–456, 2004.
- [172] J. L. Roberts, M. M. Schwartz, and E. J. Lewis, “Hereditary C2 deficiency and systemic lupus erythematosus associated with severe glomerulonephritis.,” *Clin. Exp. Immunol.*, vol. 31, pp. 328–38, 1978.
- [173] O. Meyer, G. Hauptmann, G. Tappeiner, H. Ochs, and M.-L. F, “Genetic deficiency of C4, C2 or C1q and lupus syndromes. Association with anti-Ro (SS-A) antibodies,” *Clin. exp. Immunol*, vol. 62, pp. 678–684, 1985.
- [174] Z. Chen, S. B. Koralov, and G. Kelsoe, “Complement C4 inhibits systemic autoimmunity through a mechanism independent of complement receptors CR1 and CR2.,” *J. Exp. Med.*, vol. 192, no. 9, pp. 1339–1352, 2000.
- [175] J. E. Figueroa and P. Densen, “Infectious diseases associated with complement deficiencies,” *Clin. Microbiol. Rev.*, vol. 4, no. 3, pp. 359–395, 1991.
- [176] D. Perry, A. Sang, Y. Yin, Y.-Y. Zheng, and L. Morel, “Murine models of systemic lupus erythematosus,” *J. Biomed. Biotechnol.*, pp. 271694–271694, 2011.
- [177] L. Raptis and H. a Menard, “Quantitation and characterization of plasma DNA in normals and patients with systemic lupus erythematosus.,” *J. Clin. Invest.*, vol. 66, pp. 1391–1399, 1980.
- [178] R. Licht, M. C. van Bruggen, B. Oppers-Walgreen, T. P. Rijke, and J. H. Berden, “Plasma levels of nucleosomes and nucleosome-autoantibody complexes in murine lupus: Effects of disease progression and lipopolysaccharide administration.,” *Arthritis Rheum.*, vol. 44, no. 6, pp. 1320–1330, 2001.
- [179] U. S. Gaipf, S. Franz, R. E. Voll, A. Sheriff, J. R. Kalden, and M. Herrmann, “Defects in the disposal of dying cells lead to autoimmunity.,” *Curr. Rheumatol. Rep.*, vol. 6, pp. 401–407, 2004.
- [180] E. Pieterse and J. van der Vlag, “Breaking immunological tolerance in systemic lupus erythematosus,” *Front. Immunol.*, vol. 5, pp. 1–8, 2014.
- [181] K. P. Ng, M. J. Leandro, J. C. Edwards, M. R. Ehrenstein, G. Cambridge, and D. A. Isenberg, “Repeated B cell depletion in treatment of refractory systemic lupus erythematosus,” *Ann. Rheum. Dis.*, vol. 65, no. 7, pp. 942–945, 2006.
- [182] R. Felten, E. Dervovic, F. Chasset, J. E. Gottenberg, J. Sibilia, F. Scher, and L. Arnaud, “The 2018 pipeline of targeted therapies under clinical development for

- Systemic Lupus Erythematosus: a systematic review of trials,” *Autoimmun. Rev.*, no. February, pp. 1–10, 2018.
- [183] M. Linker-israeli, R. J. Deans, D. J. Wallace, J. Prehn, T. A. L. Ozeri-chen, and J. R. Klinenberg, “Elevated levels of endogenous IL-6 in systemic lupus erythematosus . A putative role in Information,” *J. Immunol.*, vol. 147, pp. 117–123, 1991.
- [184] M. C. Carroll, “The role of complement in B cell activation and tolerance.,” *Adv. Immunol.*, vol. 74, pp. 61–88, 2000.
- [185] I. K. Mandemaker, M. Kozlowski, K. Scheffzek, J. Sporn, G. Timinszky, A. G. Ladurner, S. Huet, M. Buschbeck, I. Guberovic, R. Smith, T. Portmann, A. Gutierrez-Triana, C. Blessing, M. Hothorn, M. Treier, and D. Corujo, “MacroH2A histone variants limit chromatin plasticity through two distinct mechanisms,” *EMBO Rep.*, vol. 19, no. 10, p. e44445, 2018.
- [186] P. R. Taylor, A. Carugati, V. A. Fadok, H. T. Cook, M. Andrews, M. C. Carroll, J. S. Savill, P. M. Henson, M. Botto, and M. J. Walport, “A Hierarchical Role for Classical Pathway Complement Proteins in the Clearance of Apoptotic Cells in Vivo,” *J. Exp. Med.*, vol. 192, no. 3, pp. 359–366, 2000.
- [187] T. J. Waldschmidt, C.-M. Alexander, K. L. Legge, K. L. Wolniak, A. W. Boyden, and L. T. Tygrett, “T regulatory cells participate in the control of germinal centre reactions,” *Immunology*, vol. 133, no. 4, pp. 452–468, 2011.
- [188] M. F. Counis and A. Torriglia, “Acid DNases and their interest among apoptotic endonucleases,” *Biochimie*, vol. 88, no. 12, pp. 1851–1858, 2006.
- [189] H. Yoshida, Y. Okabe, K. Kawane, H. Fukuyama, and S. Nagata, “Lethal anemia caused by interferon- $\beta$  produced in mouse embryos carrying undigested DNA,” *Nat. Immunol.*, vol. 6, no. 1, pp. 49–56, 2005.
- [190] K. Kawane, H. Tanaka, Y. Kitahara, S. Shimaoka, and S. Nagata, “Cytokine-dependent but acquired immunity-independent arthritis caused by DNA escaped from degradation,” vol. 107, no. 45, pp. 9–14, 2010.
- [191] A. Zeigerer, J. Gilleron, R. L. Bogorad, G. Marsico, H. Nonaka, S. Seifert, H. Epstein-Barash, S. Kuchimanchi, C. G. Peng, V. M. Ruda, P. Del Conte-Zerial, J. G. Hengstler, Y. Kalaidzidis, V. Koteliansky, and M. Zerial, “Rab5 is necessary for the biogenesis of the endolysosomal system in vivo,” *Nature*, vol. 485, no. 7399, pp. 465–470, 2012.
- [192] R. Hanayama, M. Tanaka, K. Miyasaka, K. Aozasa, M. Koike, Y. Uchiyama, and S. Nagata, “Autoimmune Disease and Impaired Uptake of Apoptotic Cells in MFG-E8 – Deficient Mice,” *Science (80- )*, vol. 304, no. 5674, pp. 1147–1150, 2004.
- [193] S. Einav, O. O. Pozdnyakova, M. Ma, and M. C. Carroll, “Complement C4 Is Protective for Lupus Disease Independent of C3,” *J. Immunol.*, vol. 168, no. 3, pp. 1036–1041, 2002.
- [194] M. Zerial and H. McBride, “Rab proteins as membrane organizers,” *Nat. Rev. Mol. Cell*

- Biol.*, vol. 2, no. February, pp. 107–119, 2001.
- [195] N. Lu and Z. Zhou, *Membrane Trafficking and Phagosome Maturation During the Clearance of Apoptotic Cells*, vol. 293. 2013.
- [196] T. M. Newton and E. Reid, “An automated image analysis system to quantify endosomal tubulation,” *PLoS One*, vol. 11, no. 12, pp. 1–11, 2016.
- [197] J. Rohrer, A. Schweizer, D. Russell, and S. Kornfeld, “The targeting of lamp1 to lysosomes is dependent on the spacing of its cytoplasmic tail tyrosine sorting motif relative to the membrane,” *J. Cell Biol.*, vol. 132, no. 4, pp. 565–576, 1996.
- [198] E. C. Freundt, M. Czapiga, and M. J. Lenardo, “Photoconversion of LysoTracker Red to a green fluorescent molecule,” *Cell Res.*, vol. 17, no. 11, pp. 956–958, 2007.
- [199] J. K. Park, H. Peng, J. Katsnelson, W. Yang, N. Kaplan, Y. Dong, J. Z. Rappoport, C. C. He, and R. M. Lavker, “MicroRNAs-103/107 coordinately regulate macropinocytosis and autophagy,” *J. Cell Biol.*, vol. 215, no. 5, pp. 667–685, 2016.
- [200] A. E. González, V. C. Muñoz, V. A. Cavieres, H. A. Bustamante, V. H. Cornejo, Y. C. Januário, I. González, C. Hetz, L. L. Dasilva, A. Rojas-Fernández, R. T. Hay, G. A. Mardones, and P. V. Burgos, “Autophagosomes cooperate in the degradation of intracellular C-terminal fragments of the amyloid precursor protein via the MVB/lysosomal pathway,” *FASEB J.*, vol. 31, no. 6, pp. 2446–2459, 2017.
- [201] K. Ebine, Y. Okatani, T. Uemura, T. Goh, K. Shoda, M. Niihama, M. T. Morita, C. Spitzer, M. S. Otegui, A. Nakano, and T. Ueda, “A SNARE Complex Unique to Seed Plants Is Required for Protein Storage Vacuole Biogenesis and Seed Development of *Arabidopsis thaliana*,” *Plant Cell Online*, vol. 20, no. 11, pp. 3006–3021, 2008.
- [202] M. Sardiello, M. Palmieri, A. di Ronza, D. L. Medina, M. Valenza, V. A. Gennarino, C. Di Malta, F. Donaudy, V. Embrione, R. S. Polishchuk, S. Banfi, G. Parenti, E. Cattaneo, and A. Ballabio, “A Gene Network Regulating Lysosomal Biogenesis and Function,” *Science (80-. )*, vol. 325, no. July, pp. 473–476, 2009.
- [203] M. Sardiello, M. Palmieri, A. Di Ronza, D. L. Medina, M. Valenza, V. A. Gennarino, C. Di Malta, F. Donaudy, V. Embrione, R. S. Polishchuk, S. Banfi, G. Parenti, E. Cattaneo, and A. Ballabio, “A gene network regulating lysosomal biogenesis and function,” *Science (80-. )*, vol. 325, no. 5939, pp. 473–477, 2009.
- [204] C. Settembre, V. A. Polito, M. Garcia, F. Vetrini, S. Erdin, S. U. Erdin, T. Huynh, D. Medina, P. Colella, M. Sardiello, and D. C. Rubinsztein, “TFEB Links Autophagy to Lysosomal Biogenesis,” *Science (80-. )*, vol. 332, no. 6036, pp. 1429–1433, 2013.
- [205] J. Ahn, D. Gutman, S. Saijo, and G. N. Barber, “STING manifests self DNA-dependent inflammatory disease,” *Proc. Natl. Acad. Sci.*, vol. 109, no. 47, pp. 19386–19391, 2012.
- [206] M. K. Atianand and Katherine A. Fitzgerald, “Molecular Basis of DNA Recognition in the Immune System Maninjay,” *J. Immunol.*, vol. 190, no. 5, pp. 1–18, 2013.

- [207] X. Cai, Y. H. Chiu, and Z. J. Chen, "The cGAS-cGAMP-STING pathway of cytosolic DNA sensing and signaling," *Mol. Cell*, vol. 54, no. 2, pp. 289–296, 2014.
- [208] R. Hanayama, K. Miyasaka, M. Nakaya, and S. Nagata, "MFG-E8-Dependent Clearance of Apoptotic Cells, and Autoimmunity Caused by Its Failure," *Apoptosis Its Relev. to Autoimmun.*, vol. 9, pp. 162–172, 2006.
- [209] N. D. Barth, J. A. Marwick, M. Vendrell, A. G. Rossi, and I. Dransfield, "The 'Phagocytic synapse' and clearance of apoptotic cells," *Front. Immunol.*, vol. 8, no. DEC, pp. 1–9, 2017.
- [210] L. C. Korb and J. M. Ahearn, "C1q binds directly and specifically to surface blebs of apoptotic human keratinocytes: complement deficiency and systemic lupus erythematosus revisited.," *J. Immunol.*, vol. 158, no. 10, pp. 4525–8, 1997.
- [211] A. J. Nauta, L. A. Trouw, M. R. Daha, O. Tijms, R. Nieuwland, W. J. Schwaeble, A. R. Gingras, A. Mantovani, E. C. Hack, and A. Roos, "Direct binding of C1q to apoptotic cells and cell blebs induces complement activation," *Eur. J. Immunol.*, vol. 32, no. 6, pp. 1726–1736, 2002.
- [212] P. K. Potter, J. Cortes-Hernandez, P. Quartier, M. Botto, and M. J. Walport, "Lupus-Prone Mice Have an Abnormal Response to Thioglycolate and an Impaired Clearance of Apoptotic Cells," *J. Immunol.*, vol. 170, no. 6, pp. 3223–3232, 2003.
- [213] Y. Peng and K. B. Elkon, "Autoimmunity in MFG-E8-deficient mice is associated with altered trafficking and enhanced cross-presentation of apoptotic cell antigens," *J. Clin. Invest.*, vol. 121, no. 6, pp. 2221–2241, 2011.
- [214] K. Kawane, H. Fukuyama, H. Yoshida, H. Nagase, Y. Ohsawa, Y. Uchiyama, K. Okada, T. Iida, and S. Nagata, "Impaired thymic development in mouse embryos deficient in apoptotic DNA degradation," *Nat. Immunol.*, vol. 4, no. 2, pp. 138–144, 2003.
- [215] K. Kawane, H. Fukuyama, G. Kondoh, J. Takeda, Y. Ohsawa, Y. Uchiyama, and S. Nagata, "Requirement of DNase II for definitive erythropoiesis in the mouse fetal liver," *Science (80-. )*, vol. 292, no. 5521, pp. 1546–1549, 2001.
- [216] R. J. Krieser, K. S. MacLea, D. S. Longnecker, J. L. Fields, S. Fiering, and A. Eastman, "Deoxyribonuclease II $\alpha$  is required during the phagocytic phase of apoptosis and its loss causes perinatal lethality," *Cell Death Differ.*, vol. 9, no. 9, pp. 956–962, 2002.
- [217] K. Kawane, M. Ohtani, K. Miwa, T. Kizawa, Y. Kanbara, Y. Yoshioka, H. Yoshikawa, and S. Nagata, "Chronic polyarthritis caused by mammalian DNA that escapes from degradation in macrophages," *Nature*, vol. 443, no. 7114, pp. 998–1002, 2006.
- [218] C. A. Dinarello, "Interleukin 1 and interleukin 18 as mediators of inflammation and the NUTRITION," *Am. J. Clin. Nutr.*, vol. 83, no. April, 2006.
- [219] C. A., P. P.V., F. R., G. P., S. A., S. A.E., M. R., C. E., A. D., R. I., and M. A.,

- “Interleukin 1, interleukin 6, interleukin 10, and tumor necrosis factor (alpha) in active and quiescent systemic lupus erythematosus,” *J. Investig. Med.*, vol. 62, no. 5, pp. 825–829, 2014.
- [220] V. Umare, V. Pradhan, M. Nadkar, A. Rajadhyaksha, M. Patwardhan, K. K. Ghosh, and A. H. Nadkarni, “Effect of Proinflammatory Cytokines (IL-6, TNF- $\alpha$  and IL-1 $\beta$ ) on Clinical Manifestations in Indian SLE Patients,” *Mediators Inflamm.*, vol. 2014, 2014.
- [221] T. Lang, R. Kandane-Rathnayake, E. Lin, J. Chang, E. F. Morand, A. Y. Hoi, R. Koelmeyer, F. B. Vincent, R. Mende, and J. Harris, “Analysis of Serum Interleukin (IL)-1 $\beta$  and IL-18 in Systemic Lupus Erythematosus,” *Front. Immunol.*, vol. 9, no. June, 2018.
- [222] L. E. Muñoz, C. Janko, G. E. Grossmayer, B. Frey, R. E. Voll, P. Kern, J. R. Kalden, G. Schett, R. Fietkau, M. Herrmann, and U. S. Gaipl, “Remnants of secondarily necrotic cells fuel inflammation in systemic lupus erythematosus,” *Arthritis Rheum.*, vol. 60, no. 6, pp. 1733–1742, 2009.
- [223] R. Baum, S. Sharma, S. Carpenter, Q.-Z. Li, P. Busto, K. A. Fitzgerald, A. Marshak-Rothstein, and E. M. Gravallese, “Cutting Edge: AIM2 and Endosomal TLRs Differentially Regulate Arthritis and Autoantibody Production in DNase II-Deficient Mice,” *J. Immunol.*, vol. 194, no. 3, pp. 873–877, 2015.
- [224] S. Pawaria, K. L. Moody, P. Busto, K. Nündel, R. Baum, S. Sharma, E. M. Gravallese, K. A. Fitzgerald, and A. Marshak-, “An Unexpected Role for RNA-sensing Toll-like Receptors in a Murine Model of DNA Accrual,” *Clin Exp Rheumatol.*, vol. 33, no. 4 0 92, pp. S70–S73, 2015.
- [225] K. K. Huynh, E. L. Eskelinen, C. C. Scott, A. Malevanets, P. Saftig, and S. Grinstein, “LAMP proteins are required for fusion of lysosomes with phagosomes,” *EMBO J.*, vol. 26, no. 2, pp. 313–324, 2007.
- [226] M. Toei, R. Saum, and M. Forgac, “Regulation and isoform function of the V-ATPases,” *Biochemistry*, vol. 49, no. 23, pp. 4715–4723, 2010.
- [227] G.-H. Sun-Wada, H. Tabata, N. Kawamura, M. Aoyama, and Y. Wada, “Direct recruitment of H<sup>+</sup>-ATPase from lysosomes for phagosomal acidification,” *J. Cell Sci.*, vol. 122, no. 14, pp. 2504–2513, 2009.
- [228] D. Mijaljica, M. Prescott, and R. J. Devenish, “V-ATPase engagement in autophagic processes,” *Autophagy*, vol. 7, no. 6, pp. 666–668, 2011.
- [229] M. Ira, F. Renate, and H. Ari, “Acidification of the endocytic and exocytic pathways,” *Ann.Rev.Biochem*, no. 55, pp. 663–700, 1986.
- [230] J. M. Holopainen, J. Saarikoski, P. K. J. Kinnunen, and I. Järvelä, “Elevated lysosomal pH in neuronal ceroid lipofuscinoses (NCLs),” *Eur. J. Biochem.*, vol. 268, no. 22, pp. 5851–5856, 2001.
- [231] F. M. Platt, B. Boland, and A. C. van der Spoel, “Lysosomal storage disorders: The

- cellular impact of lysosomal dysfunction,” *J. Cell Biol.*, vol. 199, no. 5, pp. 723–734, 2012.
- [232] A. H. Futerman and G. Van Meer, “The cell biology of lysosomal storage disorders,” *Nat. Rev. Mol. Cell Biol.*, vol. 5, no. 7, pp. 554–565, 2004.
- [233] J.-H. Lee, W. Yu, K. Asok, S. Lee, P. Mohan, C. Peterhoff, D. Wolfe, M. Vicente, A. Masish, G. Sovak, Y. Uchiyama, D. Westaway, S. Sisodia, A. Cuervo, and R. Nixon, “Lysosomal proteolysis and autophagy require presenilin 1 and are disrupted by alzheimers related PS1 mutations,” *Cell*, vol. 141, no. 7, pp. 1146–1158, 2010.
- [234] R. A. Nixon, “The role of autophagy in neurodegenerative disease,” *Nat. Med.*, vol. 19, no. 8, pp. 983–997, 2013.
- [235] B. Dehay, M. Martinez-Vicente, G. A. Caldwell, K. A. Caldwell, Z. Yue, M. R. Cookson, C. Klein, M. Vila, and E. Bezdard, “Lysosomal impairment in Parkinson’s disease,” *Mov. Disord.*, vol. 28, no. 6, pp. 725–732, 2013.
- [236] C. J. Evans and R. J. Aguilera, “DNase II : genes , enzymes and function,” vol. 322, pp. 1–15, 2003.
- [237] A. Roczniak-ferguson, C. S. Petit, F. Froehlich, S. Qian, J. Ky, B. Angarola, T. C. Walther, and S. M. Ferguson, “The Transcription Factor TFEB Links mTORC1 Signaling to Transcriptional Control of Lysosome Homeostasis Agnes,” *Sci.signal*, vol. 5, no. 228, 2012.
- [238] M. Samie and P. Cresswell, “The transcription factor TFEB acts as a molecular switch that regulates exogenous antigen presentation pathways Mohammad,” *Nat.Immunology*, vol. 16, no. 7, pp. 729–736, 2015.
- [239] M. A. Gray, C. H. Choy, R. M. Dayama, E. O. Escobara, A. Somervillea, X. Xiaoa, S. M. Fergusonc, and R. J. Botelhoa, “Phagocytosis enhances lysosomal and bactericidal properties by activating the transcription factor TFEB,” *Curr. Biol.*, vol. 26(15), no. August 2016, pp. 1955–1964, 2016.
- [240] D. L. Medina, A. Fraldi, V. Bouche, F. Annunziata, G. Mansueto, C. Spampinato, C. Puri, A. Pignata, J. A. Martina, M. Sardiello, M. Palmieri, R. Polishchuk, R. Puertollano, and A. Ballabio, “Transcriptional activation of lysosomal exocytosis promotes cellular clearance,” *Dev. Cell*, vol. 21, no. 3, pp. 421–430, 2011.
- [241] C. Spampinato, E. Feeney, L. Li, M. Cardone, J. A. Lim, F. Annunziata, H. Zare, R. Polishchuk, R. Puertollano, G. Parenti, A. Ballabio, and N. Raben, “Transcription factor EB (TFEB) is a new therapeutic target for Pompe disease,” *EMBO Mol. Med.*, vol. 5, no. 5, pp. 691–706, 2013.
- [242] S. Akakura, S. Singh, M. Spataro, R. Akakura, J. Il Kim, M. L. Albert, and R. B. Birge, “The opsonin MFG-E8 is a ligand for the  $\alpha\beta 5$  integrin and triggers DOCK180-dependent Rac1 activation for the phagocytosis of apoptotic cells,” *Exp. Cell Res.*, vol. 292, no. 2, pp. 403–416, 2004.

- [243] M. Aziz, A. Jacob, A. Matsuda, and P. Wang, "Review: Milk fat globule-EGF factor 8 expression, function and plausible signal transduction in resolving inflammation," *Apoptosis*, vol. 16, no. 11, pp. 1077–1086, 2011.
- [244] M. MIKSA, D. AMIN, R. WU, A. JACOB, M. ZHOU, W. DONG, W.-L. YANG, T. S. RAVIKUMAR, and P. WANG, "Maturation-induced down-regulation of MFG-E8 impairs apoptotic cell clearance and enhances endotoxin response," *Int. J. Mol. Med.*, vol. 22, no. 2, pp. 743–748, 2008.
- [245] K. G. Shah, R. Wu, A. Jacob, E. P. Molmenti, J. Nicastro, G. F. Coppa, and P. Wang, "Recombinant human milk fat globule-EGF factor 8 produces dose-dependent benefits in sepsis," *Intensive Care Med.*, vol. 38, no. 1, pp. 128–136, 2012.

## 11 ACKNOWLEDGEMENTS

I would like to express my sincere gratitude to my supervisor Prof. Thomas Brocker for giving me the opportunity to work on this interesting project, for his critical supervision and for his great support during my PhD thesis.

I am very grateful to my advisor Dr. Jan Kranich for the continuous support during my PhD tenure, for his patience, motivation and constant quick feedback. His guidance helped me in research and also for writing this thesis.

My sincere thanks to Prof. Axel Imhof and Dr. Julia von Blume for their insightful comments who provided me an opportunity to collaborate, and also gave access to the laboratory and research facilities.

Furthermore, I would also like to thank Natalia Pacheco at MPI who contributed a lot to the success of this work for the excellent collaboration. I would thank her patience for all long confocal imaging and data processing sessions even on weekends. I also thank Merhad Pakdel at MPI for helping us with data analysis.

I thank Aga for her support with all cell culture and protein production work. Your support during last months of thesis writing really meant a lot. I like to thank Tilman Kurz and Lisa for all chats during our long stay and weekends in lab. I thank whole IFI mouse facility for maintaining the mice used in this work.

Last but not the least, I thank my husband Shri Avinash for all the support you have given me throughout my studies. It is not just moral support but for all your pep talks during my tough times and your company for most of my late-night stays in lab. It is impossible to finish this work without the emotional support you gave me all these years. I would also like to thank my whole family: late grandparents, my parents and in laws for supporting me throughout the whole process.

## 12 PRESENTATIONS

- 1) Poster presentation at the 10<sup>th</sup> ENII Summer school, 2015 in Sardinia, Italy (Title: "Identification of novel susceptibility factors for SLE").
  
- 2) Oral presentation at the Cell death, Inflammation and Cancer, EMBO workshop, 2017 in Obergurgl, Austria (Title: " Impaired degradation of DNA from apoptotic cells in C1q-KO mice contributes to SLE").